

Expression levels of MDM2 and MDMX
proteins and their associated effects on P53
in human liposarcomas

Nader Touqan

Submitted in accordance with the requirements for the degree of

Doctor of Medicine

University of Leeds

School of Medicine

August 2014

Intellectual property and publication statement

The candidate confirms that the work submitted is his own, except where work which has formed part of jointly-authored publications has been included. The contribution of the candidate and the other authors to this work has been explicitly indicated below. The candidate confirms that appropriate credit has been given within the thesis where reference has been made to the work of others.

The findings of my research on the immunohistochemical profiling of liposarcomas and the related *P53* mutation analysis were published in the following article:

Touqan N, Diggle CP, Verghese ET, Perry S, Horgan K, Merchant W, Anwar R, Markham AF, Carr I, Achuthan R. An observational study on the expression levels of MDM2 and MDMX proteins, and associated effects on P53 in a series of human liposarcomas. *BMC Clin Pathol.* 2013;13(1):32. Epub 2013/12/18.

This work forms part of the Study Materials and Methods, Immunohistochemical Profiling of Liposarcomas and Genetic Analysis of *P53* Sections of this thesis (Chapters 2, 4 and 5). The experiments that were conducted on liposarcoma tissues were performed solely by me, or with help and supervision of Dr C P Diggle and Miss Sarah Perry. Scoring of the tissue slides was performed by me, Dr E T Verghese and Dr W Merchant. Clinical elements of the study were reviewed by Mr K Horgan and Mr R Achuthan. Scientific aspects were reviewed by Dr R Anwar, Dr I Carr and Professor A F Markham.

This copy has been supplied on the understanding that it is copyright material and that no quotation from the thesis may be published without proper acknowledgement.

The right of Nader Touqan to be identified as Author of this work has been asserted by him in accordance with the Copyright, Designs and Patents Act 1988.

Acknowledgments

I first thank my supervisor, Professor Sir Alexander F Markham, for his constant guidance, generous support and his humble father-figure presence when it was most needed. I am forever indebted to him.

I would like to thank my mentors and scientific supervisors: Dr Ian Carr, Dr Rashda Anwar, Dr Christine Diggle and Miss Sarah Perry for their methodological and technical assistance during my work on this project. I am thankful to Dr Will Merchant and Dr Paul Roberts for providing invaluable histological and cytological data.

I am fortunate for the help and support provided by my clinical supervisors: Mr Kieran Horgan and Mr Raj Achuthan.

Finally, special thanks are reserved to all the patients who kindly participated in this study.

On a personal note, I dedicate this work to:

Muna and Zaki, for all the times I was away working on this.

Dad; Samer; Linda; Bushra; and Saadi, for constantly reminding me that I have to finish this.

The beautiful memory of Mum; Amru; and Ali, for inspiring me to keep going.

Abstract

Background: Inactivation of wild type P53 by its main cellular inhibitors, MDM2 and MDMX, is a well-recognised feature of tumour formation in liposarcomas (LS). MDM2 over-expression has been detected in approximately 80% of liposarcomas, but only limited information is available about MDMX expression levels. On commencing this work, we were not aware of any study that had described the patterns of MDM2 and MDMX co-expression in liposarcomas. Such information has become more pertinent as various novel MDM2 and / or MDMX single and dual affinity antagonist compounds have emerged as alternative approaches for potential targeted therapeutic strategies in LS.

Methods: After appropriate optimisation and confirmation of experimental techniques, a case series of 64 pathologically characterised liposarcomas of various sub-types was analysed by immunohistochemistry, to simultaneously assess the expression levels of P53, MDM2 and MDMX. *P53* mutation status was investigated in cases that over-expressed P53.

Results: 83% of cases over-expressed MDM2 and 69% co-expressed MDMX at varying relative levels. The relative expression levels of the two proteins with respect to each other were subtype-dependent. This apparently affected the detected levels of P53 directly, in two distinct patterns. Diminished levels of P53 were observed when MDM2 was significantly higher in relation to MDMX, suggesting a dominant role for MDM2 in the degradation of P53. Higher levels of P53 were noted with increasing MDMX levels, suggesting an interaction between MDM2 and MDMX that resulted in reduced efficiency of MDM2 when degrading P53. No increased incidence of *P53* mutations was detected in cases that over-expressed P53 compared to the general population of LSs.

Conclusions: The results of the study indicated that complex dynamic interactions between MDM2 and MDMX proteins may directly affect the cellular levels of P53 in human liposarcomas. This suggests that careful characterisation of all these markers will be necessary when considering *in vivo* evaluation of novel MDM blocking compounds as a therapeutic strategy to restore wild type P53 functions.

Table of Contents

1	Introduction	1
1.1	Soft Tissue Sarcoma	1
1.2	Liposarcoma	2
1.2.1	Liposarcoma Subtypes	3
1.2.2	Well-Differentiated Liposarcoma	3
1.2.3	Molecular Classification of Liposarcomas.....	5
1.3	P53.....	6
1.3.1	P53 Structure	7
1.3.2	Relevant P53 Functions.....	8
1.3.3	Cellular Regulators of P53.....	10
1.4	MDM2 and MDMX	10
1.4.1	Gene Amplification and Overexpression	10
1.4.2	Protein Structure.....	11
1.4.3	Intracellular Localisation	12
1.4.4	Splice Variants.....	13
1.4.5	Relevant Single Nucleotide Polymorphisms	14
1.5	P53 / MDM Interactions.....	15
1.5.1	Molecular Basis of the Interaction.....	15
1.5.2	Animal Models	18
1.5.3	The Gaps in Current Knowledge	18
1.6	Potential Novel Therapeutic Strategies	19
1.6.1	MDM2 Blockers.....	19
1.6.2	MDMX Blockers.....	20
1.6.3	Dual Affinity Blockers.....	21
1.6.4	Alternative P53 Activation Approaches.....	21

1.7	Aims of the Study	22
2	Materials and Methods.....	28
2.1	Ethical Issues	28
2.2	Patient Cohorts.....	28
2.2.1	Retrospective Cohort	28
2.2.2	Prospective Cohort	29
2.3	Materials	30
2.3.1	Eukaryotic Cell Lines	30
2.3.2	Tissue Culture Reagents.....	30
2.3.3	Cell Cycle Arrest Reagents	31
2.3.4	Immunochemical Staining Reagents.....	31
2.3.5	Reagents Used for Preparing Cell Lysates.....	32
2.3.6	Reagents Used for Protein Quantification.....	33
2.3.7	Reagents for Western Blot.....	34
2.3.8	Reagents Used for DNA Extraction	36
2.3.9	Reagents Used For Polymerase Chain Reaction	37
2.3.10	Reagents for Big Dye Sanger Sequencing	38
2.4	Methods	38
2.4.1	Tissue Samples Processing and Storage	38
2.5	Propagation of Eukaryotic Cell Lines.....	39
2.6	Cell Cycle Arrest Protocol	39
2.7	Immunochemical Staining Protocol	40
2.7.1	Immunocytochemistry (ICC)	40
2.7.2	Immunohistochemistry (IHC).....	41
2.8	Immune Blotting of Proteins	43
2.8.1	Cell Lysate Preparation and Quantification	43

2.8.2	Western Blot	45
2.9	Cytogenetic Analyses	46
2.10	Genetic Analysis	47
2.10.1	Extraction of Deoxyribonucleic Acid (DNA)	47
2.10.2	The Polymerase Chain Reaction	49
2.10.3	DNA Amplicon Dye Terminator Cycle Sequencing	51
3	Assessment of Methods.....	59
3.1	Aims.....	59
3.1.1	Choice of Control Cell Lines	59
3.1.2	Human Tissue Controls	59
3.2	Proof of Principle Experiments.....	60
3.2.1	Immunocytochemistry.....	60
3.2.2	Immunohistochemistry Control Experiments.....	60
3.2.3	Influence of Cell Cycle Phase on Expression of MDM Proteins.....	61
3.2.4	Specificity of Antibodies	62
3.2.5	PCR and Gene Sequencing for MDM2 and MDMX.....	64
3.2.6	Summary of Proof of Principle Results	65
3.3	Optimisation of Methods	65
3.4	Discussion	66
3.4.1	Choice of Primary Antibodies	66
3.4.2	Assessment of Method	66
3.4.3	Choice of Scoring Protocol.....	67
4	Immunohistochemical Profiling of Liposarcoma.....	80
4.1	Aims.....	80
4.2	Cytogenetic Results in Liposarcomas.....	80
4.2.1	Correlation between <i>MDM2</i> Amplification and Over-Expression.....	81

4.3	Subtype – Specific Expression Profile of Liposarcomas	81
4.3.1	Well-Differentiated Liposarcomas	82
4.3.2	De-Differentiated Liposarcomas	82
4.3.3	Myxoid - Round Cell Liposarcomas	83
4.3.4	All Liposarcoma Subtypes	83
4.4	Analysis of Results and Discussion	83
4.4.1	Discrepancies between Histological and Molecular Diagnostic Features	84
4.4.2	MDM2 Amplification to Overexpression	85
4.4.3	MDM / P53 Expression Profiles	86
5	Genetic Analysis of P53	102
5.1	Aims	102
5.2	DNA Extraction	102
5.3	Polymerase Chain Reaction	102
5.4	Somatic Mutations of P53	103
5.5	<i>P53</i> Arg72Pro Polymorphism - rs1042522	103
5.6	Analysis of Results and Discussion	104
5.6.1	Phenotypical Consequences of the Detected <i>P53</i> Somatic Mutations	104
5.6.2	Significance of <i>P53</i> Arg72Pro Polymorphism	106
5.6.3	<i>P53</i> Mutations in Relation to the Protein Expression Profiles	107
6	Other Soft Tissue Sarcomas and Benign Tumours	121
6.1	Aim	121
6.2	Cytogenetics	121
6.3	Immunohistochemistry	121
6.4	Discussion	122
6.4.1	Cytogenetic Results	122
6.4.2	Immunohistochemistry Results	122
7	General Discussion	125

7.1	Significance of the Study	125
7.1.1	Role in Diagnostics	126
7.1.2	Role in Therapeutic Applications	126
7.2	Limitations of the Study	127
7.3	Future Perspectives.....	128
I-	References	130
II-	List of Abbreviations	150
III-	Appendices	155
	1- Ethical Approval Letter and Leeds Teaching Hospital Trust Research and Development Approval	156
	2- Participant Information Sheet and Consent Form.....	163
	3-Full Cohort of Study Participants	169

List of Figures

Figure 1.1: P53 primary structure and frequency of somatic missense mutations in different cancers	24
Figure 1.2: MDM2 and MDMX protein structures.....	25
Figure 1.3: MDM2 splice variants	26
Figure 1.4: MDMX-S splice variant.....	27
Figure 3.1: MDM2 and MDMX positive and negative cell line controls.....	69
Figure 3.2: P53 cell line controls	70
Figure 3.3: Immunohistochemistry tissue controls	71
Figure 3.4: Intrinsic controls	72
Figure 3.5: ICC for MDM2 in different phases of the cell cycle	73
Figure 3.6: ICC for MDMX in different phases of the cell cycle.	74
Figure 3.7: Protein quantification in cell lysates.....	75
Figure 3.8: Western blot images for MDM2	76
Figure 3.9: Western blot images for MDMX and P53.....	77
Figure 3.10: Antigen retrieval examples for MDM2	79
Figure 4.1: Examples of characteristic cytogenetic alterations in liposarcomas.....	97
Figure 4.2: Subtype-specific expression levels of MDM2; MDMX; and P53	98
Figure 4.3: Co-expression patterns of MDM proteins in different subtypes of liposarcomas	99
Figure 4.4: Immunohistochemistry patterns for MDM2, MDMX and P53	100
Figure 4.5: P53 expression in relation to the Log ₂ (MDM2/MDMX) scores in liposarcomas	101
Figure 5.1: Agarose gel confirmation of genomic DNA extraction	110
Figure 5.2: Agarose gel electrophoresis of PCR products for <i>P53</i> exon 5	111
Figure 5.3: Agarose gel electrophoresis of post PCR purification products for <i>P53</i> exon 4..	112
Figure 5.4: Electropherogram of sequence surrounding codon 46 demonstrating Ser46Phe	113
Figure 5.5: Electropherogram of sequence surrounding codon 131 demonstrating Asn131Ser	114
Figure 5.6: Electropherogram of sequence surrounding codon 171 demonstrating Glu171Lys	115
Figure 5.7: Electropherogram of sequence surrounding codon 184 demonstrating Asp184Asn	116

Figure 5.8: Electropherogram of sequence surrounding codon 292 demonstrating frame shift Lys292	117
Figure 5.9: Electropherogram of sequence surrounding codon 257 demonstrating Leu257Gln	118
Figure 5.10: Electropherogram of sequence surrounding codon 72 demonstrating Arg72Pro polymorphism	119
Figure 5.11: P53 structure and detected mutations.....	120
Figure 6.1: P53 expression in relation to Log ₂ (MDM2/MDMX) scores in other STS and benign cases.....	124

List of Tables

Table 1.1: Key histological and molecular features of LS subtypes.....	23
Table 2.1: Characteristics of the retrospective patients cohort.....	53
Table 2.2: Characteristics of the prospective patients cohort.....	54
Table 2.3: Cell cycle arrest reagents	55
Table 2.4: Primary antibodies used in the study	56
Table 2.5: Details of primers used in the study	57
Table 3.1: Characteristics of the analysed cell lines	68
Table 4.1: Summary of the cytogenetic results for the liposarcoma cohort.....	90
Table 4.2: Contingency table of <i>MDM2</i> amplification and <i>MDM2</i> over-expression.....	91
Table 4.3: Stratified score summary of the analysed cohort.....	92
Table 4.4: FISH and IHC as diagnostic tools for WDLS and DDLS.....	93
Table 4.5: Characteristic features of liposarcomas with inconsistent FISH analysis	94
Table 4.6: Immunophenotype of liposarcomas in relation to their anatomical location	96
Table 5.1: Summary of <i>P53</i> somatic mutations in the analysed cohort.....	108
Table 5.2: Characteristics of <i>P53</i> mutant cases in the analysed cohort	109

1 Introduction

1.1 Soft Tissue Sarcoma

Soft Tissue Sarcomas (STSs) represent an heterogeneous group of mesenchymal tumours from various tissues of origin, which display a spectrum of distributions across age groups. These relatively rare tumours account for 1% of all cancers in adults (1), with an estimated UK incidence of 3000 cases per year according to the database of Sarcoma UK and the National Cancer Intelligence Network (NCIN) (2).

STS can arise at nearly any anatomical location. Their presentation and clinical behaviour depend largely on the type, site, size and the organs involved or in close proximity to the tumour.

STSs are morphologically classified into 21 major types and 104 categorical subtypes according to the World Health Organisation (WHO) classification agreed in 2006 (3). Such classification may be confusing to many clinicians and may also fail to truly reflect their clinical behaviour, prognosis, molecular changes or response to therapy. Additionally, histological features can be deceptive and frequently very challenging for pathologists to base an accurate diagnosis upon. Unfortunately, traditional immunohistochemical markers of differentiation may be of little use in refining the diagnosis.

In more recent years, a different approach to STS classification has attracted increasing popularity (4). This classification is based on the molecular and genetic alterations associated with sarcomas. It is mainly separated into two distinct categories: (1) STS with specific genetic alterations; and (2) STS displaying multiple, complex karyotypic abnormalities (5). This approach has provided a refreshing insight into the molecular mechanisms of sarcoma pathogenesis and has illustrated new relationships between different subtypes of STSs. Moreover, with the rise of non-traditional, targeted therapies for cancers in general and for sarcomas in particular, such classification may provide a more meaningful toolkit towards guiding a selective therapeutic approach. This methodology has influenced the most recent WHO classification of STSs, which was published in 2013 (6). The

new classification has incorporated some of the molecular and cytogenetic alterations as identifiable characteristic features. However, the traditional classification remains largely as the dominant approach (7).

The mainstay of treatment for the majority of localized STSs is radical surgical excision with adequate, generous, excision margins (8, 9). The use of adjuvant radiotherapy is adopted in intermediate and high grade tumours, or when complete excision is not feasible (10). The recurrence rate of STS is variable but is largely dependent on the surgical resection margin status (8, 11). Recurrences are therefore low in sites where a wide compartmental excision is possible. However, in sites such as the retroperitoneum, obtaining a clear margin (particularly, the posterior margin) is difficult due to the anatomical constraints (12). In such instances the recurrence rates are significantly higher. Other factors influencing recurrence rates include histological subtype, use of adjuvant radiotherapy, and tumour size and grade. Recurrence rates may range between 5 – 75% depending on these factors and the level of expertise in the treating centre (13).

It is estimated that half of all intermediate and high grade STSs in the UK develop metastatic disease eventually (2, 8). Patients with locally advanced and / or metastatic STS disease have few effective treatment options. Chemotherapy has an unproven role in the neo-adjuvant setting but is used in advanced, inoperable and recurrent cases, but with no convincing evidence of significant improvement in survival rates (14).

The overall five-year survival of STS is approximately 60%. This has remained unchanged over the past 15 years (15).

1.2 Liposarcoma

Liposarcoma (LS) is a malignant neoplasm of the adipose tissue. It is the most common STS in adult life, accounting for approximately 20% of cases (16). The NCIN reported 6370 new LS cases in England between 1985 and 2009 with an age standardised incidence rate of 6 per million population in the year 2009 (2). LS mainly presents after the age of 50 with a slightly higher incidence in males (17).

LS usually arise from deep-seated and well-vascularised structures rather than from submucosae or subcutaneous fat (18). Like most types of STS, LS may present in almost any anatomical location. However, in comparison to other STSs, they have a relative predilection for the trunk and the retroperitoneum (16).

LSs present clinically as slow growing, asymptomatic soft tumours that eventually cause symptoms from gradual pressure on neighbouring organs. Therefore, they usually have a much delayed presentation, especially when they arise in anatomical cavities, partly due to the lack of striking presenting symptoms but also due to lack of awareness of this diagnosis amongst General Practitioners.

In general, LS has a favourable prognosis compared with the other types of STSs with a median survival of 40 months (19). However, all STSs, including LS, presenting in the trunk and retroperitoneum have a poorer prognosis with a median survival of 21 months and a five year survival of 22.5% (19). This may largely be explained by the limitations in achieving satisfactory clear surgical resection margins.

1.2.1 Liposarcoma Subtypes

LSs are morphologically classified into four main subgroups: well-differentiated (WDLS); de-differentiated (DDL); myxoid - round cell (MXLS-RCLS); and pleomorphic (PLS). These major subtypes are not only histologically distinct but they also have distinctive cytogenetic and molecular signatures. Consequently, they demonstrate different clinical behaviours and prognosis.

1.2.2 Well-Differentiated Liposarcoma

Accounting for 40% of cases, WDLS is the most common subtype of LS (6, 20). It is also known as an “atypical lipomatous tumour” when it presents in a relatively superficial tissue plane. These tumours look deceptively similar to benign lipomas and the distinction between the two can frequently be challenging for pathologists. They demonstrate a characteristic feature of scattered lipoblasts with atypical hyperchromatic nuclei of variable sizes and shapes (6).

WDLS is considered as a low grade neoplasm. It rarely metastasises and has a low recurrence rate given adequate excision. However, it is known to be resistant to conventional chemotherapy (21).

1.2.2.1 De-Differentiated Liposarcoma

Morphologically, DDLS has cellular features similar to WDLS, with associated features of non-lipogenic sarcoma of high or low grade. The presence of a transition from WDLS to DDLS is used as a histological diagnostic feature (22). Clinically, DDLS is a more aggressive tumour compared to WDLS, with a higher tendency to arise in the retroperitoneum and to proliferate rapidly (18). The recurrence rates of DDLS in the retroperitoneum approach 75%, the metastatic rate is 10-20% and overall 5 year mortality is 50-75% (14). Similar to WDLS, DDLS are also resistant to chemotherapy (21).

1.2.2.2 Myxoid - Round Cell Liposarcoma

MXLS is the second most common subtype of LS accounting for a third of cases. Histologically, MXLS features an abundance of extracellular matrix, with the presence of spindle or ovoid cells. Signet ring lipoblasts and “chicken-wire” vascular arcades are pathognomonic. RCLS de-differentiation produces a similar appearance but with areas of greater cellularity (23).

These tumours are usually smaller in size but are more aggressive, with a higher metastatic rate (17%). 65% of these metastases occur in the skeleton with a 15% 5 year survival from time of first metastasis (24). MXLSs without the de-differentiated RCLS component are particularly radiosensitive in both the adjuvant and the neo-adjuvant settings (25).

1.2.2.3 Pleomorphic Liposarcoma

Accounting for 5% of LS, PLS is the rarest and most aggressive subtype. It has a tendency to arise from deep structures within the lower or upper extremities (26). The histological appearance of PLS is of high grade aggressive sarcoma showing disorderly growth patterns, extreme cellularity and bizarre giant cells. They are frequently identified by the presence of distinctive lipoblasts having multiple, small, intra-cytoplasmic fat vacuoles (27).

Approximately 45% of cases return with local recurrence and /or metastasis within 3 years of initial surgical treatment. The 5 year mortality rate is 50% in focal, non-metastatic disease at time of diagnosis (28).

1.2.3 Molecular Classification of Liposarcomas

Gene expression profiling of LS has introduced a new integral methodology into the WHO classification (29). Based on this classification, LS can generally be clustered into three main groups: LS with amplification of chromosomal regions; LS with specific chromosomal translocation(s); and LS with complex genetic alterations.

1.2.3.1 Liposarcomas with Gene Amplification

The presence of supernumerary ring or giant rod chromosomes is a characteristic feature of WDLS and DDLS. These chromosomes contain amplified segments from the 12q13-15 region (30-32).

The presence of amplified chromosomal segments can be detected by fluorescence *in situ* hybridisation (FISH) and comparative genomic hybridisation (CGH) (31). Consequently, analysing LS by FISH has become a standard routine diagnostic procedure. The Pathology Department at Leeds Teaching Hospitals NHS Trust (LTHT) has incorporated this analysis into its diagnostic protocols since 2009.

Research has identified various oncogenes encoded in this amplified region including *MDM2*, *CDK4*, *HMGA2* and *TSPAN31*. *MDM2* “the murine double minute 2” is a negative regulator of the tumour suppressor P53. It is amplified in nearly 100% of WDLS and DDLS and *CDK4* is amplified in 90% of these subtypes. Co-amplification of *MDM2* and *CDK4* is well reported (33).

Whereas FISH analysis has proved to be a valuable diagnostic tool to differentiate between WD/DDLS and benign lipomatous tumours, with high sensitivity and specificity, it does not distinguish WDLS from DDLS (20, 34).

1.2.3.2 Liposarcomas with Chromosomal Translocations

MXLS - RCLS are characterised by the recurrent translocation of the *FUS* and *CHOP* (also known as *DDIT3*) genes resulting in a t(12;16)(q13;p11) rearrangement in 95% of cases (35). A less common translocation between the *CHOP* and *EWS* genes resulting in a t(12;22)(q13;p12) rearrangement has also been reported (36). A significant body of evidence suggests that these translocations are the primary oncogenic event in MXLS-RCLS, as these tumours otherwise frequently retain a relatively normal karyotype.

1.2.3.3 Liposarcomas with Complex Genetic Alterations

PLS are reported to display an array of complex genomic imbalances, including multiple chromosome duplications, deletions and complex rearrangements, polyploidy and intercellular heterogeneity. These cytogenetic alterations more closely resemble those of other pleomorphic sarcomas than those of other subtypes of LS. However, due to the rarity of the disease, descriptive molecular studies of this subtype are confined to a limited number of cases (37).

The characteristic histological and molecular features of LS subtypes are summarised in Table 1.1.

1.3 P53

The P53 protein was first described as a transformation-related protein in chemically-induced sarcomas and other murine cancers, in 1979 (38). *P53* was initially thought to possess weak oncogenic activity, due to an initial misconception of its mutant profile as wild type (wt). It was not until 10 years later that researchers identified the actual wt sequence of *P53* and started to describe its significant spectrum of mutations in human cancers (39).

P53 knockout mouse experiments in the 1990s provided unquestionable evidence in support of the potent tumour suppressor role of wt *P53* (40). Subsequently, *P53* has become the most common site of known genetic alterations in human cancers (41).

It is known that approximately 50% of cancers have acquired inactivating mutations / deletions of *P53* (42). However, the incidence of *P53* mutations in STS had been reported to

be significantly lower, and previous analyses have estimated that only 17% of LSs have a somatic *P53* mutation (43, 44). In cancers where the wt status of *P53* is retained, its functions are often found to be compromised by other mechanisms. These include nuclear exclusion, interaction with viral proteins or, more frequently, by its main cellular inhibitors such as MDM2 protein (45).

Germline autosomal dominant mutations of *P53* are the molecular basis of the earlier-described familial cancer syndrome, currently known as Li-Fraumeni syndrome (46, 47). A recent review that utilised the International Agency for Research on Cancer (IARC) database and included 531 independent families or individuals with Li-Fraumeni syndrome has shown that STSs claimed 25% of cancers in these patients at different ages of onset (48).

In addition to its own biochemical functions, *P53* exerts numerous effects through its ability to activate multiple specific target genes. Therefore, *P53* is seen as a key regulator of the cell cycle, apoptosis, DNA repair, development, differentiation, chromosomal segregation and cellular senescence (49).

P53 belongs to a specific protein family that also includes *P63* and *P73*. These proteins are structurally and functionally related. However, *P53* has evolved in higher organisms to prevent carcinogenesis, whereas *P63* and *P73* have well characterised roles in normal cell biology (50).

It is known that non-sarcomatous malignancies with wild type *P53* usually demonstrate a clinical pattern that is more responsive to chemotherapy and radiotherapy (43). This response is not seen in STS, probably due to the lack of targeted therapies against specific pathways of particular significance in their development. The best characterised pathway of this type is the interaction of wild type *P53* with the MDM2 and its homolog “murine double minute X” (MDMX) proteins (51).

1.3.1 *P53* Structure

Human *P53* is mapped to the short arm of chromosome 17 (17p13.1). Encoded by a 20 kb gene, it contains 11 exons and 10 introns (52). Wt *P53* protein is comprised of 393 amino

acids and has a molecular weight of 53 kDa. It is composed of the following three structural and functional domains (Figure 1.1):

N- terminus (residues 1-94): contains an amino-terminal domain at residues 1-42, responsible for transactivation activity and interaction with transcription factors including MDM proteins. It also has a proline-rich region (residues 61-94), which plays a major role in P53 stability, making it more susceptible to degradation mediated by MDM2 if this region is deleted (53).

Acidic central core domain (residues 102-292): This is primarily the sequence-specific DNA binding domain. The majority of P53 missense mutations are located within this domain. In fact, more than 80% of research that described P53 mutations in cancer has focused on residues between 126 and 306 (54).

C-terminus (residues 292-393): This contains a nuclear localisation signal, a tetramerisation domain (residues 324-355), 3 nuclear export signals and a regulatory domain (residues 363-393). The *C*-terminus influences the efficiency of P53 when acting as a transcription factor. Unlike many other transcription factors, P53 has a second DNA binding domain which maps to its *C*-terminus (55).

P53 expresses up to ten different isoforms via alternative promoters, alternative splicing sites and alternative translation initiation sites. Most of these isoforms retain the central core region containing the DNA-binding domain. Recent reports suggest that some of these isoforms may act functionally as P53 antagonists (56, 57). The detailed assessment of P53 isoforms' expression in cancers may provide a better understanding of their roles in tumour formation.

1.3.2 Relevant P53 Functions

Wild type P53 may be activated in response to numerous genotoxic stressors including DNA damage, oncogenic activation, hypoxia, heat shock, viral infection, ultraviolet radiation and cytotoxic drugs (45). It exerts most of its functions through its ability to act as a sequence-specific transcription factor regulating the expression of various target genes to modulate a spectrum of cellular responses. These target genes are functionally diverse and mediate an

array of downstream cellular outcomes including cell-cycle checkpoints, cell survival, apoptosis and other metabolic processes. The extent of these cellular activities is very dynamic and largely dependent on the cell type, the extent of damage and other unidentified parameters (58).

Thirty years of extensive research has identified hundreds of P53 responsive genes. Some of the most extensively characterised of these are: *CDKN1A* and *MIR34A* for cell cycle arrest; *CDKN1A* and *PAI1* for senescence; *PUMA* and *BAX* for apoptosis; and *TIGAR*, *SCO2* and *GLS2* for metabolic processes (59).

An abridged summary of the most relevant pathways is included below. However, comprehensive narrative accounts of P53 functions and pathways can be found in several published reviews (59-61).

1.3.2.1 Cell Cycle Regulation

The ability of P53 to induce cell cycle arrest is pivotal to its tumour suppressor function, as this provides additional time for the cell to repair genomic damage before entering the critical DNA synthesis phase. P53 can induce cell cycle arrest in G1 phase through activating the cyclin- dependent kinase (CDK) inhibitor and / or p21^{waf1/Cip1}, which may be the best known downstream targets of P53 (62). P53 can also induce cell cycle arrest in G2 and S phases via other downstream targets like *GADD45* and *14-3-3δ* (63).

1.3.2.2 Apoptosis

P53 can induce apoptosis in response to severe or irreversible cellular damage. This is mainly achieved via two distinct mechanisms: Intrinsic Pathway where mitochondrial depolarisation takes place activating caspase 9 to induce apoptosis (64); and Extrinsic Pathway where expression of cell death receptors increases and inhibition of production of IAPs (inhibitor of apoptosis proteins) takes place, resulting in activation of caspase 8 and cellular death (65).

It has been shown that loss of P53-dependent apoptosis induces brain cancer in the mouse, confirming the correlation between this particular function of P53 and its ability to suppress malignant transformation (66).

1.3.3 Cellular Regulators of P53

It is not surprising that P53 is heavily regulated by a complex network of cellular proteins, bearing in mind its role in maintaining integrity of the cell and inducing apoptosis. Under normal conditions, wt P53 half-life is limited to minutes and its expression is maintained at low concentrations in a latent, inactive form (61). When cellular stress occurs, increased P53 levels are seen primarily as a result of an increase in its half-life to hours (67).

Numerous different proteins are involved in P53 regulations including HPV16/E6 (68), WT-1 (69), E1B/E4 (70), JNK (71), PIRH2 (72) and PARP1 (73). The regulation takes place on multiple cellular levels including promotion of transcription, post-translational modification and rate of degradation. However, tight control of P53 levels is primarily achieved through ubiquitinylation-mediated proteasomal degradation by its main cellular inhibitor the MDM2 (74). Mammalian cells also express an MDM2 homolog called MDMX (also known as MDM4), which is an equally important regulator of P53. A significant body of evidence suggests that MDMX is a negative regulator of P53, independent of MDM2 (75).

Details of the regulatory interactions between P53, MDM2 and MDMX are discussed in Section 1.5 of this Chapter. The functional regulators of P53 have been comprehensively reviewed in recent publications (57, 76).

1.4 MDM2 and MDMX

1.4.1 Gene Amplification and Overexpression

The human MDM2 and MDMX genes have been mapped to the chromosomal locations 12q13-14 and 1q32, respectively (77, 78). *MDM2* contains 12 exons and *MDMX* has 11. Whereas *MDM2* amplification has been accepted as a characteristic feature in nearly 100% of WDLD / DDLS (79), *MDMX* amplification has been reported in only 17% of human LS (80).

Recent studies have also reported *MDMX* co-amplification with *MDM2* in STS, and particularly in LS (81, 82). In addition to LS, amplification of *MDM2* or *MDMX* has also been noted in other tumours including glioblastoma (83), cutaneous melanoma (84), osteosarcoma (81), oesophageal (85), colorectal (86) and breast cancer (87).

Overexpression may or may not occur in conjunction with amplification of these genes (80, 88). *MDM2* overexpression was detected in approximately 75% of WDLS / DDLS subtypes by immunohistochemistry (89, 90). High levels of *MDM2* mRNA have been reported as a negative prognostic factor in STS, including liposarcomas (91). It may be of particular significance to the studies described herein that the phenomenon of *MDM2*-mediated P53 inactivation has a tendency to occur more often in retroperitoneal LS, compared to those that arise in the extremities (34).

Work on established cancer cell lines has shown that the incidence of *MDMX* overexpression is variable amongst different types of human cancers and seems to occur in between 20-40% of tumours, including STS (80, 92, 93). Overexpression of *MDMX* was also reported without either *P53* mutations or *MDM2* amplification, in glioblastomas (94). This observation supported the suggestion of an independent role for *MDMX* in the transformation process. It has been noted that the overexpression of *MDM2* and / or *MDMX* in tumour cells generally correlates with retained wild type P53 (93, 95).

1.4.2 Protein Structure

The *MDM2* and *MDMX* proteins share striking structural similarities. Their full length proteins are comprised of 491 and 490 amino acid residues, respectively (78). They have a similar predicted molecular weight of 56 kDa, with several conserved structural domains (Figure 1.2) including:

N-terminal hydrophobic pocket: Both *MDM2* and *MDMX* bind to P53 through this domain. There is approximately 50% amino acid sequence identity between the two *MDM* proteins in this domain (96). However, the small structural differences between the two proteins in this region have important implications for the design of blocking antagonists to prevent *MDM* / P53 interactions. DNA damage induces phosphorylation at the *N*-termini of both

MDM2 and MDMX, by damage-activated kinases, and is reported to disrupt MDM binding to P53 *in vitro* (97, 98).

Central acidic domain: This region contains nuclear export and import signals, which are vital for proper nuclear-cytoplasmic trafficking of MDM2. Phosphorylation of this domain is again important for the regulation of function for both proteins.

C-terminal domain: The C-termini of MDM2 and MDMX have a rare C2H2C4 protein - protein binding domain which consists of two RING domains (Really Interesting New Gene), while one of the RING domains has the classical 4 cysteine structure (C4), the other consists of 2 histidine and 2 cysteine residues binding the zinc atom (99). This RING domain is critical for the binding of the MDM2 / MDMX heterodimers to P53 leading to subsequent ubiquitinylation and degradation. Despite conservation of the RING domain in MDMX, it apparently lacks an intrinsic ubiquitin ligase activity towards P53 (100).

1.4.3 Intracellular Localisation

MDM2 is primarily a nuclear protein. However, many cell-line studies have reported abundant expression in the cytoplasm, suggesting cytoplasmic localisation might also be important for its function. This observation is not unexpected due to the presence of a nuclear export domain in MDM2, which has been reported to enhance P53 translocation from the nucleus to the cytoplasm, with MDMX possibly modulating this process (101).

Since MDM2-mediated proteasomal degradation of P53 occurs in the cytoplasm, the ability of MDM2 to move to the cytoplasm may therefore be important in MDM2-mediated P53 turnover (102).

The intracellular localisation of MDMX varies between different cell lines, with some studies showing predominantly cytoplasmic localisation (103, 104). However, MDMX is translocated into the nucleus upon co-expression of MDM2 or P53 (104-106). Therefore, MDMX may depend on MDM2 for nuclear redistribution in order to deactivate P53.

The cellular localisation of P53 is equally dynamic and correlates with many variables including cell cycle phase, mutational status, cancer cell type and interaction with other

proteins (107, 108). Uncontrolled cellular division due to loss of P53 functions is generally seen in cells with P53 localised predominantly in the cytoplasm.

1.4.4 Splice Variants

Multiple MDM2 and MDMX splice variants have been reported in the literature. Only the functional and the most common variants are discussed below.

1.4.4.1 MDM2 Splice Variants

Over 40 splice variants of MDM2 have been identified in both tumours and normal tissues (109, 110). In humans, MDM2-A and MDM2-B are the most common and potentially functional splice variants of MDM2. They were first identified in paediatric rhabdomyosarcomas in 2002 (111). However, the exact function(s) of these variants remain somewhat controversial and not yet fully understood (112).

MDM2-A and MDM2-B are missing exons 4-9 and 4-11, respectively, from the full length MDM2 RNA. Consequently, their resulting protein isoforms lack the P53 binding domain (Figure 1.3). However, MDM2-A retains the central acidic and the carboxy-terminal RING finger domains, the latter being important for binding with other proteins as well as ubiquitinyllating P53.

Previous data suggested that both MDM2-A and MDM2-B isoforms interacted with full length MDM2 to sequester it in the cytoplasm, away from P53 (113). Therefore they may act like MDM2 inhibitors, blocking its anti-P53 activity (114). However, these data are not consistent with the frequent expression of these splice variants found in various tumours (115).

Mdm2-A transgenic mouse models have been created to examine the effects of this isoform on P53 functions. P53-dependent death *in-utero* was observed in the Mdm2-A homozygous group. Growth inhibition, enhanced senescence and accelerated aging were demonstrated in the Mdm2-A heterozygous group, with some of these effects occurring in a P53-dependent manner (112). These findings could indicate that Mdm2-A expression may

protect against cancer formation through enhanced P53 activity. However, further studies are needed to clarify the exact physiological effects of MDM2-A in human cells.

More recent studies have described the MDM2-C splice variant as a functional oncogenic protein that is over-expressed in some human cancers (116). MDM2-C lacks amino acid residues corresponding to exon 5 through 9, which include part of the P53 binding domain and hence its functions may be P53-independent.

1.4.4.2 MDMX Splice Variants

Numerous splice variants of MDMX have been identified in a variety of murine and human tumour cell lines (117). The most extensively described of these is MDMX-S, characterised by loss of exon 6, which results in a frame shift and incorporation of 26 unique amino acids followed by a premature stop codon (see Figure 1.4). MDMX-S is the commonest splice variant in STS, detected in 14% of cases (80). A recent study has proposed that the MDMX-S/MDMX ratio positively correlates with early metastasis and poor prognosis (118). Other functional MDMX splice variants have been described including MDMX-A, characterised by loss of exon 9 sequences encoding the acidic domain and MDMX-G, which lacks the P53 binding domain (119).

In contrast to MDM2, a major proportion of MDMX splice variants described in the literature are functional and may even be more effective than full length MDMX in inhibiting P53-mediated induction of apoptosis (117, 119). An MDMX-L isoform with 18 amino acid *N*-terminal extension has been reported as a potent promoter of P53 degradation. This isoform is induced by P53 itself under specific circumstances (120).

1.4.5 Relevant Single Nucleotide Polymorphisms

Perhaps the most relevant P53 single nucleotide polymorphism (SNP) reported in STS is the replacement of arginine by proline at codon 72 (Arg72Pro, rs1042522). This polymorphism occurs in the proline-rich domain of P53 resulting in decreased apoptotic potential (121) and increased susceptibility to degradation by MDM2 (122). Interestingly, a recent report analysing 174 STS cases has reported the over-representation of Pro72 occurred mainly in LS

patients and particularly those with WDLS (>60%). The same study reported *P53* mutations in only 6% of these cases (123).

An *MDM2* polymorphism, rs2279744, changes a base from *T* to *G* at position 309 in the *MDM2* promoter resulting in higher levels of *MDM2* RNA and protein, consequently attenuating *P53* pathways both *in vitro* and *in vivo*. Homozygosity of the *G* allele is strongly associated with *MDM2* amplification and is frequently seen in LS (81).

No *MDMX* polymorphisms have been reported to be important in either the occurrence or progression of STS. However, a polymorphism replacing *A* with *C* at the 3'-untranslated region (3'-UTR) of *MDMX*, rs4245739, may contribute to breast cancer susceptibility (124) and may have a prognostic role in other cancers including ovarian and retinoblastoma (125).

1.5 P53 / MDM Interactions

The *P53* / *MDM* interactions are complex and multi-layered. Below is a brief summary of the most relevant of these interactions in the context of this study.

1.5.1 Molecular Basis of the Interaction

MDM2 and *P53* regulate each other's functions through an auto-regulatory feedback loop. When activated, *P53* transcribes the *MDM2* gene and, in turn, the *MDM2* protein inhibits *P53* activity (126). This inhibition is achieved by various mechanisms, but mainly through *MDM2* binding to *P53*, shielding its *N*-terminus from recruitment of transcriptional activators (127), or by *MDM2* acting as an ubiquitin E3 ligase targeting *P53* for proteasomal degradation (128). Whereas activated *P53* was thought to exclusively upregulate *MDM2* (128), recent data has also shown a *P53*-dependent increase in *MDMX-L* expression under specific cellular conditions (120).

Similar to *MDM2*, *MDMX* binding to *P53* occludes the *N*-terminal alpha helix of *P53*, which is essential for the recruitment of transcriptional co-activators. Therefore, this binding inhibits *P53* transactivation functions (76). Generally, chains of poly-ubiquitylation are needed to initiate protein degradation, whereas mono-ubiquitylation modulates target protein

function. The MDM axis interactions with P53 are not an exception. In certain circumstances, mono-ubiquitylation of P53 by MDM2 has been reported to modulate the function of p53, affecting transcription, DNA repair and its intracellular localisation (129-131).

In contrast to MDM2, MDMX alone does not mono-ubiquitylate P53. Several study models have suggested that MDM2 / MDMX hetero-dimers recruit E2 ubiquitin-conjugating enzymes resulting in a more potent complex for P53 degradation when compared to MDM2 homodimers (132, 133). No MDMX homodimers have been identified *in vitro* or *in vivo*, which may suggest that MDMX is monomeric (96).

MDM2 and MDMX regulate one another through a series of dynamic interactions. MDM2 has the ability to ubiquitylate itself and MDMX in order to maintain the negative feedback loop (119, 134). However, this function may be limited and becomes futile beyond a certain threshold of activity (135). On the other hand, MDMX enhances the effect of MDM2 by increasing its relatively short cellular half-life and therefore promoting P53 degradation (136). Other studies, however, have suggested that MDMX may stabilise P53 and, in fact, antagonise the MDM2-targeted degradation of P53 (106, 137).

It appears that the cellular levels of MDM2 and MDMX relative to one another, play an important role in their vibrant interactions. One report suggested that MDMX promotes MDM2 auto-ubiquitylation when the latter exceeds a certain threshold of cellular abundance (100). The mutual dependence model described by Gu *et al.*, in modified cell lines, suggested that the actual cellular functions of MDMX vary between activation and inhibition of MDM2, depending on their relative expression levels (105). This model may have provided an explanation for some of the controversies surrounding MDMX function in cell lines, in a relatively coherent manner. However, it lacks support from careful descriptive studies performed on actual human cancer tissue.

Overall, the literature demonstrates that MDM2 and MDMX are proteins that compete with each other in complex patterns to bind to P53 in a process designed to maintain the critical correct level of P53 activity (138, 139). MDMX expression by cells is vital for efficient MDM2-mediated P53 degradation (140). However, the co-expression of MDMX has to be finely tuned in order to optimise this crucial function of MDM2.

1.5.1.1 Fine Tuning of the Interactions

Additional layers of post-transcriptional modifications of MDM proteins have also been reported as fine tuning modulators of their interactions. For example, phosphorylation of MDM2 at Ser166 and Ser186 (141), and MDMX at Ser 367 (142) can lead to their stabilisation and therefore inhibition of P53. In response to genetic stress, DNA-dependent protein kinase (DNA-PK) phosphorylates Ser17 of MDM2 (97) and ABL phosphorylates Tyr99 of MDMX (98) leading to dissociation of P53 from its negative regulators.

The complex series of interactions between P53 and the MDM axis, also involves active participation of other proteins that regulate these pathways. Collectively, these interactions are responsible for maintaining the balance between cell viability and apoptosis. Although these interactions have been the focus of many studies, there continues to be a need for more research effort to fully understand the details of the mechanisms involved. Perhaps the most relevant of these interactions is that involving the Alternative Reading Frame protein (ARF) (143). ARF interacts with MDM2, blocking the shuttling of MDM2 between the nucleus and the cytoplasm, by sequestering it in the nucleolus. In effect, this prevents MDM2-mediated P53 degradation and so results in activation of P53 (144). ARF also promotes MDM2 ubiquitinylation of MDMX (135). On the other hand, overexpression of RAS proteins has been reported to upregulate both MDM2 and MDMX, leading to P53 inhibition (145, 146).

It is important to mention that both MDM proteins have been reported to have P53-independent oncogenic activities through interacting with other downstream targets (147). For example, MDM2 inhibits the potent tumour suppressor retinoblastoma protein (RB) (148) and promotes proliferation through the formation of complexes with the transcriptional activators E2F/DP1, resulting in DNA synthesis (149). This may explain the reported cellular overexpression of MDM2 and MDMX in tumours that have a mutant P53 profile. In turn, it may also explain the selection of mut P53 (and not only the wt P53) tumours for deregulation of MDM pathways.

1.5.2 Animal Models

In vivo experiments have convincingly proven the importance of P53 / MDM axis interactions to maintain life. Mouse models lacking functional *Mdm2* do not survive embryogenesis, but can be completely rescued by the elimination of P53 activity (150, 151), with similar observations noted in *MdmX* null mice (152). Neither *Mdm2* nor *MdmX* loss could be compensated for by the presence of the other. This demonstrates that both proteins work collectively on the balance of P53 activity, but possibly via independent mechanisms.

The synergistic affiliation of MDM2 and MDMX in inhibiting P53 was also observed during CNS development, in mouse models. Loss of *Mdm2* activity in the CNS resulted in hydranencephaly at embryonic day 12, whereas *MdmX* deletion resulted in pronencephaly at embryonic day 17. Much earlier and more severe CNS phenotypes were seen when both *Mdm2* and *MdmX* were deleted and all these phenotypes were rescued by associated deletion of *P53*.

Other animal studies have also confirmed the critical role of the C-terminal RING domain of MDM2 and MDMX in inhibiting P53. Point mutation in *MdmX* disturbing its RING domain and its *Mdm2* binding site for forming heterodimers was embryonically lethal in a P53-dependent manner (153). Similar observations were found with matching *Mdm2* point mutations (154). Collectively, these observations confirmed the vital interactions between the two MDM proteins to maintain a viable level of P53 activity. The regulatory effects of important phosphorylation sites in MDM2 to stabilise P53 in response to DNA damage were confirmed in mice models, bearing altered *Mdm2* alleles. Substituting Serine by Alanine at the *Mdm2* 394 residue (S394A), prevented phosphorylation and consequently resulted in accelerated tumour formation (155).

1.5.3 The Gaps in Current Knowledge

Quantitative studies have proven that the relative nuclear abundance of MDM proteins in relation to P53 correlated with limiting P53 activity in culture-grown cells (51). However, only a few studies have described the simultaneous expression levels of MDM2 and MDMX proteins in cancer cells, their expression levels relative to each other and the possible

effects of this on P53 (87, 105). Furthermore, these studies were limited to cell lines and may not be applicable to actual cancer tissues. Such characterisation is pivotal to clarify the putative utility of novel, single and dual affinity MDM2/MDMX blocking compounds in the treatment of STS and other cancers.

1.6 Potential Novel Therapeutic Strategies

As approximately 50% of tumours retain a wt P53 that is presumed to be inhibited by interacting with MDM proteins, it is expected that targeting this interaction would be an attractive approach towards selective cancer treatment. However, as both MDM2 and MDMX are required for normal tissue functions, it is clearly challenging to provide maximal therapeutic benefit with minimal mechanism-based toxicity. In other words, the therapeutic index may be a narrow one. Targeting the P53-MDM interaction may be achieved in different ways including modulating MDM protein expression and targeting E3 ubiquitin ligase activity. However, the most promising and widely explored approach has been through inhibiting the various protein-protein interactions using selective antagonists.

1.6.1 MDM2 Blockers

Since the discovery of MDM2 and the recognition of its cellular functions, large libraries of small molecules have been screened using high throughput techniques in the search for targeted blockers. In addition, structure-based molecular design methods have been employed to yield three major groups of P53-MDM2 interaction inhibitors. These groups are: the Nutlins (156); the Benzodiazepinediones (157); and the Spiro-oxindoles (158).

These sets of compounds bind to MDM2 with high affinity, disrupting the P53-MDM2 interaction to re-establish wt P53 activity. Of these compounds the activity of Nutlin-3a is the best defined and studied.

In vivo experiments with Nutlin-3a, have demonstrated selective activity against tumours that over-express MDM2 and retain wt P53, with very encouraging results (159).

Furthermore, several studies have suggested that rational combinations of Nutlin-3a with other chemotherapeutic agents may potentiate their effects and perhaps protect normal cells from cytostatic agents (160).

The other most promising MDM2 antagonist compound, from the Spiro-oxindole family, is MI-219. MI-219 has a superior pharmacokinetic profile compared to Nutlin-3a. Both compounds have not shown visible toxicity in related animal studies (161, 162).

Two orally active MDM antagonists have recently entered phase I clinical trials, RG7112 (a second generation of Nutlin-3a) from Hoffmann La Roche (Switzerland) and JNJ-26854165 from Johnson and Johnson (USA). Some proof of mechanism of action, from clinical applications of RG7112 in LS patients, has recently been published, with potentially encouraging prospects (163).

However, due to the low binding affinity of Nutlins to MDMX, they do not appear to disrupt P53-MDMX interactions (164, 165). Therefore, they are not effective in tumours selectively over-expressing MDMX. This observation has led to a search to identify and design compounds that do disrupt P53-MDMX complexes, with either a specific or dual MDM antagonist activity.

1.6.2 MDMX Blockers

The first specific MDMX antagonist compound was identified and characterised in 2010 (166). SJ-172550 has significant affinity for MDMX, binding to it in a reversible manner. This compound has shown significant anti-cancer activity in retinoblastoma cells that over-express MDMX. It also displayed a synergistic apoptotic effect when used with Nutlins. However, later studies have shown that this compound may be unstable *in vivo* and has a complex mechanism of action that involves covalent adduct formation in the P53-binding domain of both MDM2 and MDMX, which hinders its further development (167).

The stabilised α -helix of p53 variant 8 (SAH-p53-8) is a new modified peptide antagonist to MDM2 and MDMX interactions with P53 (168). It has 25 fold greater affinity for MDMX compared to MDM2. Its structural modification has increased its *in vivo* stability and improved its cellular uptake (169). This has introduced an encouraging new approach in drug development as peptides can antagonise protein-protein interaction more efficiently due to their large interaction surfaces.

1.6.3 Dual Affinity Blockers

Computational studies, Ensemble-based virtual screening technologies and phage display techniques have allowed the identification of compounds with comparable dual MDM2 and MDMX affinity (170-175). These studies provided proof-of-concept for the feasibility of joint MDM2 and MDMX blocking, introducing the first generation of dual specificity blocking compounds. Essentially, all MDM blockers have dual-affinity properties to some degree. However, finding an appropriate balance of affinities in a potent “druggable” compound would be a significant result in this area of research.

These compounds have gone through patent review (176) and are progressing swiftly in the pre-clinical development phase to define and optimise their therapeutic properties. However, their activities on cancer tissue have not been reported. Should structure / activity optimisation of these compounds provide lead drugs, then employment of these in clinical trials would be an important novel step in targeted cancer management.

1.6.4 Alternative P53 Activation Approaches

Small molecules that inhibit MDM2 ubiquitin ligase activity have been identified including HLI98 (177) and MEL23, MEL24 (178). These compounds bind to MDM2 and P53, enhance their stability and eventually lead to P53 activation (179). However, these compounds have usually shown p53-independent cytotoxicity, probably by inhibiting other cellular RING domain E3 ubiquitin ligases (95).

Another small molecule compound named RITA (reactivation of p53 and induction of tumour cell apoptosis) has been described, which binds directly to the amino terminal domain of P53 causing conformational changes and dissociation from MDM2 (180). This compound was found to have high toxicity due to its ability to cause protein-DNA crosslinks. However, its utility may be improved in conjunction with other selective therapies like MDM2 blockers (181).

1.7 Aims of the Study

The hypothesis to be tested was that a careful characterisation of MDM2, MDMX and P53 expression profiles in resected LS tumour specimens might reveal distinct relative expression patterns and therefore add to current, cell line-based, understanding of the complex interactions between these proteins in LS tissues. It was anticipated that such insights might also guide the selection of novel blocker compounds, of variable specificities and affinities, in future functional and clinical studies.

The aim of this study was therefore to characterise the simultaneous expression levels of MDM2, MDMX and P53 in human LS tissues. The study examined:

- The different patterns of MDM2 and MDMX expression.
- The effect of their relative expression levels on the cellular levels of P53.
- The genetic make-up (P53 mutation status) of tumours that over-expressed P53 by immunohistochemistry.

Table 1.1: Key histological and molecular features of LS subtypes

Subtype	Histological features	Molecular changes
WDLS	Similar features to benign lipomas but with scattered lipoblasts and atypical hyperchromatic nuclei of variable sizes and shapes	<i>MDM2</i> amplification (nearly 100%) <i>CDK4</i> amplification (90%)
DDLS	Similar to WDLS with progression to components of non-lipogenic sarcoma of high or low grade	<i>MDM2</i> amplification (nearly 100%) <i>CDK4</i> amplification (90%)
MXLS-RCLS	Abundance of extracellular matrix with the presence of spindle or ovoid cells	t(12;16)(q13;p11) (95%) t(12;22)(q13;p12)
PLS	Features of high grade aggressive sarcoma, disorderly growth patterns, extreme cellularity and bizarre giant cells	Complex genomic imbalances

A tabular summary of the key histological and molecular features of different subtypes of liposarcomas. Note the high sensitivity of the integrated molecular changes as an aiding diagnostic tool. WDLS = well-dedifferentiated liposarcoma; DDLS = De-differentiated liposarcoma; MXLS = Myxoid liposarcoma; RCLS = Round cell liposarcoma; PLS = Pleomorphic liposarcoma.

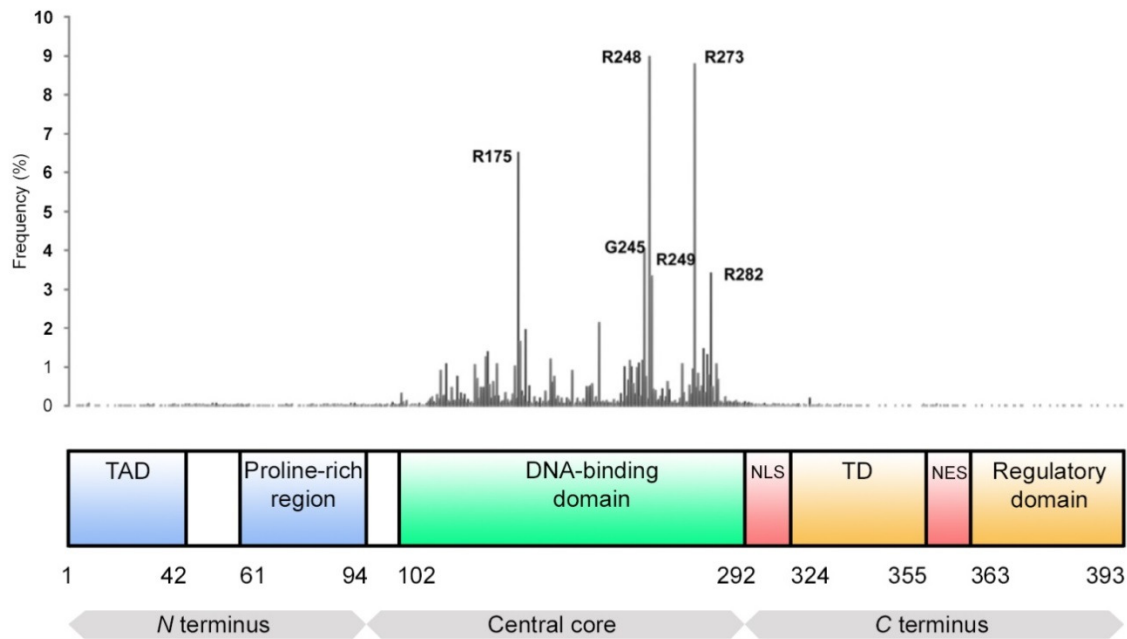


Figure 1.1: P53 primary structure and frequency of somatic missense mutations in different cancers

This is a schematic presentation of P53 structure and its domains. The numbers are for amino acids. The graph shown illustrates the reported missense mutational spectrum in human cancers (n=19,262). Data was obtained from the P53 International Agency for Research on Cancer IARC website (p53.iarc.fr) and plotted as a function of amino acid position. Majority of mutations are located within the DNA-binding core domain. TAD = Transactivation domain; TD = Tetramerisation domain; NES = nuclear export signal; NLS = nuclear localisation signal. Adapted from WA Freed-Pastor *et al.*, 2013 (54).

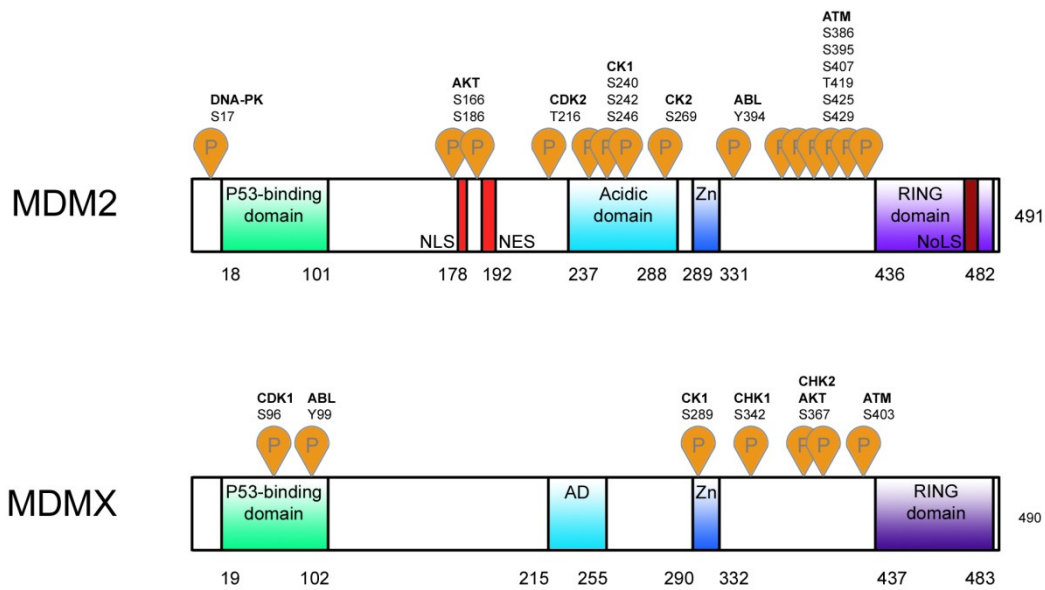


Figure 1.2: MDM2 and MDMX protein structures

This is a schematic presentation of MDM2 and MDMX protein structures showing the common phosphorylation sites (as indicated by P orange signs). The two proteins share structural similarities and are extensively phosphorylated by kinases of different classes. These include damage induced kinases: ATM, CHK1, CHK2, DNA-PK, ABL; and proliferation / survival kinases AKT, CK1, CK2, CDK1, CDK2. NES = nuclear export signal; NLS = nuclear localisation signal; NoLS = nucleolar localisation signal. Adapted from M Wade *et al.*, 2010 (103) with permission from author (Professor G M Wahl).

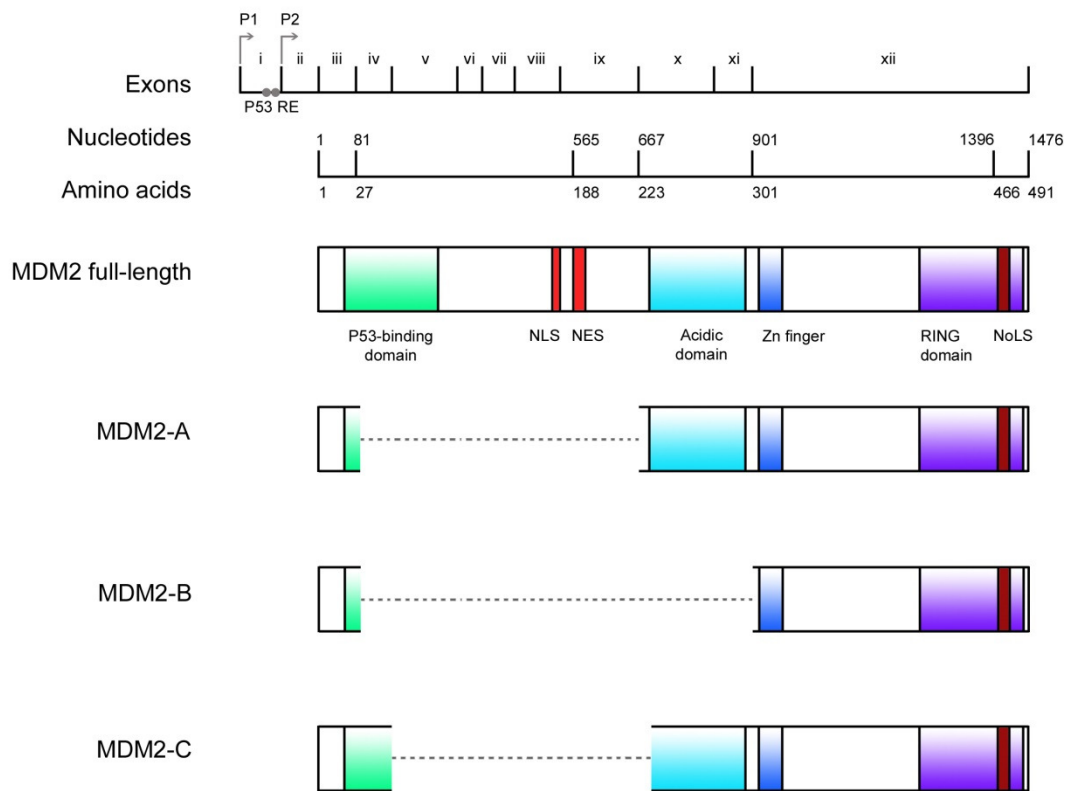


Figure 1.3: MDM2 splice variants

This is a schematic representation of full length MDM2 protein and its common splice variants. P1 and P2 = promoters 1 and 2 respectively; P53 RE = P53 response elements; NES = nuclear export signal; NLS = nuclear localisation signal; NoLS = nucleolar localisation signal. Adapted from K Schuster *et al.*, 2007 (182) with permission from publisher (American Association of Cancer Research).

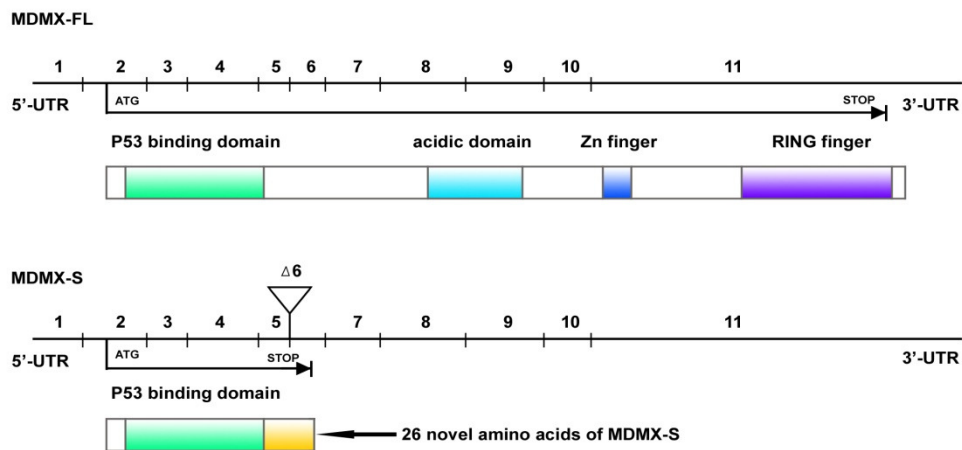


Figure 1.4: MDMX-S splice variant

This is a schematic presentation of full length MDMX and MDMX-S splice variant. MDMX-S consists of the P53-binding domain and 26 unique amino acids that are generated after a shift in the open reading frame due to the loss of exon 6. Adapted from reference F Bartel *et al.*, 2005 (80) with permission from author (Dr F Bartel).

2 Materials and Methods

2.1 Ethical Issues

Ethical approval was applied for by the author. The study was reviewed and approved by the Leeds Central Research Ethics Committee (Reference number 10/H1313/34). The Committee approval permitted the use of archived STSs and other tumours held by the Pathology Department at LTHT. It also allowed prospective collection of fresh tissue from patients at the time of surgical intervention, after obtaining appropriate informed consent. The approval permitted the researcher to perform tissue studies and genetic analysis. This study complied with the Human Tissue Act. This approval was also verified by the LTHT Research and Development Department (Reference number MM10/9511). The ethical approval letter is attached in Appendix 1.

2.2 Patient Cohorts

Two cohorts were created for the study, a retrospective cohort of archival tissues and a prospective cohort of fresh samples from patients presenting to the LTHT for surgical intervention during the 3 year recruitment period of the study.

2.2.1 Retrospective Cohort

Four different sources were explored to identify liposarcoma patients who had presented to the LTHT since the year 2008 and the retrieved data was cross matched to avoid repetition. These sources included: the Sarcoma Specialist Nurse log which was kindly made available by Ms Emma Brown (Sarcoma Specialist Nurse, LTHT); the Electronic Hospital Records at LTHT via the Patient Pathway Manager (PPM) software; the LTHT Pathology Department electronic record; and the LTHT Cytogenetics Department Annual Audit Data, which was kindly provided by Dr Paul Roberts (Head of Cytogenetics Department, LTHT). The PPM system was able to correctly identify 90% of patients as the remaining 10% were inaccurately coded under other STS non-specified subtypes.

The relevant clinical details for the identified cohort were retrieved from the PPM system and occasionally from the historical medical notes, if necessary. All samples were then given serial numbers and anonymised accordingly. In concordance with the ethical conduct requirements of the study, no participant's personal information was kept on record after the initial identification process.

A total number of 64 cases were identified with a median age of 64 years. The cases were of a broad presentation of variants, including sex, anatomical location and histological subtype. The characteristics of the cohort are summarised in Table 2.1 and the full cohort is provided in Appendix 3.

2.2.2 Prospective Cohort

The Sarcoma Multi-Disciplinary Team (MDT) meetings records at LTHT were reviewed regularly to identify potential candidates presenting with STS or large benign lipomas, which required surgical resection. These candidates were first approached in the Out-Patient Department at the time of their surgical consultation and they were given the study information sheet. Candidates were then consented at their subsequent hospital admission for operation. The participant's information sheet and consent form used in the study are attached in Appendix 2.

A total of 16 patients were recruited prospectively in the study. These were comprised of: 11 STS including 7 LS, 3 angiosarcomas and 1 fibroblastic tumour, with a median age of 66 years; and 5 cases of benign tumours with a median age of 45 years. The benign tumours were recruited with either a known benign diagnosis or with a subsequent diagnosis based on histology findings supported by cytogenetic analysis. The characteristics of the prospective cohort are summarised in Table 2.2.

2.3 Materials

2.3.1 Eukaryotic Cell Lines

Three control cell lines were selected for analysis in this study: U2OS and SW-872 were obtained from the American Type Culture Collection (ATCC[®], Manassas, USA, catalogue numbers. HTB-96 and HTB-92, respectively); HT29 was kindly donated by Sarah Perry (Senior Research Technician, Leeds Institute of Biomedical & Clinical Sciences, Wellcome Trust Brenner Building) and was originally obtained from ATCC[®] (catalogue no. HTB-38). When the cells lines were first obtained, multiple stock vials containing the cells were frozen down in liquid nitrogen. Cells that were cultured beyond 25 passages from their first use were discarded and a new vial of frozen cells was thawed and used.

2.3.2 Tissue Culture Reagents

All tissue culture plastics were supplied by Corning Coaster (Buckinghamshire, UK). All solutions and buffers were made up in deionised filtered water, unless otherwise specified. The pH of all buffered solutions was adjusted to its required pH at 25°C.

2.3.2.1 1 x Dulbecco's Phosphate-Buffered Saline (DPBS) (pH 7.0 – 7.2)

500 ml stocks were obtained from Life Technologies, Carlsbad, USA (catalogue no. 14190).

2.3.2.2 Tissue Culture Media

Roswell Park Memorial Institute (RPMI) + GlutaMax™ –I

500 ml stocks were obtained from Invitrogen, Carlsbad, USA (catalogue no. 61870).

Dulbecco's Modified Eagle's Medium (DMEM) + GlutaMax™ –I

500 ml stocks were obtained from Invitrogen, Carlsbad, USA (catalogue no. 31966).

2.3.2.3 Foetal Calf Serum (FCS)

500 ml stock was obtained from Sigma Aldrich, St. Louis, USA (catalogue no. F7524).

2.3.2.4 10 x Trypsin

100 ml stock, obtained from Life Technologies, Carlsbad, USA (catalogue no. 15400-054).

Components of 10 x Trypsin stock are:

Trypsin	0.5% (w/v)
Ethylene di-amine tetra-acetic acid disodium salt (EDTA)	0.9 mM
Sodium chloride (NaCl)	146.5 mM

2.3.3 Cell Cycle Arrest Reagents

2.3.3.1 Cell Cycle Arrest Drugs

Nocodazole, Aphidicolin and Hydroxyurea were individually utilised as cell cycle arrest agents. They were prepared and used according to manufacturer's instructions. Table 2.3 summarises the conditions of use for these agents with a brief description of their mechanisms of action.

2.3.3.2 Dimethyl sulfoxide (DMSO)

500 ml stock was obtained from Sigma Aldrich, St. Louis, USA (catalogue no. D8418).

2.3.4 Immunochemical Staining Reagents

2.3.4.1 1 x Tris-Buffered Saline (TBS) (pH 7.4)

Components of 1 x TBS are:

Sodium chloride	0.15 M
Tris-Hydrochloric acid (Tris-HCl)	0.02 M

1 L of 1 x TBS was made by mixing 60 ml of stock solution of 2.5 M NaCl and 20 ml 1 M Tris-HCl (pH 7.4) in deionised water.

2.3.4.2 Goat Serum in TBS

The desired concentration (v/v) of goat serum in TBS was prepared by adding normal goat serum (Dako, Santa Clara, USA, catalogue no. X0907) to TBS.

2.3.4.3 Citrate Buffer 10 mM (pH 6.0)

Components of Citrate Buffer 10mM are:

Citric acid monohydrate (Prolabo, Radnor, USA, catalogue no. 20275.298)	10 mM
Sodium hydroxide	26 mM

1 L of 10 mM Citrate Buffer was prepared by dissolving the 2.10 g of citric acid monohydrate in deionised water, then adding 13 ml of 2 M sodium hydroxide, under constant pH monitoring using a calibrated pH meter (Mettler-Toledo, model no. MP220). Few drops of 2 M sodium hydroxide may be added to achieve the desired pH before the final volume was set to 1 L.

2.3.4.4 Primary Antibodies

Four primary antibodies were used in the study, these are summarised in Table 2.4.

2.3.4.5 Antibody Diluent

250 ml stock was obtained from Life Technologies, Carlsbad, USA (catalogue no. 00-3118).

2.3.4.6 Primary Antibody Detection Kit

To detect the primary Abs, the NovoLink Max Polymer Detection System was used according to manufacturer's instructions (Leica[®] Microsystems, Newcastle,UK, catalogue no. RE7150). Reagents used in the detection kit are described in the Manufacturer's Manual.

2.3.5 Reagents Used for Preparing Cell Lysates

2.3.5.1 Radioimmunoprecipitation Assay (RIPA) Buffer

100 ml stock was obtained from Thermo Scientific, Waltham, USA (catalogue no. 89900).

Components of RIPA buffers are:

Tris-HCl (pH 7.6)	25 mM
Sodium chloride	150 mM
Sodium deoxycholate	1% (w/v)
Sodium dodecyl sulphate (SDS)	0.1% (w/v)

Nonyl phenoxy polyethoxy ethanol (NP-40) 1% (w/v)

2.3.5.2 Dithiothreitol (DTT)

25 g DTT was obtained from Sigma Aldrich, St. Louis, USA (catalogue no. D0632).

DTT 1 M stock was prepared by dissolving DTT in deionised water. It was stored at -20°C in small aliquots and used when needed to avoid repetitive thawing.

2.3.5.3 Phenylmethanesulfonyl fluoride (PMSF)

5 g PMSF was obtained from Thermo Scientific, Waltham, USA (catalogue no. 36978).

PMSF 10 mM stock was prepared by dissolving PMSF in isopropanol. It was stored at -20°C in small aliquots and used when needed to avoid repetitive thawing.

2.3.5.4 RIPA Buffer Working Solution

Components of RIPA Buffer Working Solution are:

RIPA Buffer	1 ml
Protease Inhibitor Cocktail (Sigma Aldrich, St. Louis, USA, catalogue no. P8340)	1% (v/v)
PMSF	1 mM
DTT	1 mM

2.3.6 Reagents Used for Protein Quantification

2.3.6.1 Bovine Serum Albumin (BSA) Protein Standards

(Novagen, Billerica, USA, catalogue no. 71285) 2 mg/ml

A gradient of BSA protein standards was prepared according to manufacturer's recommendations. Deionised water was used to prepare the following dilutions 0; 25; 125; 250; 500; 750; 1000; 1500; and 2000 µg/ml.

2.3.6.2 Bicinchoninic Acid Assay (BCA) Working Reagent Solution

500 ml stock of BCA Solution was obtained from Novagen, Billerica, USA (catalogue no. 71285).

To make BCA Working Reagent Solution, the following component was added:

4% (w/v) cupric sulphate	2% (v/v)
--------------------------	----------

2.3.7 Reagents for Western Blot

2.3.7.1 4 x NuPage® Lithium Dodecyl Sulphate (LDS) Sample Buffer (pH 8.5)

10 ml stock was obtained from Life Technologies, Carlsbad, USA (catalogue no. NP0007).

Components of 4 x NuPage® LDS Sample Buffer (10 ml) are:

Glycerol	10 % (v/v)
Tris base (pH 8)	424 mM
Tris-hydrochloric acid	564 mM
LDS	2% (w/v)
Ethylene di-amine tetra-acetic acid (EDTA)	0.5 mM
Serva blue G250	1 mM
Phenol red	0.7 mM

2.3.7.2 20 x NuPAGE® MOPS SDS Running Buffer (pH 7.2)

500 ml stock was obtained from Life Technologies, Carlsbad, USA (catalogue no. NP0001)

Components of 20 x NuPAGE® MOPS SDS Running Buffer (500 ml) are:

3-(<i>N</i> -morpholino) propane sulphuric acid (MOPS)	1.0 M
Tris base (pH 8)	1.0 M
Sodium Dodecyl Sulphate (SDS)	70 mM
EDTA (pH 8)	20 mM

2.3.7.3 20 x NuPAGE® MOPS SDS Transfer Buffer (pH 7.2)

500 ml stock was obtained from Life Technologies, Carlsbad, USA (catalogue no. NP0006)

Components of 20 x NuPAGE® MOPS SDS Transfer Buffer (500 ml) are:

Bicine	500 mM
Bis-Tris	500 mM

EDTA (pH 8) 20 mM

2.3.7.4 β -Mercaptoethanol

(Sigma Aldrich, St. Louis, USA, catalogue no. M3148) 14.3 M

2.3.7.5 Precast NuPAGE® Novex® 4-12% Bis-Tris Gel (0.1 mm, 10 wells)

(Invitrogen, Carlsbad, USA, catalogue no. cat no. NP0321)

2.3.7.6 Protein Molecular Weight Markers

A- Magic Mark™ XP (range: 20 - 220 kDa)

50 μ l stock was obtained from Life Technologies, Carlsbad, USA (catalogue no. LC5603)

B- Precision Plus Protein Standards – Dual colour (range: 10 – 250 kDa)

500 μ l stock was obtained from Bio-Rad, Hercules, California (catalogue no. 161-0374)

C- Pre-stained Protein Marker (range: 6 – 175 kDa)

500 μ l stock was obtained from BioLabs Inc., Ipswich, USA (catalogue no. P7708)

2.3.7.7 Amersham Hybond-P Polyvinylidene difluoride (PVDF) membrane

(GE Healthcare, Little Chalfont, UK, catalogue no. RPN2020F)

2.3.7.8 Tween-20

100 ml stock was obtained from Fisher Scientific, Waltham, USA (catalogue no. BP337-100)

2.3.7.9 TBS Tween (TBST)

TBS (pH 7.4) as described in Section 2.3.4.1

Tween -20 0.1 % (v/v)

2.3.7.10 Secondary Antibodies Used in Western Blot

A- Polyclonal rabbit anti mouse horseradish peroxidase (HRP) conjugated

5 ml stock was obtained from Dako, Santa Clara, USA (catalogue no. P0260)

B- Polyclonal swine anti rabbit HRP conjugated

5 ml stock was obtained from Dako, Santa Clara, USA (catalogue no. P0217)

2.3.7.11 SuperSignal® West Femto Chemiluminescent Substrate

100 ml stock was obtained from Thermo Scientific, Waltham, USA (catalogue no. 34095)

2.3.8 Reagents Used for DNA Extraction

A- DNA extraction from FFPE tissue blocks

2.3.8.1 QI Amp® DNA FFPE Tissue Kit

(Qiagen, Venlo, Netherlands, catalogue no. 56404) 50 tests

B- DNA extraction from tissue culture

2.3.8.2 QI Amp® DNA Mini Kit

(Qiagen, Venlo, Netherlands, catalogue no. 51304) 50 tests

2.3.8.3 Agarose Gels (variable concentrations)

Agarose (Severn Biotech Ltd, Kidderminster, UK, catalogue no. 30-17-50) % (w/v)

1 x Tris-Acetate EDTA (TAE) (pH 8) (volume as required) ml

(Severn Biotech Ltd, Kidderminster, UK, catalogue no. 20-6001-50)

Ethidium bromide (10mg/ml) 2µg/100ml

(Promega, Madison, USA, catalogue no. H5041)

2.3.8.4 Gel Electrophoresis 6 x loading dye

1 ml stock was obtained from Promega, Madison, USA (catalogue no. G1881)

2.3.8.5 Genomic Molecular Weight Markers

A- **GeneRuler™ 100 bp DNA Ladder** (range: 100 – 1000 bp)

1 ml stock was obtained from Fermentas, Waltham, USA (catalogue no. SM0241)

B- **Lambda DNA / Hind III Marker** (range: 125 – 23130 bp)

1 ml stock was obtained from Fermentas, Waltham, USA (catalogue no. SM0103)

2.3.9 Reagents Used For Polymerase Chain Reaction

2.3.9.1 5 X Go *Taq* flexi PCR buffer (pH 8.5)

20 ml stock was obtained from Promega, Madison, USA (catalogue no. M890)

2.3.9.2 Magnesium Chloride (MgCl₂) Solution (25 mM)

1.5 ml stock was obtained from Promega, Madison, USA (catalogue no. A5311)

2.3.9.3 Primers

The *P53*, *MDM2* and *MDMX* primers used in the study are summarised in Table 2.5.

Stocks of 10 micromolar (μM) of each primer were stored at -20°C .

2.3.9.4 Deoxynucleoside Triphosphates (dNTP)

10 mM stock of dNTP was prepared from the following and stored at -20°C :

100 mM deoxyadenosine triphosphate (dATP)	
(Fisher Scientific, Waltham, USA, catalogue no. BP2564-1A)	100 μl
100 mM deoxycytidine triphosphate (dCTP)	
(Fisher Scientific, Waltham, USA, catalogue no. BP2564-1B)	100 μl
100 mM deoxyguanosine triphosphate (dGTP)	
(Fisher Scientific, Waltham, USA, catalogue no. BP2564-1C)	100 μl
100 mM deoxythymidine triphosphate (dTTP)	
(Fisher Scientific, Waltham, USA, catalogue no. BP2564-1D)	100 μl

2.3.9.5 GenElute PCR Clean up Kit

(Sigma Aldrich, St. Louis, USA, catalogue no. NA1020) 100 tests

2.3.10 Reagents for Big Dye Sanger Sequencing

2.3.10.1 BigDye® Terminator v3.1 Cycle Sequencing Kit

(Applied Biosystems Inc., Warrington, UK, Catalogue no. 4337455)

Components of kit are:

Big Dye 3.1	800 µl
5 x Sequencing Buffer	4 ml

2.3.10.2 Ethylene di-amine tetra-acetic acid (EDTA)

500 g stock was obtained from Duchefa, Haarlem, Netherlands (catalogue no. E0511)

2.3.10.3 Highly Deionised (HiDi) Formamide

25 ml stock was obtained from Life Technologies, Carlsbad, USA (catalogue no. 4311320)

2.4 Methods

2.4.1 Tissue Samples Processing and Storage

2.4.1.1 Retrospective Samples

Archival tissue blocks were collected from the Pathology Department at LTH after the appropriate approvals were granted. In accordance with the Human Tissue Authority (HTA) regulations and the ethical permissions for the study, the samples were afterwards stored in a secure, HTA-registered tissue storage facility (room 9.04f, Wellcome Trust Brenner Building).

2.4.1.2 Prospective Samples

Fresh tissue samples were delivered immediately to the Pathology Department at LTH after surgical resection, in a fresh preservative-free state. The specimen was marked and cut by a consultant histopathologist with the researcher attending. A fresh sample was collected for

the purpose of the study. It was immediately cut into small cubes of tissue (approximately 1 cm³ in size) and the cubes were stored in pre-labelled cryo-tube vials (Thermo Scientific, Waltham, USA, catalogue no. 366656). They were immediately immersed in liquid nitrogen for 2 minutes, before being frozen at -80°C. An updated log of all archival and fresh specimens prepared for the study was maintained and kept securely.

2.5 Propagation of Eukaryotic Cell Lines

The materials used in these experiments are detailed in Section 2.3.2.

U2OS and HT29 were routinely maintained in RPMI + GlutaMax™ –I with 10% (v/v) FCS and SW-872 was maintained in DMEM + GlutaMax™ –I with 10% (v/v) FCS. They were incubated in a humidified incubator with 5% CO₂ at 37°C and the media were changed every three days. The cells were passaged once they reached 90 – 95% confluence. No antibiotic or antifungal reagents were used. For passage, cells were rinsed in DPBS for 1 minute, before incubation in 1 x trypsin solution in DPBS for 10 minutes. Single cell suspensions were passaged at a ratio of 1:10.

2.6 Cell Cycle Arrest Protocol

The materials used in these experiments are detailed in Section 2.3.2.

Cells were grown on 22 x 22 mm, 0.13 – 0.16 mm thick cover slips (VWR International, Leicestershire, UK) in 6-well tissue culture plates, in aseptic controlled conditions. They were then incubated at 37°C in 5% CO₂ until they had reached the desired confluence (approximately 40%). Their cell cycle was arrested across different phases using one of three cell cycle arrest agents (Nocodazole, Aphidicolin and Hydroxyurea). To establish the optimum doses, increasing concentrations of each of these agents, in the relevant tissue culture media, were used until the lethal doses were identified. The tissue cultures were then incubated with each of the cytotoxic agents at the highest, non-lethal dose (Table 2.3) for 24–48 hours (hrs). Control samples were incubated in 1 mM DMSO at similar (v/v) concentrations to each of the cell cycle arrest agents. The cells were inspected under inverted light microscope (Olympus, model no. CKX41). They were used after visual confirmation of their viability and unanimous morphology. Subsequently, slides were fixed

in neat methanol (-20°C) for 10 minutes, then washed and maintained in DPBS. Fixed slides were kept in the fridge (4°C) afterwards and ICC was performed within 24 hrs of fixation.

2.7 Immunochemical Staining Protocol

The materials used in these experiments are detailed in Section 2.3.3.

2.7.1 Immunocytochemistry (ICC)

To perform ICC, cells were grown on 22 x 22 mm cover slips (until 40% confluent), fixed in methanol and then washed and maintained in DPBS, as described in Section 2.6. ICC was performed within 24 (hrs) of fixation. No antigen retrieval procedures were required.

After the slides were washed in TBS, endogenous peroxidase was neutralised by 3% (v/v) hydrogen peroxide in water for 20 minutes, followed by protein block with 3% (v/v) casein in DPBS (as provided in the NovoLink Max Polymer Detection System) for 10 minutes to reduce non-specific primary antibody (Ab) binding. Subsequently, the slides were incubated with the optimally diluted primary Abs in Invitrogen® Antibody Diluent as follows: P53, 1:100 for 12 hrs at 5°C; MDM2 (SMP-14), 1:300; and MDMX, 1:200, both for 1 hr incubation time. The primary Abs used in the study are summarised in Table 2.4.

2.7.1.1 Detection of the Primary Antibody

To detect the primary Abs the NovoLink Max Polymer Detection System was used. The system employs a controlled polymerisation to prepare polymeric Horseradish Peroxidase (HRP)-linker antibody conjugates. After TBS wash of the primary Ab, slides were incubated for 30 minutes in a serum-based post-primary block to enhance penetration of the polymer reagents. They were then incubated for another 30 minutes in the HRP polymer-conjugated secondary Ab, which had positive reactivity to mouse IgM, mouse IgG and rabbit IgG. Subsequently, the slides were incubated for 5 minutes in 3,3'-diaminobenzidine (DAB) chromogen, which produces a visible brown precipitate at the antigen site when oxidised by HRP of the secondary Ab. All the previous steps were separated by 5-minute washes in TBS, repeated twice. The counterstaining was performed with 0.02 % (v/v) haematoxylin in

water, for 2 minutes. After a brief wash in tap water, coverslips were then mounted on slides, which were visualised under a light microscope (Nikon, model no. Eclipse E600).

2.7.2 Immunohistochemistry (IHC)

Formalin-fixed and paraffin-embedded (FFPE) tissue blocks were cut at 4 μm thickness with a microtome (Leica, model no. RM 2255), to obtain sequential sections. Sections were floated in a water bath at 39 – 42 °C before transfer onto Superfrost Plus slides (Thermo Scientific, Waltham, USA, catalogue no. 4951PLUS4). They were incubated overnight at 37°C. Slides were de-waxed by serial immersion in a xylene-to-ethanol (3 x 100% xylene washes followed by 3 x 96% ethanol washes). Antigen retrieval was performed by immersing the slides in a hot bath of 1mM citrate buffer (pH 6.0) at 95 -98°C for 20 minutes. After cooling for 20 minutes at room temperature, the slides were washed for 5 minutes in deionised water and a further 5 minutes in TBS. Endogenous peroxidase was blocked by 3% (v/v) hydrogen peroxide in water for 20 minutes, then non-specific primary Ab binding was blocked with 20% (v/v) goat serum in TBS for 30 minutes. The slides were incubated with primary Abs diluted in 5% (v/v) goat serum in TBS at the concentrations found after optimisation, which were within the ranges recommended by the manufacturers, as follows: for MDM2 (SMP-14) at a dilution of 1:250 for 90 minutes; for MDMX at 1:250 dilution; and for P53 at a 1:600 dilution. Both of the latter were incubated for 18 hours at 5°C. All previous steps were separated by 5-minute washes in TBS, repeated twice.

To detect the primary Abs, the NovLink Max Polymer Detection System was used, as detailed in Section 2.7.1.1. The slides were counter-stained with haematoxylin, dehydrated through an ethanol-to-xylene solvent gradient and mounted under glass cover slips.

2.7.2.1 Optimisation of Immunochemical Protein Detection

Conditions for use of the antibodies in ICC and IHC with cell lines and LS cancer tissue were optimised by series of experiments, which included adjusting the following parameters:

A- Optimisation of Antigen Retrieval Techniques

Multiple antigen heat retrieval techniques, using 1 mM citrate buffer solution (pH 6.0) were employed. These included: microwave oven heat application at 800 watt for 10 minutes; pressure cooker retrieval for 2 minutes and immersing the slides in sub-boiling citrate buffer bath (95-98 °C) for 5 - 30 minutes.

B- Optimisation of the Blocking Compounds

To block the non-specific Ab binding, two blocking compounds were used either separately or in conjunction with one another. These included: 0.4% casein in phosphate-buffered saline (as provided in the NovoLink Max Polymer Detection System), for an incubation period of 5 - 10 minutes and 20% (v/v) goat serum in TBS for 10 minutes.

C- Optimisation of the Primary Antibodies

Decreasing primary Ab concentrations were used until a negative signal was obtained, to achieve optimal dilution results. Variable incubation periods from 1 hr to overnight were performed until the most specific results were achieved. Different antibody diluents were used including Invitrogen Antibody Diluent and 5% (v/v) goat serum in TBS.

2.7.2.2 Routinely Used Immunochemical Staining Controls

No primary and no secondary Ab controls were included in each ICC and IHC run. At least one positive and one negative tissue controls were analysed with each IHC run.

The negative controls for P53, MDM2 and MDMX included: normal fat from breast tissue kindly provided by Professor Valerie Speirs (Professor of Experimental Pathology and Oncology, University of Leeds) and a fully characterised, subcutaneous benign lipoma.

P53 positive control was a metastatic adenocarcinoma in a lymph node. MDDM2 and MDMX positive controls included two fully characterised LSs with known *MDM2* or *MDMX* amplification, respectively. All control samples were tested and validated for use by the Pathology Department at LTHT. They were kindly provided and proof read by Dr Will Merchant (Consultant Histopathologist, LTHT).

2.7.2.3 Immunohistochemistry Scoring Protocol

Scoring for the IHC stained tissue slides was performed on a light microscope (Olympus multi-viewer, model no. BX41) at 40 x magnification. This was done simultaneously but independently by the author and an experienced histopathologist. Both were blinded to the actual histological diagnosis. 100 cells per slide were scored (maximum of 20 cells per high power field). Particular care was taken to mark the sequential slides of each case identically, so as to score corresponding fields for the three different antibodies.

Only clear nuclear staining was considered positive. Blood cells, inflammatory cells, non-specific cells and capillary endothelium cells were not included in the scoring process. Mitotic figures were excluded (as will be explained in Section 3.2.3). Scoring was stratified for MDM2 and MDMX as (-, + and ++) where <11, 11-40 and >40 of the 100 cells were stained positive, respectively. P53 was considered over-expressed (+) if 10% or more cells had positive nuclear staining. The slides were then proof read and re-scored separately by a specialist consultant histopathologist.

2.7.2.4 Data Analysis

Basic statistical tests were performed in the study. Statistical analysis was done using SPSS software - version 21, (SPSS Inc., Illinois, USA). *P* values <0.05 were considered significant.

The project statistics were reviewed and approved by Dr Helene Thygesen, biostatistician (Cancer Research UK, Leeds Centre).

2.8 Immune Blotting of Proteins

2.8.1 Cell Lysate Preparation and Quantification

The materials used in these experiments are detailed in Sections 2.3.5 and 2.3.6.

2.8.1.1 Preparation of Lysate from Cultured Cells

Western blots for a protein of interest were performed using lysates prepared with Radioimmunoprecipitation Assay (RIPA) buffer. Cells were grown in T75 flasks until 40 – 50%

confluent, media were removed and cells were washed in their relevant, cold and FCS-free media. To counteract endogenous enzymes, Protease Inhibitor Cocktail; PMSF; and reducing agent (DTT) were added to make the RIPA Buffer Working Solution (see Section 2.3.5.4). The cells were incubated with 1 ml of the RIPA Buffer Working Solution and allowed to stand for 10 minutes at 4°C before dislodging the cells with a tissue scraper and transferring the solution to a 1.5 ml microfuge tube (Eppendorf). The solution was pipetted up and down to break up any clumps, and then incubated on ice for another 10 minutes. Subsequently, the solution was centrifuged for 10 minutes at 16,000 g at 4°C. The supernatant lysate was quantified for protein concentration (as per Section 2.8.1.3) and stored at -80°C.

2.8.1.2 Preparation of Lysate from Frozen Tissue

Frozen tissue sections were mounted on a chuck using mounting medium (VWR, Leuven, Belgium, cat no. 361603E) before being cut with a cryostat (Leica, model no. CM3050 S) at 5 µm thickness. The first two sections were discarded and the subsequent four sections were transferred into 1.5ml Eppendorfs containing 500 µl of RIPA Buffer Working Solution. The samples were then processed and stored as described in Section 2.8.1.1.

2.8.1.3 Quantification of Proteins

The protein concentration of the lysates was quantified using a Bicinchoninic Acid Assay (BCA) protein assay kit. This analysis is based on a colourimetric assay of a Biuret reaction, which utilises the reduction of Cu^{+3} to Cu^{+2} by proteins in an alkaline solution, in a concentration-dependent reaction leading to a measurable violet colour. 10 µl of either the cell lysate, RIPA buffer standard, or serial dilutions of the BSA protein standard (see Section 2.3.6.1) with 15 µl of deionised water were added to each well of a 96-well microtitre plate, then 200 µl of BCA Working Reagent Solution containing cupric sulphate (see Section 2.3.6.2) was added to each well and mixed thoroughly before incubation at 37°C for 30 minutes. Optical density was subsequently measured using a microplate reader (Dynex Technologies Ltd, model no. OpsyS MRTM) at 570 nm. The protein concentration of the lysate samples were first corrected for the RIPA buffer standard measurement, then calculated from the standard curve obtained from the serial dilutions of the BSA protein standards.

2.8.2 Western Blot

The materials used in these experiments are detailed in Section 2.3.7.

2.8.2.1 Gel Electrophoresis of Proteins

A mass equivalent of 20 µg of protein was added to 1 x LDS sample buffer (pH 8.5) containing 5% (v/v) β-mercaptoethanol, to make up a total volume of 20 µl. Samples were briefly mixed, spun and placed in a hotplate at 100°C for 5 minutes before being transferred into ice for 5 minutes. Afterwards, samples were centrifuged for 30 seconds, gently suspended and kept on ice, before being loaded onto the gel.

Twenty µg of samples was loaded onto Precast NuPAGE® Novex® 4-12% Bis-Tris Gel with 5 µl molecular weight markers in adjacent lanes (either Precision Plus Protein Standards or Prestained Protein Marker were used). 5 µl of Magic Mark™ XP was added to each ladder to allow band visualisation on the running gel. Electrophoresis was then performed in Xcell SureLock™ Mini-Cell system (Life Technologies, model no. EI0001), in 1 x NuPAGE® MOPS SDS Running Buffer, at a constant current of 180 V for 1 to 1.5 hrs.

2.8.2.2 Transblotting of Bis-Tris Gels

Proteins that were separated using the gel electrophoresis were then transferred onto Amersham Hybond-P Polyvinylidene difluoride (PVDF) membrane. The membrane was activated by being soaked in neat methanol for 30 sec then washed in deionised water for 10 minutes with constant agitation on a shaker. Proteins were then transferred in 1 x NuPAGE® MOPS SDS transfer buffer with 10% (v/v) methanol, using the XCell II Blot Module (Life Technologies, Carlsbad, USA, catalogue no. EI9051) for 16 hrs at 12 V.

2.8.2.3 Immunoblotting of Proteins

The PVDF membrane with the transferred protein was blocked with TBS containing 0.1% (v/v) Tween-20 (TBST) and 5% (w/v) skimmed dried milk (Marvel) for 1 hour at room temperature with gentle agitation. It was then transferred to 1% (w/v) skimmed dried milk (Marvel) in TBST containing the primary Ab in appropriate dilutions as follows: 1:5000 for P53 (DO-7) and MDMX; 1:2500 for MDM2 (SMP-14); and 1:4000 for MDM2 (2A10). The

membrane was allowed to incubate with the primary Ab for 90 minutes at 37°C, it was then washed, thrice, with TBST, for ten minutes each time.

The membrane was then transferred to 1% (w/v) dried skimmed milk (Marvel) in TBST containing the appropriate secondary Abs in 1:2000 dilution as follows: for P53 and MDM2, polyclonal rabbit anti mouse HRP conjugated; and for MDMX, polyclonal swine anti rabbit HRP conjugated. The membrane was incubated with the secondary Ab for one hour at room temperature, then washed, thrice, TBST for 15 minutes. To rule out non-specificity of secondary Ab, samples incubated without primary Ab were included in the early stages of the investigation.

To detect the bound Abs, the membrane was incubated with 200 µl of SuperSignal® West Femto Chemiluminescent Substrate for 5 minutes, before being visualised using ChemiDoc® MP imaging system (Bio-Rad, model no. 170-8280), with exposure time periods of 1 minute to 1 hr depending on the level of signal intensity.

2.9 Cytogenetic Analyses

Cytogenetic analyses were performed by the Yorkshire Regional Genetics Services (Ashley Wing, St James's University Hospital) as part of the diagnostic protocols of LSs. This service was introduced in 2008 and has subsequently become a routine diagnostic tool. Two separate tests were performed for LSs including Giemsa banding for karyotype analysis as a "road map" for subsequent Fluorescence *in situ* hybridization (FISH) analysis to detect *MDM2* amplification.

2.9.1.1 Fluorescence *in situ* Hybridization

The methods adopted by the Yorkshire Regional Genetics Services to perform FISH analysis can be summarised as follows. FISH analysis was performed on FFPE tissue slides, guided by a complementary haematoxylin and eosin pre-stained slide provided by histopathologist and marked for the areas of tumour cells. Briefly, the slides were de-waxed and dehydrated in a gradient of xylene and ethanol. They were then incubated in 0.2M HCl for 30 minutes to compromise the integrity of the nuclear membranes, before being washed with distilled water. Slides were pre-treated by pepsin and incubated in a hybrite for 45 minutes.

Hybridisation was achieved by adding 5 µl of DNA probe which hybridises to the MDM2 locus at 12q15 with a 12 centromere control (Keratech, Amsterdam, Netherlands, catalogue no. KBI-10717 MDM2(12q15)/SE12) and the slides were kept on a hot plate (80°C) for 5 minutes to denature the DNA for probe attachments, they were then incubated at 37°C overnight. Finally, more washes and 4',6-diamidino-2-phenylindole (DAPI) counterstaining were performed before the slides were ready for analysis.

2.9.1.2 Fluorescence *in situ* Hybridization Scoring Protocol

A total of 100 cells were scored independently by two trained technicians using fluorescent microscopes (Leica DMLB; Leica DMR; and Zeiss Axioplan 2) and the scorers were blinded to the provisional histological diagnosis. Only cells with clear cell boundaries were scored. Overlapping nuclei were also excluded. A fourfold increase in MDM2 (red) signal, compared to centromere (green) signal, was considered positive for *MDM2* amplification. At least 5 of the scored 100 cells had to demonstrate these changes to conclude the case was positive for *MDM2* gene amplification. Other characteristic features of gene amplification that were occasionally seen included the presence of supernumerary rings or a giant chromosome in karyotype analysis.

2.10 Genetic Analysis

2.10.1 Extraction of Deoxyribonucleic Acid (DNA)

The materials used in these experiments are detailed in Section 2.3.8.

2.10.1.1 DNA Extraction from Formalin-Fixed Paraffin-Embedded Blocks

QI Amp[®] DNA FFPE Tissue Kit was used to extract genomic material from FFPE tissue blocks for subsequent analysis. The kit utilises the selective binding properties of a silica-based membrane to purify DNA from small samples, and the manufacturer's instructions were followed accurately. The tissue blocks were first cut using a microtome at 5 µm thickness, the first two sections were discarded and the subsequent 3 – 5 sections (no more than 25 mg) were kept in 1.5 ml Eppendorf tubes. De-waxing and rehydration were done by adding

1.2 ml of xylene with rigorous vortexing followed by centrifugation at 13,000 g for 2 minutes. The supernatant was removed and the pellet was resuspended in 1.2 ml of 100% ethanol to remove any residual xylene. Gentle vortex was then followed by centrifugation at 13,000 g for 2 minutes, the supernatant was removed and the obtained pellet was allowed to air dry at room temperature for 10 minutes. The tissue pellet was then re-suspended in 180 µl of ATL buffer with 20 µl proteinase K (20mg/ml) and was incubated for 1 hr at 56°C to ensure adequate sample lyses. This was followed by 1 hour incubation at 90°C to reverse formalin crosslinking, and the sample was then dissolved in 200 µl of Buffer AL with 200 µl of 100% ethanol, before being transferred to QI Amp spin column and centrifuged at 6000 g for 1 minute. The filtrate was discarded as DNA was bound to the silica membrane in the column. The residual contaminants were washed with 500 µl of Buffers AW1 and AW2 consecutively, separated by 6000 g centrifuge for 1 minute each. DNA was subsequently eluted into a clean 1.5 ml Eppendorf in 40 µl of nuclease-free water (or ATE Buffer). The eluate containing DNA was stored at -20°C until further use. Nucleic acid concentration was measured using a NanoDrop™ 1000 Spectrophotometer (Thermo Scientific, Waltham, USA).

2.10.1.2 DNA Extraction from Cultured Cells

QI Amp® DNA Mini Kit was used to extract genomic material from cultured cell lines. The kit utilises a silica membrane column as described in Section 2.7.6.1. Cells were grown in T75 Corning tissue culture flasks in their appropriate media. When they reached 50% confluence, media was removed and cells were washed in DPBS then incubated with 1 x trypsin for 10 minutes at 37°C, until they had detached from the flask. They were then resuspended in 10 ml of their culture media into a collection tube. The cell suspension was centrifuged at 300 g for 10 minutes and the media supernatant was discarded. The pellet was resuspended in DPBS to a final volume of 200 µl before 20 µl proteinase K (20mg/ml) and 200 µl of Buffer AL were added separately. The solution was incubated at 56°C for 10 minutes and then 200 µl of 100% ethanol was added with gentle vortex. The solution was transferred to QIAamp Mini spin column and centrifuged at 6000 g for 1 minute, the filtrate was discarded and the DNA was bound to the silica membrane in the column. Subsequently

the contaminants were washed off in Buffers AW1 and AW2 and DNA was eluted and stored as described in Section 2.7.6.1.

2.10.1.3 Agarose Gel Confirmation of DNA Extraction

1 % (w/v) agarose gel was prepared by adding the required weight of agarose to a volume of 1 x TAE, the solution was warmed in a microwave oven until agarose had dissolved, then cooled to 50⁰C, an equivalent of 2 µg/100ml ethidium bromide was added and mixed well. The gel was then poured into an appropriate sized rig with a comb in place. Once cooled, the comb was removed to reveal the wells.

4 µl of each DNA eluate with 3 µl of 6 x agarose gel loading dye was loaded into the ethidium bromide- stained agarose gel, and an appropriate genomic molecular weight ladder was loaded into adjacent lane. Horizontal gel electrophoresis was performed in a gel casting system (Life Technologies, model no. Horizon[®] 58 or Bio-Rad, model no. Sub-Cell[®] GT) in 1 x TAE buffer, at a constant current of 60 V (5V per cm of distance between electrodes) for 40 minutes. The gel was then visualised under ultra-violet (UV) light at 306 nm, via the fluorescence of intercalated ethidium bromide, using the ChemiDoc[®] MP imaging system (Bio-Rad, model no. 170-8280).

2.10.2 The Polymerase Chain Reaction

The materials used in these experiments are detailed in Section 2.3.9.

2.10.2.1 Oligonucleotide Primer Design

Oligonucleotide primers for Polymerase Chain Reaction (PCR) amplification and sequencing of MDM2 and MDMX sequences were designed against the human genome (Genome Reference Consortium Human Build 37) as annotated by University of California, Santa Cruz (UCSC) genome browser (183). Primers were designed to flank each coding exon, the donor and acceptor splice sites and about 100 bp of flanking intronic DNA. The oligonucleotide primer sequences for amplification and sequencing of P53 coding sequences were reproduced from reference (184).

2.10.2.2 The Polymerase Chain Reaction Protocol

Stocks of 10 μM primers and 20 $\text{ng}/\mu\text{l}$ DNA extracts were prepared by dilution in sterile water. All PCRs were initially performed on a thermal gradient (45°C – 65°C) using Peltier Thermal Cycler (Bio-Rad, model no. PTC0220), to determine the optimal annealing temperature for each primer pair reaction. This standard protocol was sufficient to identify the optimal annealing temperatures for all different primers (Table 2.5).

PCRs were performed in 25 μl total reaction volumes containing: 1 x Go *Taq* flexi PCR reaction buffer, 1.5 mM MgCl_2 , 200 μM of each (dNTP) [(dATP); (dGTP); (dCTP); (dTTP)], 200 nanomolar (nM) of each primer, 1.5 units of *Taq* DNA polymerase and template genomic DNA (approximately 50 ng). Double-stranded DNA was denatured by heating to 95°C for 3 minutes, followed by 40 cycles of the following steps: denaturing at 95°C for 30 seconds; cooling to 50-59°C for 30 seconds to allow the primers to anneal to their complementary sequences; heating to 72°C for 30 seconds to extend the annealed primers with *Taq* DNA polymerase. The final cycle was complemented by an extension of 72°C for 2 minutes. A negative control of all reagents excluding genomic DNA was included in all experiments, as was a positive control of previously analysed DNA (from human blood), which was kindly made available by Dr Christine Diggle (Senior Research Fellow, Wellcome Trust Brenner Building).

2.10.2.3 Standard Agarose Gel Electrophoresis

At the conclusion of each PCR, standard 1% (w/v) agarose gel electrophoresis was performed to confirm a successful reaction was achieved by the detection of a transluminant band, which corresponded with the expected PCR amplicon size against 100 bp DNA ladder. 4 μl of PCR products was added to 3 μl of 6 x agarose gel loading dye and horizontal agarose gel electrophoresis was performed according to the protocol detailed in Section 2.7.6.3.

2.10.2.4 Purification of PCR Products

The PCR products were purified of unincorporated oligonucleotide primers using GenElute PCR clean up kit. The kit is designed for purification of single-stranded or double-stranded

PCR amplification products of a size range between 100 bp to and 10 kb. The purification was achieved by first activating the silica membrane of the GenElute plasmid mini spin column with 0.5 ml of Column Preparation Solution to maximise the DNA binding. The column was centrifuged at 16,000 g for 1 minute, and the eluate was discarded. Then, the PCR products were diluted in 5 x (v/v) Binding Solution and passed through the silica membrane (by centrifugation at 16,000 g for 1 minute) to allow DNA binding to the membrane. The eluate was discarded. The bound DNA was then washed and cleaned by 0.5 ml of Wash Solution, centrifuged at 16,000 g for 1 minute, twice and the eluate was discarded. Finally the PCR products were eluted in 25 µl nuclease-free water into a clean Eppendorf and stored at -20°C until further use.

The purified products were quantified for nucleic acid concentrations using Nanodrop and standard agarose gel electrophoresis was performed, as per protocol detailed in Section 2.7.6.3, for confirmation of retained purified PCR products.

2.10.3 DNA Amplicon Dye Terminator Cycle Sequencing

DNA analysis of *MDM2* and *MDMX* was performed in the control cell lines and of *P53* in selected FFPE tissue blocks. The materials used in these experiments are detailed in Section 2.3.10.

The DNA sequencing was performed using BigDye® Terminator v3.1 Cycle Sequencing Kit, according to the manufacturer's instructions. DNA sequencing of *P53* exon 4 to 9; *MDM2* exon 1 to 11; *MDMX* exon 1 to 10 and flanking intervening sequences was performed using PCR fragments covering these regions. Sequencing was performed on purified PCR amplicons (as described in Section 2.7.7.4) using the same oligonucleotide primers that were used for exon amplification. The sequences were aligned to reference sequences: NT_010718.16 for *P53*; NT_029419.12 for *MDM2*; and NT_00487.19 for *MDMX*. Sequencing was obtained from both forward and reverse strands.

2.10.3.1 Sequencing Reaction

Sequencing reactions were performed in a 96-well plate and consisted of the following: 1 µl of the template PCR product; 1 µl BigDye™ 3.1 Terminator ready Reaction Mix; 1.5 µl 5 x

Sequencing Buffer, 1.6 picomolar (pM) of the forward or reverse corresponding primer, sterile water to make up the solution to a final volume of 10 µl. The reagents were pipetted and mixed well. Cycle sequencing was performed with rapid thermal ramping on a Peltier Thermal Cycler (Bio-Rad, model no. PTC0220), using 25 cycles of the following steps: 96°C for 10 seconds; 50°C for 5 seconds and 60°C for 4 minutes. Each change in temperature was performed by ramping the temperature up or down at the rate of 1 °C per second.

2.10.3.2 Ethanol Precipitation to Remove Unincorporated Dyes

DNA material and its extension products were precipitated by adding 5 µl of 125 mM EDTA (pH 8.0) and 60 µl of 100% ethanol to each 10 µl reaction solution. The mixture was thoroughly mixed and centrifuged at 3060 g for 30 minutes at room temperature, the plate was then inverted on a clean tissue and re-centrifuged at 8 g for 1 minute.

The resulting pellet was then washed with 60 µl of freshly-prepared 70% ethanol and immediately centrifuged at 780 g for 15 minutes at 4°C to remove EDTA and the unincorporated dye-terminators. The plate was then inverted and centrifuged at 8 g for an additional minute before it was left to air-dry. Each ethanol-precipitated products pellet was re-suspended in 10 µl highly deionised (HiDi) formamide and the sequencing reactions were visualised by electrophoresis on a Genetic Analyser (Applied Biosystems, model no. 3130xL).

2.10.3.3 Sequence Analysis

Data from the 3130xL Genetic Analyser were exported as (.ab1) files and analysed using GeneScreen, a program developed by Dr Ian Carr (Lecturer, University of Leeds), for high-throughput mutation detection in DNA sequence electropherograms (185) (<http://dna.leeds.ac.uk/genescreen>). Identification, verification and annotation of sequence variants were performed using this software.

Table 2.1: Characteristics of the retrospective patients cohort

Category	Subcategory	Result (n)
Sex	Female	33 (median age = 63)
	Male	31 (median age = 64)
Anatomical location	Trunk	29 (15 retroperitoneal)
	Extremities	35
Histological subtype	WDLS	43 (including 1 inflammatory and 1 mixed type)
	DDLS	9
	MXLS-RCLS	12

This is a tabular summary of the characteristics of the retrospective clinical cohort demonstrating a homogenous distribution amongst gender, age and tumour subtypes and anatomical locations.

Table 2.2: Characteristics of the prospective patients cohort

Category	Subcategory	Results (n)
Sex	Female	12 (median age = 58.5)
	Male	4 (median age = 57.5)
Anatomical location	Trunk	6
	Retroperitoneum	10
Histology		
Malignant (n = 11) (median age = 66)	WDLS	5
	DDLS	2
	Angiosarcoma	3
	Inflammatory myofibroblastic tumour	1
Benign (n=5) (median age = 45)	Lipoma	3
	Myxoma	1
	Leiomyoma	1

This is a tabular summary of the characteristics of the prospective clinical cohort demonstrating recruitment of various STS subtypes and benign cases.

Table 2.3: Cell cycle arrest reagents

Agent	Mechanism of action	Cell cycle arrest phase	Range of concentrations	Optimal concentration	Exposure time	Source	Catalogue no.
Nocodazole	Interferes with the polymerization of microtubules	M -Phase	500 ng/ml – 1 ng/ml	5 ng/ml	24 hrs	Acros Organics, Geel, Belgium	358240100
Aphidicolin	Specific inhibitor of DNA Polymerase- α	G 1 - S Phase	50 μ g/ml – 5 μ g/ml	12.5 μ g/ml	24 hrs	Sigma Aldrich, St. Louis, USA	A0781
Hydroxyurea	Inhibits DNA synthesis	S – Phase	100 μ g/ml – 5 μ g/ml	25 μ g/ml	48 hrs	Sigma Aldrich, St. Louis, USA	H8627

This is a tabular summary detailing the cell cycle arrest reagents used in the study, a brief description of their mechanisms of action, the range of concentrations tested and the optimum concentration dose used and exposure times in cell cycle arrest experiments.

Table 2.4: Primary antibodies used in the study

Recognition	Name	Clonality	Epitope	Reactivity	Source	Catalogue no.
P53	DO-7	Mouse monoclonal IgG	35-45	Human	Leica Microsystems	NCL-L-p53-DO7
MDM2	SMP-14	Mouse monoclonal IgG	154-167	Human	Santa Cruz Biotechnology, Inc.	Sc-965
MDM2†	2A10	Mouse monoclonal IgG	249-339	Human	Abcam	Ab16895
MDMX	MDM4	Rabbit polyclonal IgG	125-175	Human	Bethyl Laboratories	IHC-00108

This is a tabular summary of the primary antibodies used in the study. † the MDM2 (2A10) Abcam antibody was abandoned from use in the cohort analysis after Proof of Principle experiments.

Table 2.5: Details of primers used in the study

Exon	Nucleotide Sequence	Size of PCR Product	Tm°
P53 Exon 4	F: 5'-d(TCCAAGCAATGGATGATT) R: 5'-d(TTCTGGGAAGGGACAGAAGA)	194 bp	63°C
P53 Exon 5*	F: 5'-d(CTCTCCTGCAGTACTCCCCTGC) R: 5'-d(GCCCCAGCTGCTCACCATCGCTA)	211 bp	55°C
P53 Exon 6*	F: 5'-d(GATTGCTCTTAGGTCTGGCCCCTC) R: 5'-d(GGCCACTGACAACCACCCTTAACC)	182 bp	55°C
P53 Exon 7*	F: 5'-d(GCTTGCCACAGGTCTCCCCAAG) R: 5'-d(AGGCTGGCAAGTGGCTCCTGAC)	192 bp	59°C
P53 Exon 8*	F: 5'-d(TGGTAATCTACTGGGACGGA) R: 5'-d(GCTTAGTGCTCCCTGGGGGC)	134 bp	50°C
P53 Exon 9*	F: 5'-d(GCCTCTTTCCTAGCACTGCCAAC) R: 5'-d(CCCAAGACTTAGTACCTGAAGGGTG)	102 bp	50°C
MDM2 Exon 1	F: 5'-d(TTCAGACACGTTCCGAAACTG) R: 5'-d(AGACACGATGAAAAGTGGAAATCAT)	263 bp	55°C
MDM2 Exon 2	F: 5'-d(AGCACCGACTTGCTTGTAGC) R: 5'-d(CAGAGCCATGCTACAATTGAGG)	296 bp	55°C
MDM2 Exon 3	F: 5'-d(CATAATGATTAGATCCTCCCCAGCAT) R: 5'-d(CGACCACAAAATTAATGTTGCTGC)	338 bp	55°C
MDM2 Exon 4	F: 5'-d(GTTCCTGGTTGTTACCCCTAT) R: 5'-d(GAATGAGGGTAGAGGTGAAGT)	310 bp	55°C
MDM2 Exon 5	F: 5'-d(GAAGTCTGGTTAGATCCAGCTT) R: 5'-d(CCTCAGTATGTGGTTTTAGTTCATATG)	310 bp	55°C
MDM2 Exon 6	F: 5'-d(GCCACCACCAAGTTTCTGA) R: 5'-d(GTACAAGGTCCTAAGCATTAGGAA)	242 bp	55°C
MDM2 Exon 7	F: 5'-d(GGTGGGAGTGATCAAAAGGTAA) R: 5'-d(ACTCAGAGGTTAATTCATCTCAACC)	365 bp	55°C
MDM2 Exon 8	F: 5'-d(CTGCTGTAACAGTTGGACAGAT) R: 5'-d(CCGTATCCTTATTAGGACTGCC)	387 bp	55°C
MDM2 Exon 9	F: 5'-d(ACAGAGGTCAAGAGGTGATGTTTAT) R: 5'-d(GGCTATAATCTTCTGAGTCGAGAGA) (or) R: 5'-d(CCTCAAGTCCACAAACCAATGTGT)	168 bp 363 bp	55°C
MDM2 Exon 10	F: 5'-d(CCATTGTGGGTAAGGATTTCTCTC) R: 5'-d(GCTACAGGTCTCATCACAACAAAT)	438 bp	55°C
MDM2 Exon 11	F: 5'-d(AGTCCTCATGCTGTTTACAGTGACT) R: 5'-d(CACTATTCCACTACCAAAGTAGGTC)	898 bp	55°C
MDMX Exon 1	F: 5'-d(CTGCTGGTTGCCTTTGTGTG) R: 5'-d(GCTTCCTGCCTTGACTTCTC)	307 bp	55°C
MDMX Exon 1 (transcript 3)	F: 5'-d(GCTCAGCCTTCTAGCTCTC) R: 5'-d(ACCCACCTCTCAAGCTCCTC)	330 bp	55°C
MDMX Exon 2	F: 5'-d(AGGCGACAGAGCAAGACCTT) R: 5'-d(GGAGCTTGCAAGTATCTGAG)	1168 bp	55°C
MDMX Exon 3	F: 5'-d(GGAGCGGCTTTCCTGTTGTA) R: 5'-d(CAGTGCCTCATAGGCTACCT)	432 bp	55°C

MDMX Exon 4	F: 5'-d(AGATTCTGCCTTTGTATGCCTTAC) R: 5'-d(CCAGTCATGCCAAAGATAGCATTTC)	307 bp	55°C
MDMX Exon 5	F: 5'-d(CTAGGGACTAAACCTGGCTC) R: 5'-d(ACTCTGTCCCTGGTCTGTGA)	320 bp	55°C
MDMX Exon 6	F: 5'-d(CACACTAACTGGTGAGCCAG) R: 5'-d(GGGTTGCTAAAATAGCACTACCTC)	378 bp	61.8°C
MDMX Exon 7 (transcript 2)	F: 5'-d(GGGAGGAGATTTGAGCTCTG) R: 5'-d(CATCTGGAACTGAAGTTGGGC)	535 bp	61.8°C
MDMX Exon 8 (transcript 2)	F: 5'-d(TGGCGATGTAGTGTGACGAC) R: 5'-d(GCTTTTAAGGCAGCCCTGGTTA)	439 bp	55°C
MDMX Exon 9 (transcript 2)	F: 5'-d(AAGCTGTCTCCTTAAGTGCTAGAG) R: 5'-d(CAAGGTAGGGAGAGGATAAGATCAA)	434 bp	55°C
MDMX Exon 10 (transcript 2)	F: 5'-d(AGCAGTTGTGGCACTATCAGTGTA) R: 5'-d(CTGTTCTTCATTGTTAGCTCCAGT)	927 bp	55°C

This is a tabular summary of the primers used in the study. F = forward; R = reverse; T_m^o = actual annealing temperature used for each primer. * Primers were reproduced from Y Oda, 2000 (184).

3 Assessment of Methods

3.1 Aims

The aim of this Section is to examine the efficacy of the Abs utilised in this study and the related methodology, in detecting the relevant biomarkers by immune-staining techniques. The Section also includes brief examples of the optimisation of the methods experiments.

3.1.1 Choice of Control Cell Lines

HT29, U2OS and SW-872 cell lines were chosen as controls for the immune-staining experiments, as they have been widely utilised and extensively characterised regarding their P53, MDM2 and MDMX expression status (as shown in Table 3.1). Previous studies have shown that U2OS and HT29 over-expressed MDM2, whereas SW-872 had normal MDM2 expression. U2OS over-expressed MDMX whereas SW-872 had normal expression. All three cell lines had expressed P53 in different intensities. Wild type P53 was retained in U2OS but the other two cell lines had mutant genotypes for P53. Therefore, the selected three cell lines provided a sufficiently diverse platform for the proof of principle experiments.

3.1.2 Human Tissue Controls

The following controls were included in proof of principle experiments, after being verified and fully characterised by a Specialist Consultant Histopathologist (Dr Will Merchant, LTHT):

- (A) Negative controls: This included 1 sample of normal fat from breast tissue and 3 benign large lipomas, with confirmed normal *MDM2* by FISH.
- (B) Positive controls: Three samples of fully characterised liposarcoma, with confirmed *MDM2* amplification by FISH.

3.2 Proof of Principle Experiments

A series of experiments were performed on control cell lines and FFPE human tissues as “proof of principle”. These experiments included Immunochemical staining; Western blotting; and Sanger sequencing of genomic DNA.

3.2.1 Immunocytochemistry

ICC experiments for MDM2, MDMX and P53 were performed on the control cell lines, according to the protocol described in Section 2.7.1. The aim was to examine the specificity of the primary antibodies used (refer to Table 2.4) and the reproducibility of the results obtained. No primary or no secondary Ab controls were included as per protocol. Examples of ICC results are provided in Figures 3.1 and 3.2.

Negative staining (blue stain) was observed in all control experiments lacking primary and / or secondary Abs. The expression patterns of MDM2, MDMX and P53 were mosaic and appeared to be affected by the cell cycle phase. Strongly positive MDM2 nuclear staining (brown stain) was obtained in HT29 and U2OS. On the other hand, weaker and infrequent stain was detected in SW-872, which in this case was limited to cells undergoing division (mitosis). Similarly, strong positive MDMX staining was seen in U2OS but not in SW-872. All three cell lines stained positive for P53 with varying intensities. Reproducibility of results was confirmed upon repeating the control experiments.

The ICC results obtained demonstrated high specificity of the primary Abs used as they agreed with what has been previously described in the literature (Table 3.1).

3.2.2 Immunohistochemistry Control Experiments

IHC experiments were performed on FFPE human tissue controls (Section 3.1.2) as per the protocol detailed in Section 2.7.2.

These experiments showed negative nuclear stain for MDM2, MDMX and P53 proteins in all the 4 negative control tissues. Positive nuclear stains for MDM2, MDMX and P53 were obtained in all the 3 LS positive controls (as shown in Figure 3.3).

IHC results correlated with the known amplification status of *MDM2* by FISH. Additionally, intrinsic controls were demonstrated by a negative vascular endothelial stain within the positive control tissue slides (Figure 3.4).

3.2.3 Influence of Cell Cycle Phase on Expression of MDM Proteins

The ICC experiments had revealed a mosaic pattern of different MDM2 and MDMX stain intensities and intracellular localisations within each of the analysed cell lines. This observation agreed with the natural cellular behaviour of cell cycle regulatory proteins, like P53, MDM2 and MDMX, as the expression of these proteins may fluctuate during different phases of the cell cycle. To further elaborate on this observation and to examine if this phenomenon might influence the IHC scoring results, bearing in mind that LSs are slow growing tumours with limited mitotic figures, ICC analysis for MDM2 and MDMX was performed on the 3 control cell lines, after incubation of the tissue cultures with each of the cell cycle arrest agents shown in Table 2.4. The protocols for these experiments are detailed in Section 2.6.

Figures 3.5 and 3.6 illustrate the staining intensities and the intracellular locations of MDM2 and MDMX in response to cell cycle arrest reagents, respectively. Two cell lines were selected for the purpose of demonstration in these figures: SW-872, as it had normal expression of both MDM2 and MDMX; and HT29, as it over-expressed both proteins.

3.2.3.1 MDM2 Expression Influenced by Cell Cycle Phase

Predominantly nuclear MDM2 stain was seen in early S-phase, when cell cultures were under the influence of Aphidicolin. In comparison, when cell lines were held in a late S-phase and M-phase under the influence of Hydroxyurea and Nocodazole, respectively, the positive (brown) stain was detected in the cytoplasm, with distinct negative nuclear staining. These changes were noticeable in both the intracellular localisations and the intensities of staining signal and they were obvious both in cells that had apparently normal MDM2 expression (SW-872) and in those that over-expressed MDM2 (HT29, U2OS).

3.2.3.2 MDMX Expression Influenced by Cell Cycle Phase

For MDMX, no substantial effects on the expression intensities or intracellular locations were observed in the MDMX over-expressing cell lines (U2OS and HT29) in response to the cell cycle arrest agents. Only weak and predominantly cytoplasmic expression was noted in cell lines that did not overexpress MDMX in stress-free conditions (SW-872) when subjected to the influence of cell cycle arrest agents.

3.2.3.3 Implications of MDM Expressions in Response to Cell Cycle

While the expression patterns for both MDM2 and MDMX appeared to be influenced by the cell cycle phase, it seemed that MDM2 was significantly more affected than MDMX. However, to eliminate this potential source of bias in subsequent IHC profiling experiments, it was decided that dividing cells (mitotic figures) would not to be included in the scoring protocol.

It is noteworthy that different shift patterns of cellular MDM2 and MDMX expression were observed in response to the cell cycle arrest reagents. For example, Nocodazole-treated HT29 tissue cultures were noted to have negative nuclear MDM2 expression, but high nuclear and cytoplasmic MDMX. This observation confirmed lack of cross reactivity between the MDM2 and MDMX Abs used in the study.

3.2.4 Specificity of Antibodies

In order to examine the specificity of the Abs utilised in the study, Western blot experiments were performed in the control cell lines and FFPE tissue controls, according to the protocol described in Section 2.7.4. These experiments were performed to ensure that only Abs detecting appropriate single bands would be selected in subsequent IHC profiling experiments.

3.2.4.1 Protein Quantification

Cells were cultured and cell lysates were prepared as described in Section 2.7.3. Cell lysates from frozen tissues were prepared using the same buffer as that used for cultured cells. Protein concentration was analysed using a Bicinchoninic Acid Assay, according to the

protocol described in Section 2.7.3. Figure 3.7 illustrates the standard curve of the diluted BSA protein-gradient and the calculated protein concentrations for HT29, U2OS, SW-872 and a LS control. Results are shown in $\mu\text{g/ml}$. Despite culturing cells to similar confluency, U2OS contained the lowest protein content per unit volume of cell lysate.

3.2.4.2 Western Blot Experiments

Western blotting was performed for a mass equivalent of 20 μg of proteins per lysate, according to the protocol detailed in Section 2.7.4. A wide range molecular weight markers (Precision Plus Protein Standards – Dual colour [range: 10 – 250 kDa]) was used for MDM2 and MDMX Abs to scrutinise their specificities.

A- MDM2

Two different mouse monoclonal Abs were used: Abcam (2A10); and Santa Cruz (SMP-14) (see Table 2.4). Figure 3.8 shows the Western blot images of these 2 Abs for the three control cell lines. Multiple bands were detected when Abcam (2A10) was used and a single band, within 10% of the predicted molecular weight of MDM2 (56 kDa) was detected with Santa Cruz (SMP-14). Furthermore, the band intensities with the latter Ab corresponded with the ICC results and agreed with the described expression level of MDM2 in U2OS and HT29 in previous reports (186-189). The SW-872 control, which demonstrated normal (weak) MDM2 expression on ICC did not show a visible band on Western blot with Santa Cruz (SMP-14) Ab.

B- MDMX

While MDMX expression levels were not previously described in HT29, cell lines SW-872 and U2OS were known to have normal expression levels and over-expression of MDMX, respectively (refer to Table 3.1). Consequently, U2OS and a fresh LS sample, from the study cohort, which over-expressed MDMX on IHC, were used as positive controls and SW-872 was used as a baseline (weak) control. MDMX Western blot images obtained for these controls, demonstrated a single band, within 10% of the predicted molecular weight for MDMX (56 kDa), in positive controls and no visible band for SW-872 (Figure 3.9).

A single band within the predicted molecular weight range for P53 (53 KDa) was obtained for each of the control cell lines, when the experiment was replicated on a fresh blot, as seen in Figure 3.9.

3.2.4.3 Implications of Antibody Specificity Tests

For MDM2, Santa Cruz (SMP-14) Ab was selected for subsequent ICC and IHC optimisation experiments and in the analysis of the patient cohorts, since this demonstrated a single Western band of approximately the correct molecular weight. The Abcam (2A10) Ab was rejected.

For MDMX, Bethyl Laboratories (MDM4) Ab; and for P53, Leica Microsystems (DO7) Ab were accepted for subsequent experiments, as they each showed a single band within 10% of the predicted molecular weights of their corresponding proteins.

3.2.5 PCR and Gene Sequencing for MDM2 and MDMX

3.2.5.1 Rationale

It was important to examine if the detected MDM2 and MDMX proteins in the control cell lines were encoded by mutant genes, since mutations can affect the protein expression levels and this may potentially introduce bias in the subsequent planned experiments.

3.2.5.2 PCR and Sanger Sequencing

DNA was extracted from the control cell lines, as described in Section 2.7.6. All MDM2 and MDMX gene exons were amplified by PCR. The PCR products were purified prior to Sanger sequencing using the protocols described in Sections 2.7.7 and 2.7.8.

No mutations were detected in any of the exons for MDM2 and MDMX in all three control cell lines. The results are not shown for abbreviation.

3.2.5.3 Implications of PCR and Sanger Sequencing Experiments

As no mutations were detected in *MDM2* or *MDMX*, in any of the control cell lines, it was therefore demonstrated that the Abs used in immunochemical staining experiments were able to detect, at least, the wild type status of MDM2 and MDMX proteins.

3.2.6 Summary of Proof of Principle Results

In summary, the immunochemical staining results for MDM2, MDMX and P53 in cell lines and FFPE blocks demonstrated a reliable sensitivity and reproducibility of results for the utilised Abs, as they matched what had been described in the literature. The specificity of the Abs was demonstrated by a single band in the Western blot analyses and the Sanger sequencing results provided evidence that the detected MDM2 and MDMX proteins were of wild type status. Consequently, optimisation of methods and subsequent implementation of protocols for further sample analyses in the study was considered appropriate.

3.3 Optimisation of Methods

As described in Section 2.7.2.1, multiple and successive steps of IHC method optimisation were performed leading to enhanced sensitivity and specificity of the adopted methods in detecting the biomarkers of interest. LS tissues are naturally sensitive and fragile due to their minimal stromal epithelial components. Therefore, perhaps the most critical and challenging optimisation step was in the antigen retrieval techniques, as briefly discussed in this Section below.

Three antigen retrieval methods, utilising heat application in 10mM citrate buffer (pH 6.0) solution, were tried. It was noted that some conventional retrieval methods routinely used for other tissues, including the utility of microwave oven or pressure cooker, were too harsh on LSs and occasionally resulted in false positive results. Figure 3.10 illustrates false positive, strong MDM2 staining in the negative tissue controls (normal fat and benign lipomas), including non-specific positive staining of their vascular endothelium. However, when gentle retrieval by heated citrate buffer bath at sub-boiling temperature was employed, more specific nuclear staining was achieved. This has been demonstrated by no staining in negative controls; specific nuclear staining of lipoblasts in LS tissues; and negative staining

of vascular endothelium (internal controls) of examined controls. Therefore, the latter method was adopted in the subsequent cohort analysis experiments ensuring utility of negative controls with each run of IHC.

3.4 Discussion

3.4.1 Choice of Primary Antibodies

The primary antibodies selected for this project have been used in related studies and have produced a single band in Western blots in previously published work (190-192), which has been subsequently confirmed by Western blot experiments in this study. The MDM2 antibodies are sensitive to epitopes that are lost in the described non-functional MDM2 splice variants (refer to Figure 1.3, MDM2 splice variants). The MDMX epitope recognised by the antibody used maps to a region between residues 125 – 175, which is lost in the functional MDMX-S splice variant and therefore may have resulted in under-representation of MDMX functional cellular abundance. While MDMX-S is estimated to be over-expressed in 17% of STS, its over-expression in LSs appears to be far less common (80). P53 antibody is sensitive to both wild type and mutant proteins. It was raised to an epitope that does not reside within the P53 – MDM interaction domain and therefore has the ability to detect free and MDM-interacting P53.

3.4.2 Assessment of Method

Sensitivity and specificity of the antibodies used here for detecting the relevant biomarkers have been demonstrated by the following criteria:

1. Negative staining in no primary and no secondary Ab negative controls and reproducibility of results.
2. Matching ICC results of the control cell lines with what has been already published in the literature.
3. Satisfactory positive and negative IHC controls for benign and malignant tissues of confirmed *MDM2* status by FISH.

4. Satisfactory intrinsic controls showing specific staining of tumour cells and negative staining of vascular endothelium within the same examined tissue slides.
5. Distinct patterns of MDM2 and MDMX expression in cell cycle arrest experiments.
6. Western blot analysis resulted in a single band at the expected molecular weight for each of the analysed proteins. Antibodies producing multiple bands were rejected.
7. Successful optimisation of method experiments leading to increased specificity of IHC staining, sharper and easily interpretable results, leading to objective scoring.

3.4.3 Choice of Scoring Protocol

IHC assessments in this study were based on full tissue-block sections. Because the density of malignant cells (that are eligible for scoring) in LSs may be very low, implementing tissue microarray systems may not have permitted adequate scoring. While the researchers acknowledge the benefits of microarray-based IHC assessments in terms of experimental uniformity, implementation of this technique in LS tissue characterisation studies can potentially compromise the obtained results. Previous similar LS tissue-characterisation studies have also used full tissue blocks (34, 88).

The scoring protocol employed in this study was adapted from related LS studies (90). The protocol took into account the diversity of LS tissue characteristics, the sporadic paucity of malignant lipoblasts, the potential effects of cell cycle division in over-scoring and potential for inter-observer discordance. Disputed cases were revised jointly by the two scorers and then independently proof read and re-scored by a specialist consultant histopathologist.

Table 3.1: Characteristics of the analysed cell lines

Cell line	Origin	Genotype	Phenotype	Reference(s)
U2OS	Type: Human osteosarcoma Site: Tibia Ethnicity: Caucasian Age: 15 years	P53 wild type <i>MDM2</i> not amplified	<i>MDM2</i> : over-expression <i>MDMX</i> : over-expression P53: over-expression	(135, 164, 186-188)
SW-872	Type: Human liposarcoma Site: Unknown Ethnicity: Caucasian Age: 36 years	P53 mutant <i>MDM2</i> not amplified	<i>MDM2</i> : normal-expression <i>MDMX</i> : normal-expression P53: over-expression	(188, 193)
HT29	Type: Human adenocarcinoma Site: Colon Ethnicity: Caucasian Age: 44 years	P53 mutant <i>MDM2</i> amplification status is unknown	<i>MDM2</i> : over-expression <i>MDMX</i> : unknown P53: over-expression	(189)

This is a tabular summary for the relevant characteristic features of the analysed cell lines in the study with their related references as described in the literature.

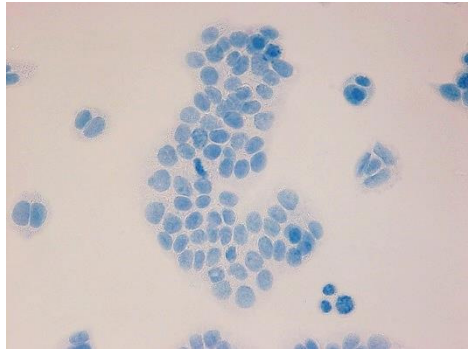
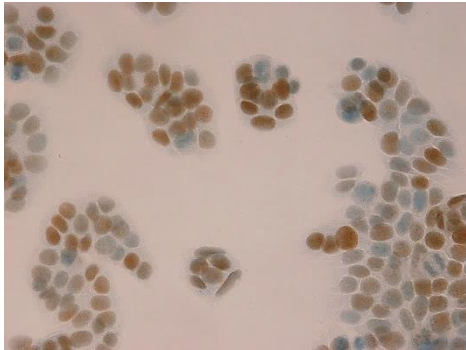
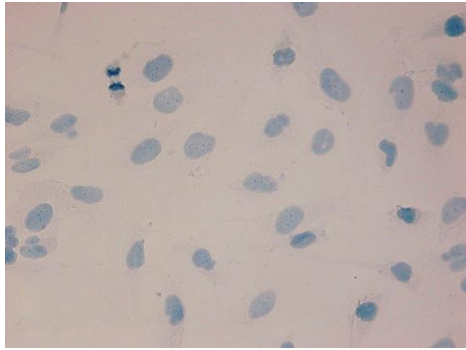
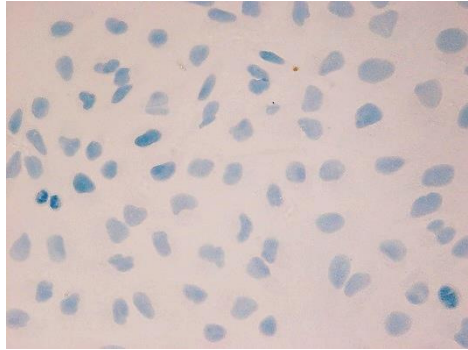
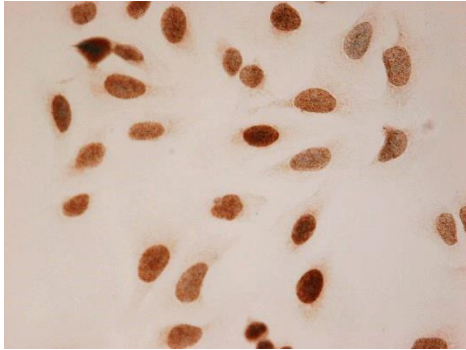
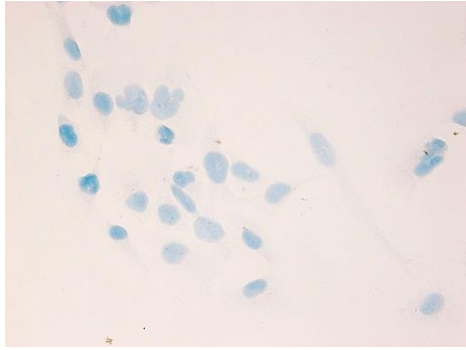
	No primary antibody control	Positive control	Negative control
MDM2 controls	<u>HT29</u> 	<u>HT29</u> 	<u>SW-872</u> 
MDMX controls	<u>U2OS</u> 	<u>U2OS</u> 	<u>SW-872</u> 

Figure 3.1: MDM2 and MDMX positive and negative cell line controls

A representative sample of cell line controls for MDM2 and MDMX. Note the negative (blue stain) in samples with no primary antibodies. Positive (brown stain) was seen in cell lines known to over-express MDM2 and MDMX. No brown stain was seen in negative cell line controls. All images were taken at 40 x magnification.

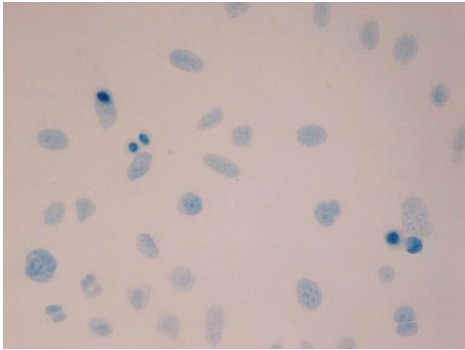
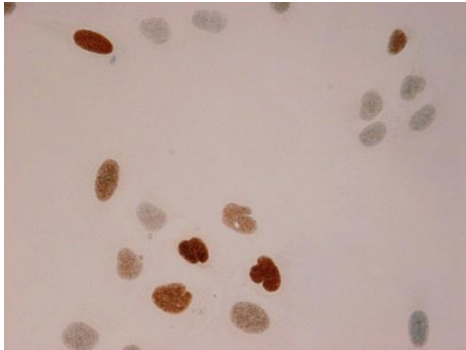
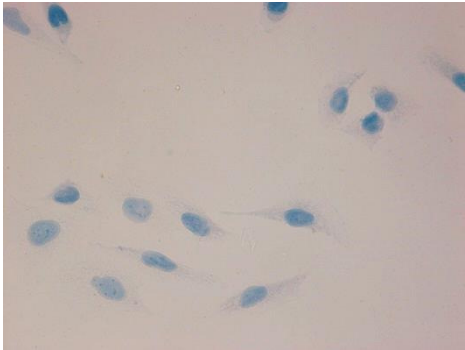
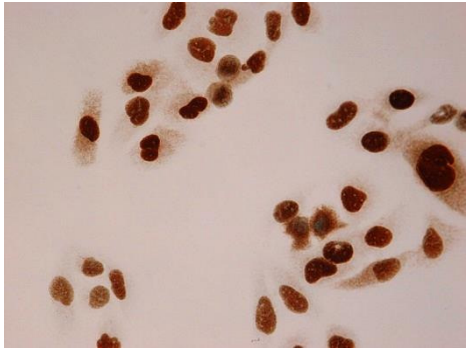
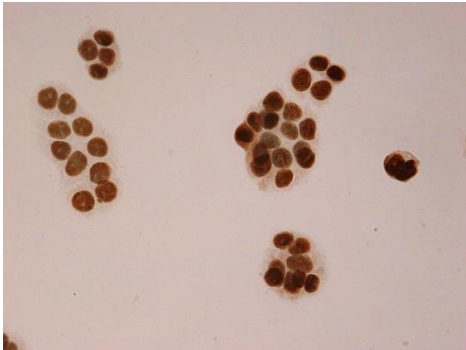
	No primary antibody control	P53	P53
Wild type P53 control	<u>U2OS</u> 	<u>U2OS</u> 	
Mutant P53 controls	<u>SW-872</u> 	<u>SW-872</u> 	<u>HT29</u> 

Figure 3.2: P53 cell line controls

A representative sample of P53 cell line controls. Uniform over-expression of P53 was seen in cell lines with mutant P53 compared to wild type status. The figure illustrates the ability of the primary antibody to detect both mutant and wild type P53. All images were taken at 40 x magnification.

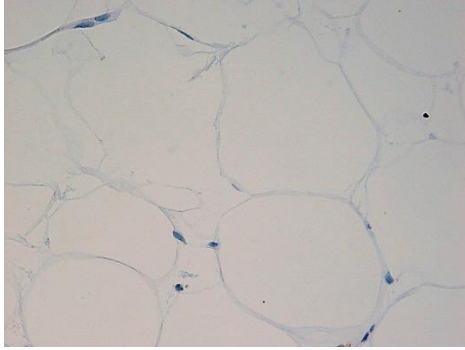
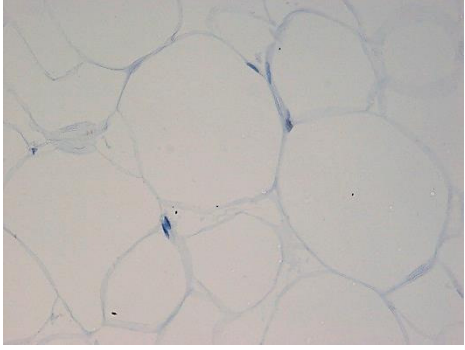
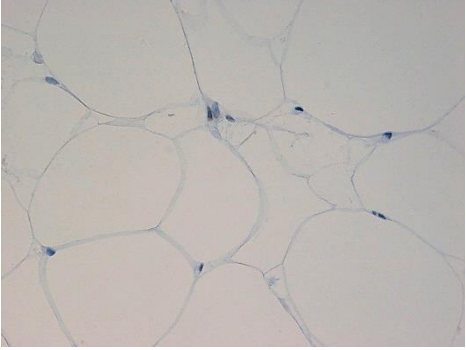
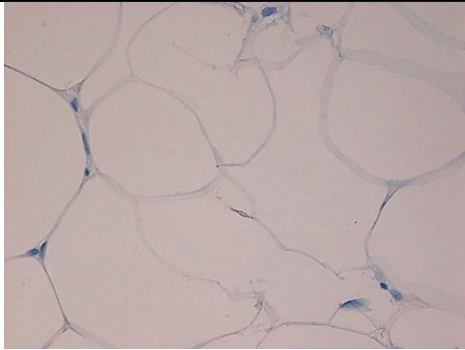
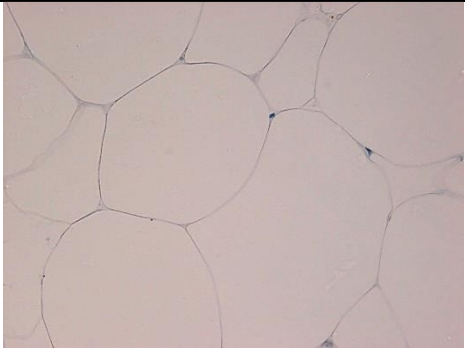
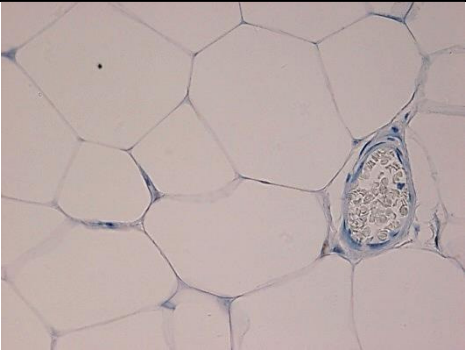
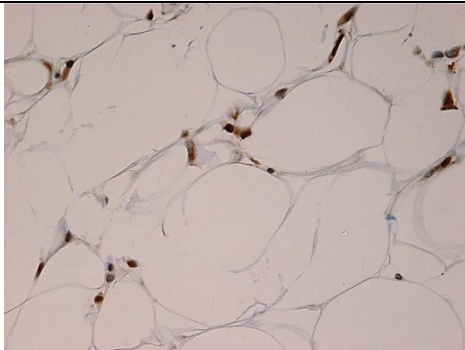
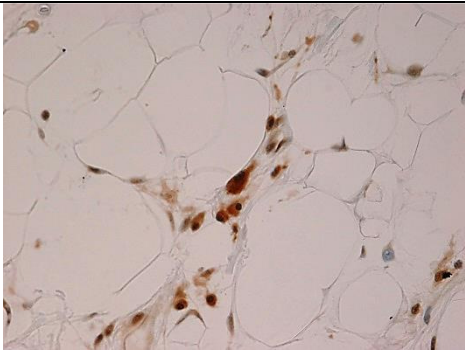
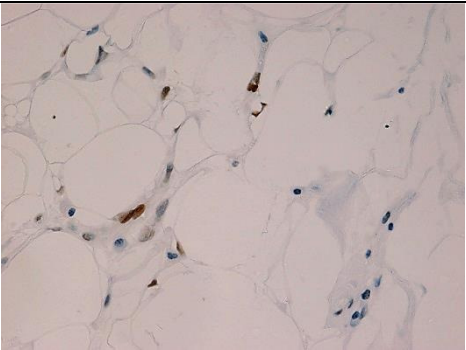
	MDM2	MDMX	P53
Normal fat from breast tissue (negative control 1)			
Lipoma (negative control 2)			
WDLS (positive control) <i>MDM2</i> amplified P53 wild type Sample no. 16			

Figure 3.3: Immunohistochemistry tissue controls

Sample IHC results from control tissues demonstrated negative staining in normal fat and lipomas and positive staining in liposarcoma. All images were taken at 40 x magnification.

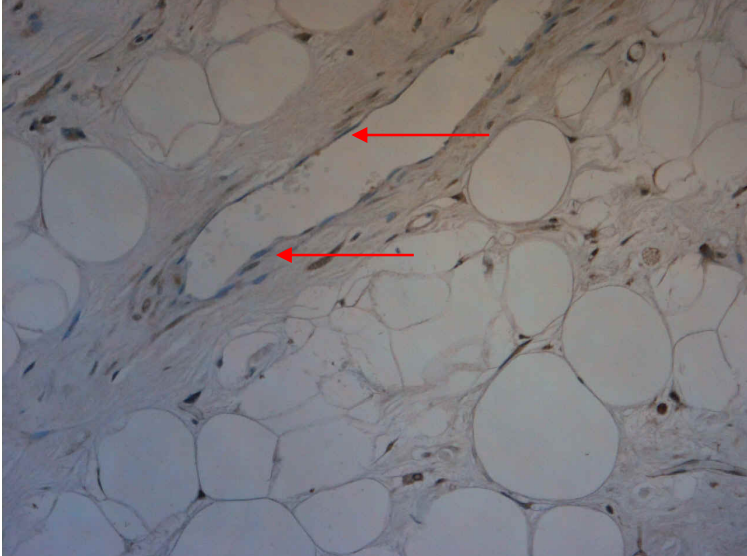
Tissue characteristics	Intrinsic Positive / Negative controls
<p>WDLS</p> <p><i>MDM2</i> amplified</p> <p>MDM2 controls:</p> <p>Positive: MDM2 over-expression</p> <p>Negative: no staining in vascular endothelium</p>	
<p>WDLS</p> <p>MDMX controls</p> <p>Positive: MDMX over-expression</p> <p>Negative: no staining in vascular endothelium</p>	

Figure 3.4: Intrinsic controls

Illustration of intrinsic tissue controls showing positive MDM2 / MDMX staining in lipoblasts and negative staining in vascular endothelium (as indicated by the red arrows). Images were taken at 60 x magnification.

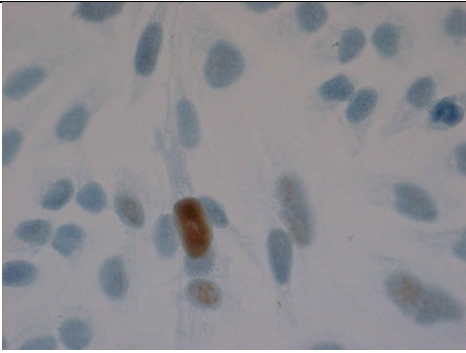
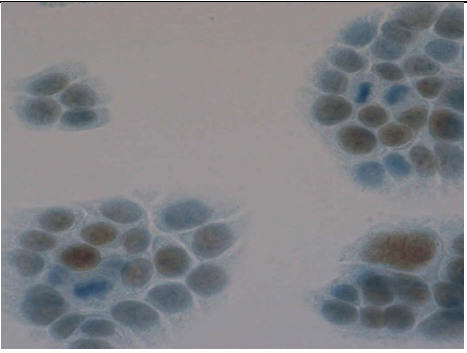
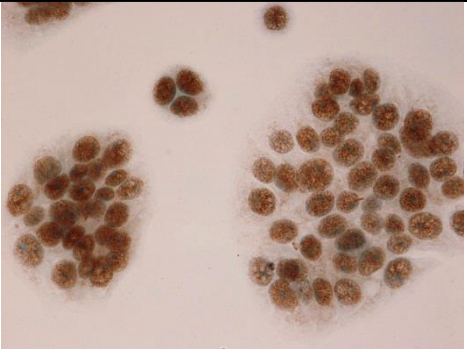
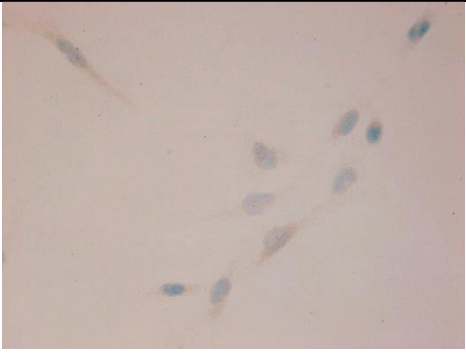
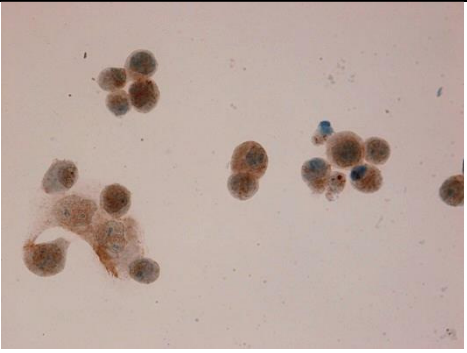
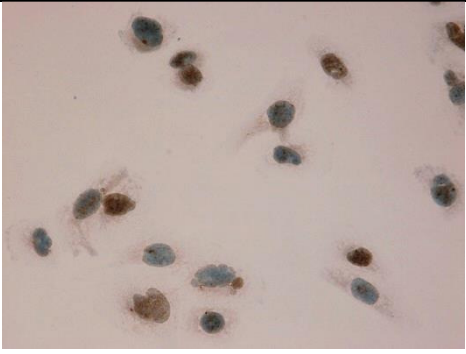
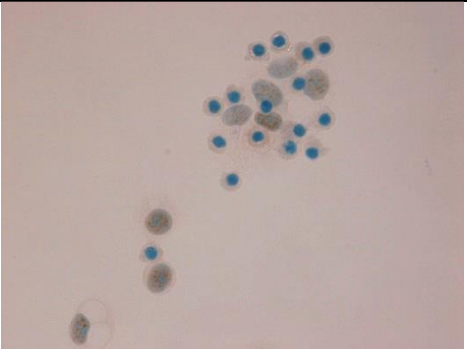
Immunocytochemistry - MDM2, cycle arrest reagents		
Agent	SW-872	HT29
DMSO control vehicle		
Aphidicolin Early S-phase		
Hydroxyurea Late S-phase		
Nocodazole M-phase		

Figure 3.5: ICC for MDM2 in different phases of the cell cycle

Note the SW-872 DMSO control sample showing negative staining except for cells in division, the intensities and intracellular localities of MDM2 were affected in response to different cell cycle arrest reagents. All images were taken at 40 x magnification.

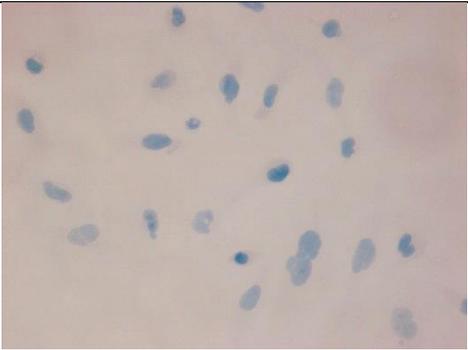
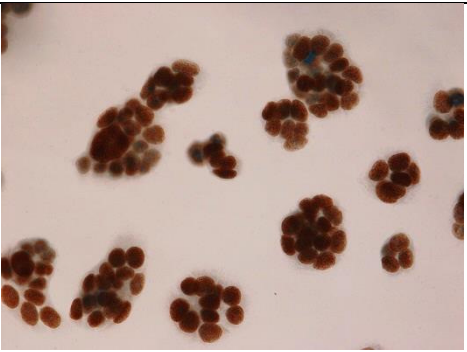
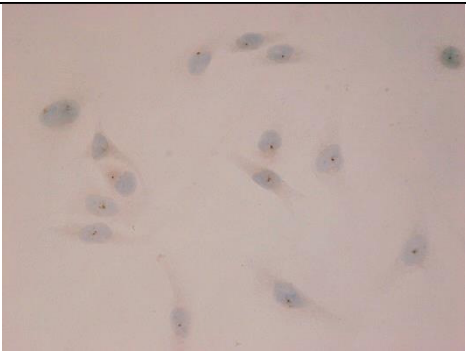
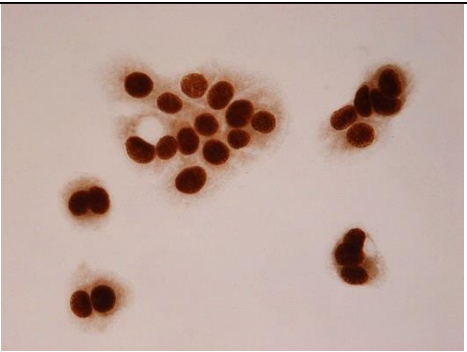
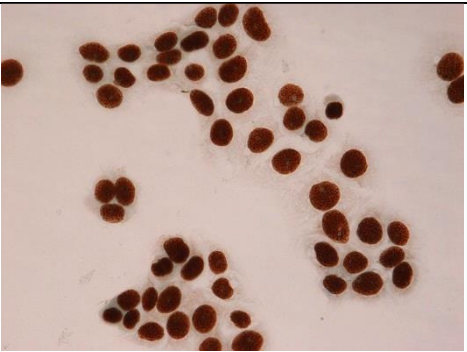
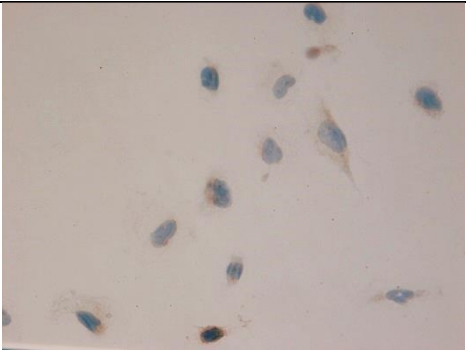
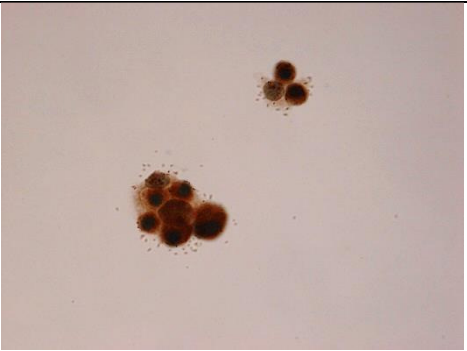
Immunocytochemistry – MDMX, cell cycle arrest reagents		
Agent	SW-872	HT29
DMSO control vehicle		
Aphidicolin Early S-phase		
Hydroxyurea Late S-phase		
Nocodazole M-phase		

Figure 3.6: ICC for MDMX in different phases of the cell cycle.

SW-872 showed weakly positive cytoplasmic stain in response to cell cycle manipulation. Note how the strongly positive HT29 remained non affected by the cell cycle arrest reagents. All images were taken at 40 x magnification.

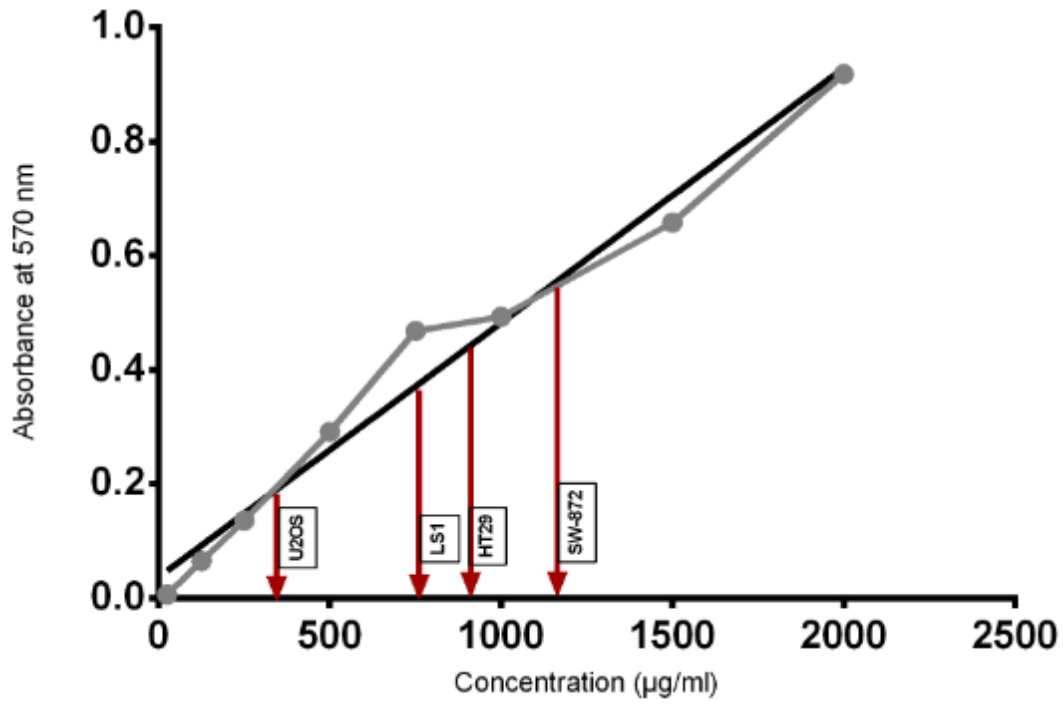


Figure 3.7: Protein quantification in cell lysates

Adjusted linear curve from standard protein concentration gradient showing the calculated protein concentrations of the analysed samples.

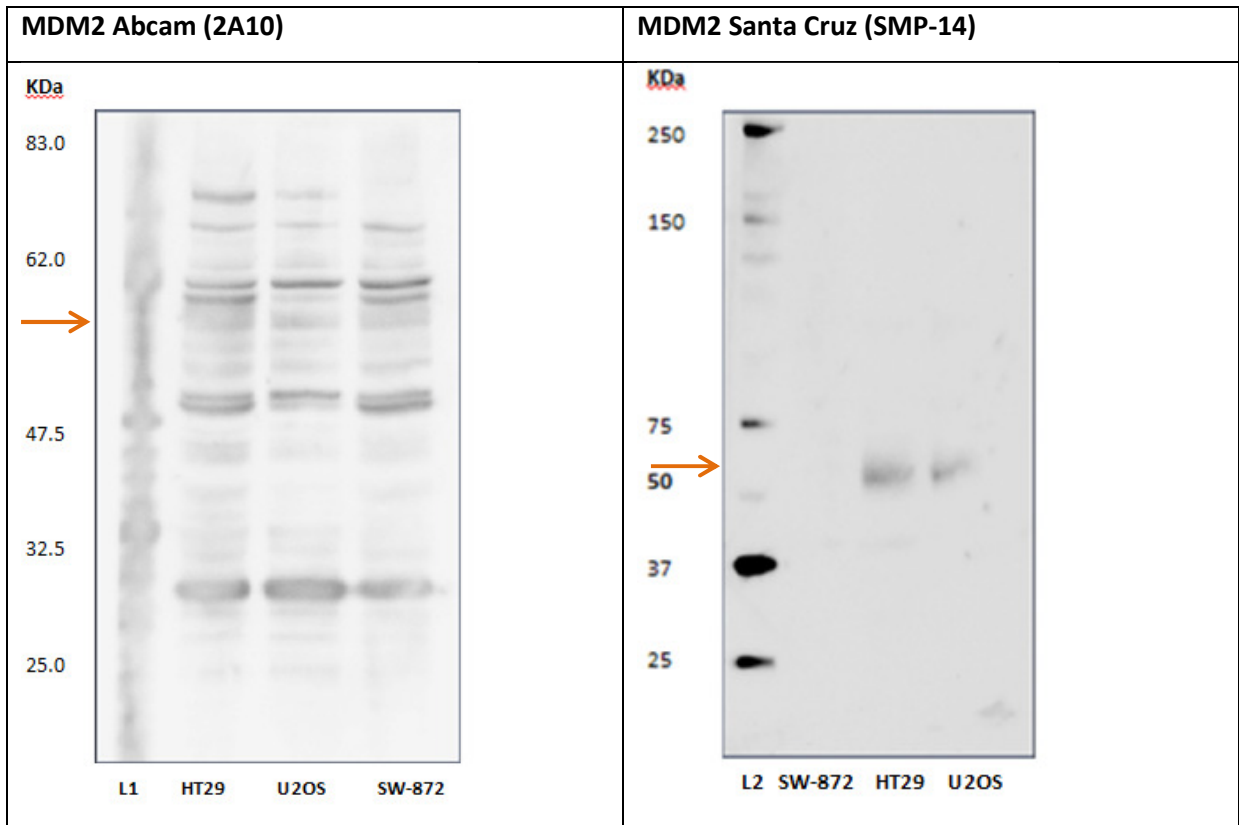


Figure 3.8: Western blot images for MDM2

Western blot images for different MDM2 antibodies demonstrating multiple, nonspecific bands with Abcam (2A10) Ab, compared to single band within 10% of predicted molecular weight of MDM2 when using Santa Cruz (SMP-14) Ab. The arrows indicate the predicted location of MDM2 band within the molecular weight ladder. Note the higher intensity of HT29 band similar to ICC scores and no band was seen in the base line (weak) control cell line (SW-872) when Santa Cruz (SMP-14) Ab was used. L1 = ladder1 (Pre-stained Protein Marker); L2 = ladder2 (Precision Plus Protein Standards). Wider range molecular weight markers were intentionally used for MDM2 and MDMX study-approved Abs to confirm their specificities.

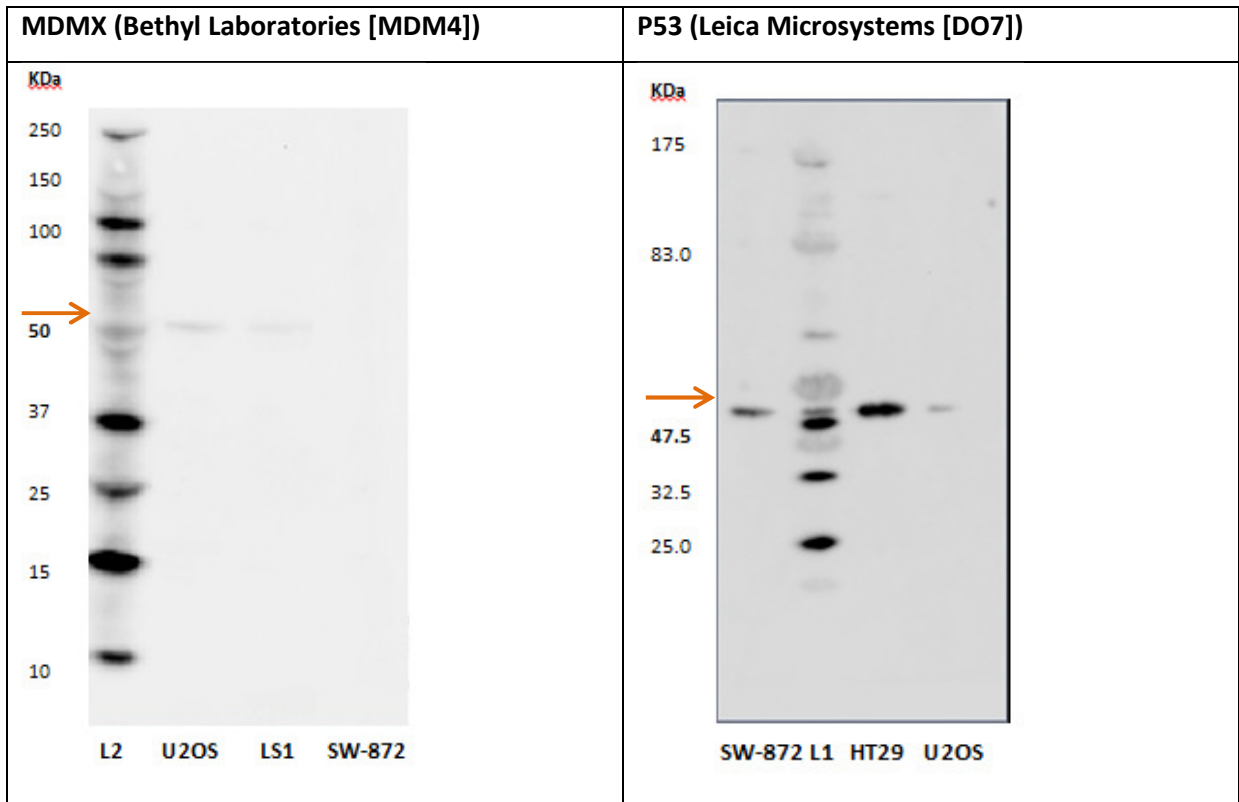


Figure 3.9: Western blot images for MDMX and P53

Western blot images for MDMX and P53 showing visible bands within 10% of the predicted molecular weights. The arrows indicate the predicted location of the protein within the molecular weight ladder. Note no band was detected for MDMX in SW-872 cell line. A high Intensity P53 band in HT29 similar to its ICC results. LS1, liposarcoma control case; . L1 = ladder1 (Pre-stained Protein Marker); L2 = ladder2 (Precision Plus Protein Standards). Wider range molecular weight markers were intentionally used for MDM2 and MDMX study-approved Abs to confirm their specificities.

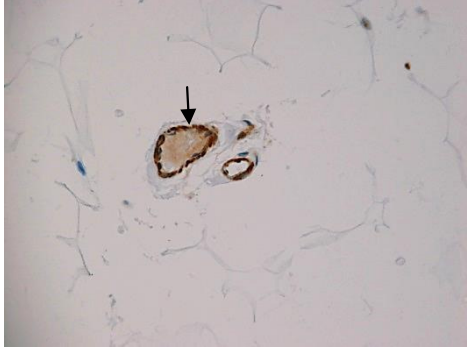
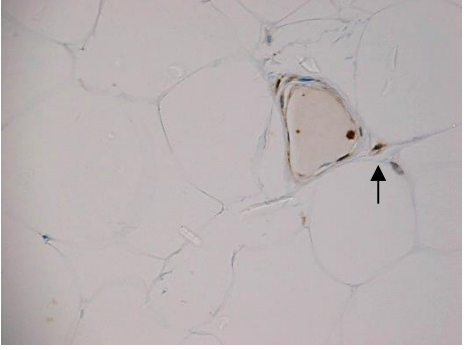
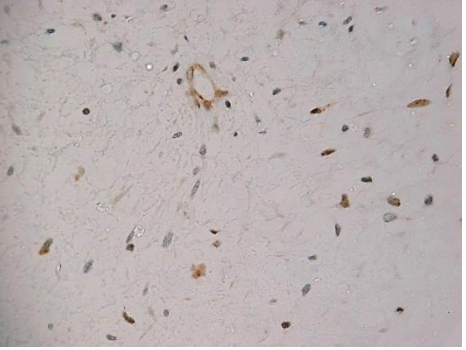
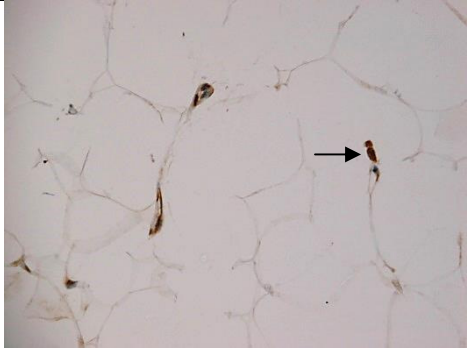
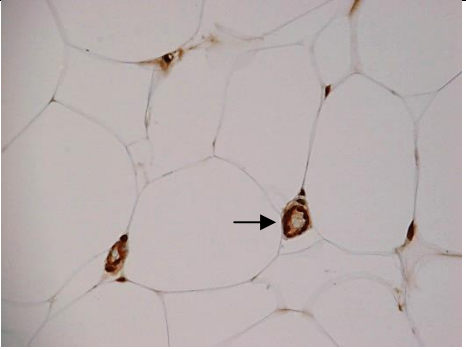
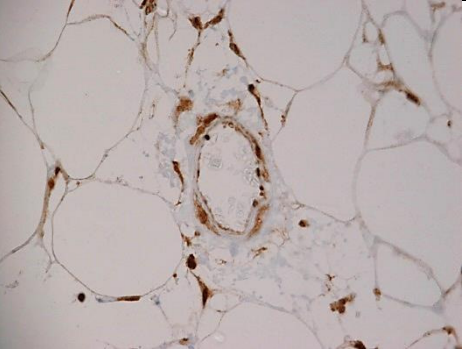
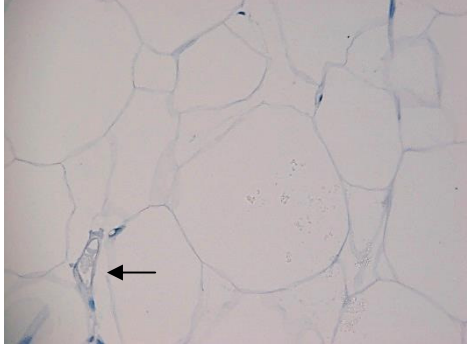
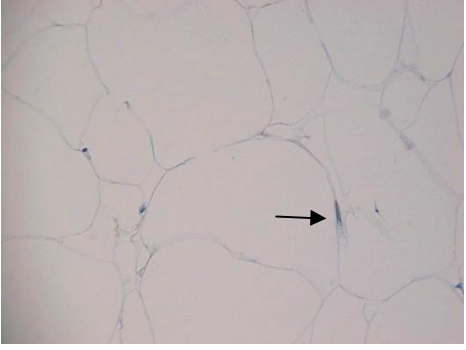
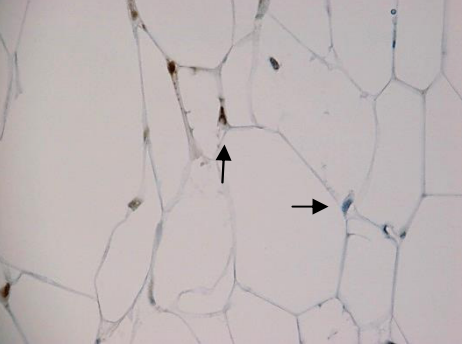
Method	Normal fat from breast tissue	Lipoma	Liposarcoma	Comments
A- Microwave oven heat application at 800 watt in for 10 minutes				Non-specific staining including vascular endothelium, false positives in fat and lipoma
B- Pressure cooker retrieval for 2 minutes				Unanimous non-specific staining, false positives in fat and lipoma
C-Gentle retrieval in hot bath at (95-98 °C) for 20 minutes				Preserved tissue architecture, specific staining, adequate negative and internal controls

Figure 3.10: Antigen retrieval examples for MDM2

Illustrative example of different antigen retrieval techniques. All methods used 1mM citrate buffer solution (pH 6.0). Note a false positive MDM2 staining, including a vascular endothelium, in negative control samples (normal fat and lipoma) when microwave oven heat and pressure cooker methods are applied. Specific nuclear staining in LS positive control was obtained with satisfactory negative controls (including negative vascular endothelium) when gentle retrieval in hot citrate buffer bath was used.

4 Immunohistochemical Profiling of Liposarcoma

4.1 Aims

The primary aim of this Section is to describe the expression profiles of *MDM2*, *MDMX* and *P53* in different subtypes of LS, and to examine the effect of *MDM2* and *MDMX* co-expression on *P53*.

The secondary aims are to assess the correlation between *MDM2* amplification and over-expression, and explore the value of IHC, as a complementary tool to FISH, in making the diagnosis of WDLS and DDLS.

4.2 Cytogenetic Results in Liposarcomas

Cytogenetic analysis was performed by the Yorkshire Regional Genetics Services, as described in Section 2.9. The results were retrieved and analysed by the researcher. Cytogenetic testing (G band analysis and / or FISH) was attempted in 60 of the 64 LS cases in the cohort. It provided additional molecular data to the histopathologist to aid the diagnosis in 55 cases and completely failed in 5 cases (92% success rate). Failure to provide interpretable results was largely due to inadequate primary cell culture growth, required for metaphase spread in G band analysis, or due to overgrowth of fibroblasts and other normal cells. Occasionally FISH analysis failures were from low numbers of malignant cell in the LS sections provided to the Cytopathologist. An example of cytogenetic analysis results is provided in Figure 4.1. A summary of the cytogenetic results of the liposarcoma cohort analysed here is presented in Table 4.1 and any variations specific to a subtype are described below.

Cytogenetic analysis was attempted in 10 of the 12 MXLS-RCLS cases and completely failed in one case. The majority of the successfully-analysed MXLS-RCLS cases (n=7/9) displayed the characteristic chromosomal translocation t(12;16)(q13;p11). However, one case displayed multiple complex translocations and another showed a probable *MDM2* amplification.

Cytogenetic analysis was attempted in all but one of the 43 WDLs and failed in 3 cases. It confirmed the diagnosis of WDL by a detected *MDM2* amplification in 33 of the 39 successfully-analysed cases. However, it revealed some inconsistencies between the histological diagnosis and the molecular features in 6 cases, as FISH analysis in these failed to show the characteristic *MDM2* amplification to support the histological diagnosis. In contrast, all DDLs analysed by FISH (n=7) had *MDM2* amplification.

This study identified four WDLs and two DDLs that had apparently normal karyotyping by G band examination and were not originally subjected to FISH analysis to examine for *MDM2* amplification. These cases underwent specialist review and subsequent FISH analysis on their stored tissue blocks at the Pathology Department, LTHT. FISH analysis of these cases revealed *MDM2* amplification in the DDLs and in 2 of the 4 WDLs.

Collectively, successful cytogenetic analysis confirmed the histological diagnosis in 48 of the attempted 60 cases (80%); provided results inconsistent with the histological features in 7 cases (12%); and failed to provide results in 5 cases (8%).

4.2.1 Correlation between *MDM2* Amplification and Over-Expression

78% of all WDL and DDL that demonstrated amplification of the *MDM2* gene by FISH showed *MDM2* over-expression on subsequent analysis (n=31/40). On the other hand, all 6 WDLs with no apparent *MDM2* amplification by FISH were found to have over-expressed the *MDM2* protein. A contingency table of *MDM2* amplification and *MDM2* over-expression is provided in Table 4.2.

4.3 Subtype – Specific Expression Profile of Liposarcomas

Sixty four, histologically-characterised, LS cases were analysed by IHC (Table 4.3) according to the protocols detailed in Section 2.7. These comprised the following sub-types: WDL (n=43) including 1 case of inflammatory and 1 case of mixed differentiation; DDL (n=9); and MXLS-RCLS (n=12). The subtype-specific expression levels of each of the analysed proteins are demonstrated in Figure 4.2.

4.3.1 Well-Differentiated Liposarcomas

77% (33/43 cases) of WDLS over-expressed MDM2, mostly at high intensity (++) score = 56%) with a median MDM2 score of 43. Co-expression of MDMX was seen in 56% of all cases, as 9 of the 33 cases that over-expressed MDM2 did not co-express MDMX. The solitary MDM2 over-expression was not featured in the other LS subtypes. MDMX expression was not only less frequent than MDM2 in WDLS but also had lower scores per individual case. Only 10 cases scored (++) , with a median MDMX score of 14.

10 cases had apparently diminished expression levels of both MDM2 and MDMX. This expression profile mainly correlated with normal P53 expression. However, two of these cases showed P53 over-expression, suggesting a possible *P53* mutation.

P53 over-expression was seen in 26% of cases (n=11). Excluding the two cases mentioned above that had normal MDM2 and MDMX, P53 over-expression was mainly detected in cases that co-expressed both MDM2 and MDMX in abundant levels (++) .

A trend of normal (low) cellular expression of P53 was largely observed in cases that over-expressed MDM2 solely (n= 8/9) or in association with MDMX, where the relative expression levels of the MDM2 were significantly higher in relation to MDMX (n=14/14).

4.3.2 De-Differentiated Liposarcomas

All 9 cases of DDLS showed MDM2 and MDMX over-expression, in relatively high intensities. The expression level of the two proteins was comparable to one another with a median MDM2 score of 92 and MDMX score of 60. Both median scores are within the (++) stratification of the scoring protocol.

P53 over-expression was seen in 7 of these cases (78%). The two cases that did not over-express P53 had relatively higher expression levels of MDM2 in relation to MDMX. This observation is in agreement with the P53 expression trend noted in WDLS.

4.3.3 Myxoid - Round Cell Liposarcomas

The majority of the 12 MXLS-RCLS had positive MDM2, MDMX and P53 staining. A predilection to over-express MDMX at higher relative levels, compared to other LS subtypes, was noted with a median MDMX score of 88.5 and median MDM2 score of 84.5. Ten of these cases also had positive P53 expression (83%). Only 1 case had apparently normal expression of the three proteins. Round cell de-differentiation was detected histologically in 3 cases. It did not influence the staining pattern.

4.3.4 All Liposarcoma Subtypes

As shown in Table 4.3, MDM2 over-expression (+/++) was detected in 83% of cases (n=53/64). MDMX co-expression (+/++) was seen in 69% of cases (n=44/64) in varying ratios compared with MDM2. The co-expression pattern was subtype-dependent. WDLS displayed abundant levels of MDM2 in relation to MDMX, whereas all other subtypes had comparable levels of MDM2 and MDMX expression. No solitary MDMX (without MDM2) over-expression was detected in any of the analysed cases. 44% of cases (n=28/64) had positive P53 expression (+). Perhaps unexpectedly, most of these cases (n=25/28) co-expressed both MDM2 and MDMX as well.

4.4 Analysis of Results and Discussion

Due to real challenges in attaining accurate histological diagnoses in some LSs, it has been an acceptable practice for pathologists to stream their diagnoses into: certain; probable; and possible categories, based on the index of suspicion provided by the clinical and the histological features. This approach is subjective and the proportion of cases allocated into these categories is related to the experience and the expertise of an individual pathologist. However, this streaming provides a practical tool to the certainty of the diagnosis, which is used in daily practice (194). The practice at LHTH adopts the safest approach principle and a patient's diagnostic coding of LS may be based on reasonable clinical and histological suspicions in some instances.

4.4.1 Discrepancies between Histological and Molecular Diagnostic Features

The integration of molecular analysis into the diagnostic classification of LSs has added a valuable tool to the provision of a more accurate histological diagnosis. However, this integration has its own imperfections: the success rate to provide an interpretable result is approximately 90% (a similar rate was seen in this study); and the results obtained may not always match the given histological diagnosis, which may occasionally provide an additional source of diagnostic conflict. Therefore, it has been accepted that the input from molecular analysis may confirm a malignant diagnosis but will not provide a gold-standard alternative to the classical morphological histological diagnosis made by a specialist pathologist. This consensus is practiced at the MDT meeting of the Sarcoma Department at LTHT. In fact, it is also clearly documented in a recent review that involved 763 STSs including 220 LSs. The review showed *MDM2* amplification in 96% of cases where the histological diagnosis was “certain” and in 79% in those where the diagnosis was “probable” (194). In contrast, a separate review of 50 LSs has revealed 50-70% concordance between histological diagnosis and molecular analysis (81). Such variations may represent the natural spectrum of diversities in LSs and the genuine challenge to establish a clear and objective distinction between certain types of benign lipomatous tumours and certain subtypes of LS (mainly WDLS).

Upon reviewing the relevant literature, as summarised in Table 4.4, some studies report identifying WDLS and DDLS cases that lack *MDM2* amplification. Collectively, these account for about 8% of cases. This is comparable with the findings of our study, as *MDM2* amplification was seen in 73% of the successfully-analysed WDLS and DDLS. Discrepancies between the histological and molecular findings were identified in 7 cases among all LS subtypes of the analysed cohort. Most of these discrepancies (6 of 7 cases) were, unsurprisingly, among the WDLS subtype as these tumours are the closest mimickers of benign lipomas in their histological appearance and occasionally their clinical behaviour. Five of these 6 cases presented in the extremities and one in the chest wall. They were relatively smaller in size compared to the remainder of WDLSs cases in the cohort, with a median size of 234 cm³, compared to 1080 cm³ for WDLSs with *MDM2* amplification. In depth analysis, revealed that one of these cases had chromosome 12 gain (4x) where *MDM2* maps; and 2 cases had a somatic P53 mutation (as will be discussed in Section 5.4). These

changes may present the driving force for carcinogenesis in this specific cohort. Polyploidy of chromosome 12 has been previously reported in LS (195). The other discrepancy was seen in a MXLS that presented in the retroperitoneum and demonstrated a possible *MDM2* amplification. However, the molecular findings were not certain in this case.

All these 7 cases underwent an independent review by a specialist histopathology consultant outside the research group. Additionally, further cytogenetic testing including 13q deletion, which is a characteristic of benign and low-malignant lipomatous tumours (196), was performed on the archival tissue blocks, to aid the revised diagnosis. Three cases were found to have 13q deletions of which two may be alternatively pleomorphic or spindle-cell lipomas. However, the site of presentation (thigh) is extremely rare for such tumours. Diagnoses of the other four cases remained unchanged after the review. Table 4.5 summarises the key features of these cases.

It is worth mentioning that the status of *MDMX* amplification was not assessed in the tumours in our study and we are not aware of any preceding published reports that characterised LS in this aspect. However, *MDMX* amplification and over-expression, without a concomitant *MDM2* amplification or *P53* mutation, has been reported, as the potential driving mechanism of transformation, in a subset of Glioblastomas (197). It may be legitimate to ask if a similar subset of cases exists within LSs, especially since two of the *MDM2* non-amplified WDLS cases over-expressed *MDMX*.

4.4.2 *MDM2* Amplification to Overexpression

Gene amplification can result in *MDM2* or *MDMX* protein over-expression. The relevant literature review (Table 4.4) showed that approximately 80% of WDLS and DDLS, including those with confirmed *MDM2* amplification, were found to over-express *MDM2* protein. These findings are in agreement with the results of this study (Table 4.2).

Similarly, many tumours over-express *MDM2* and *MDMX* without increased copy numbers. These include: retinoblastoma (198); melanoma (84); Ewing sarcoma (192); and colon cancer (146). In our study, all WDLS cases without *MDM2* amplification, over-expressed *MDM2* (n=6). This may emphasise the complementary role of IHC in obtaining an accurate diagnosis and suggests that different mechanisms may have triggered the protein over-

expression, other than amplification. Therefore, assessment of tumours based on gene amplification alone may underestimate the numbers of cases in which MDM2 and / or MDMX over-expression contributes to cancer initiation and progression. Consequently, it may underestimate the potential candidates for selective blocking strategy treatments based on MDM / P53 interactions.

4.4.3 MDM / P53 Expression Profiles

In agreement with previous reports (90, 199), MDM2 over-expression was frequently detected across the various subtypes of LS. MDMX co-expression was also a common feature and probably more frequent than previously reported (80, 118). However, the previous reports on MDMX expression had relatively limited numbers of LSs within their STS cohorts (n=18 and 37, respectively) and they were mainly focused on MDMX-S splice variant as a prognostic indicator. At the time of writing this report, we were not aware of any large study that described MDMX expression patterns in LS to compare our results with.

A previous analysis that included 74 LSs has reported 96% IHC positivity (>10% of cells) for MDM2 and P53 in retroperitoneal WDLS and DDLS, compared to only 33% in non-retroperitoneal LSs of the same histological subtypes (34). This observation was not replicated in our study, as no specific patterns of MDM2, MDMX or P53 expression, in relation to their anatomical distribution, were observed in our cohort (Table 4.6). This variation may be explained by the discrepancies in the antigen retrieval techniques, the primary Abs used and the scoring systems employed. Whereas retroperitoneal LSs generally have a worse prognosis, this is believed to be due to late presentation and difficulty in obtaining clear microscopic margins surgically (200). To explore whether distinct phenotypical characteristics are retained in retroperitoneal LSs that would make them more aggressive, may prove to be a complex task with multiple variables, which is beyond the scope of this study.

As MXLS-RCLS feature cytogenetic alterations that do not implicate amplification or direct alterations to MDM2 or MDMX genes, previous studies regarding the expression levels of these proteins are limited and often MXLS - RCLS subtypes are excluded from LS immunohistochemical characterisation studies for the same reason (201). However, the

available results from the literature, regarding MDM2 over-expression in MXLS are essentially inconsistent. Some studies claimed normal MDM2 expression in all these cases (34, 88) (n=26 and 23, respectively) and others reported over 50% incidence of MDM2 over-expression (90, 199) (n=8 and 8, respectively). However, a more recent report that analysed 56 cases of LS with myxoid stromal features has shown MDM2 over-expression in 95% of cases (202). These differences may also be explained by the use of different, relatively new, primary Abs and the alterations in the IHC techniques. On the other hand, they may be genuine manifestations of tumour and intra-tumour heterogeneity (203) or genetic variations amongst the population of these subtypes of cancers, including *MDM2* amplification, which was reported in 14% of MXLS in a previous study that included 22 cases (81). The results of our study are consistent with higher expression of both MDM2 and MDMX proteins. Again, no previous analysis has described MDMX expression pattern in MXLS-RCLS subtypes.

The described pattern of MDM2 and MDMX co-expression in the different subtypes of LS, was analysed further. The results confirmed that the same cases expressed the two proteins concomitantly, as shown in the following scatter plots (Figure 4.3), representing the actual expression values of MDM2 and MDMX across the different subtypes of LS.

The observation of MDMX co-expression with MDM2 may invite further in-depth analysis of the dynamic, complex interactions between these proteins and their effect on P53. The co-expression pattern, commonly seen in WDLS, in which MDM2 levels are higher in relation to MDMX (MDM2 : MDMX ratio >1) agrees with the previously-described cytological interactions between the two proteins, where MDMX increases the short half-life of MDM2 (105) and in turn, MDM2 degrades MDMX (134). However, the observed comparable expression levels of the two proteins in DDLS and MXLS-RCLS may, in turn, represent how the ability of MDM2 to degrade MDMX becomes futile beyond a certain threshold of activity (135). This observation, therefore, invites further assessment to elaborate the precise MDM2 activity in these subtypes.

In this study, MDM2 and MDMX co-expression was noted to correlate with the expression levels of P53 in two distinct patterns as shown in Figure 4.4:

A) A collaborative pattern: where diminished or no P53 expression was detected. This pattern was mainly observed in cases where MDMX was co-expressed with MDM2 but at relatively lower levels (+) (represented in Table 4.3 by the blue cell). This pattern could have resulted from MDMX collaborating with MDM2 to inhibit P53 by targeting it for degradation and leading to diminished P53 expression, in line with MDMX acting as an MDM2 stabiliser. Tumours with this expression pattern may respond well to MDM2 blockers or dual specificity antagonists of higher MDM2 affinity.

B) A competitive pattern: where higher scores of P53 were observed (>10% of cells). This pattern was mainly noted in cases where MDMX was co-expressed at relatively high levels (++) (represented in Table 4.3 by the pink cell). This pattern may be explained by MDMX possibly “competing” with MDM2 in binding to P53, resulting in reduced P53 degradation by MDM2 and therefore higher cellular expression levels, in line with MDMX acting, here, as a P53 stabiliser (137, 204). Tumours that express this profile may best be targeted by dual blocker compounds. One could argue that MDMX single affinity blockers may have a reduced therapeutic potential in these cases, as the resulting MDMX-freed P53 may then be subject to degradation by the over-expressed MDM2, if no MDM2 antagonist is used in conjunction.

As no cases of LS that over-expressed MDMX exclusively (in the absence of MDM2) were detected, there must be questions about the utility of single affinity MDMX blockers in LS. However, antagonising MDMX-mediated P53 suppression may still have some beneficial therapeutic effect in these cases and functional studies will be needed to clarify this.

These observations regarding patterns of co-expression are in agreement with the previously described mutual dependence model from modified cell lines (105). Furthermore, a recent review recognised the emerging awareness of the significance of the cellular proportions of MDM2 and MDMX to each other in determining P53 stability and activity (138). Despite the different genetic alterations involved in the malignant transformation of the different sub-types of LS, it is noted that the expression level of P53 was largely affected by the MDM2/MDMX ratio in all sub-types, with a statistically significant negative correlation between MDM2/MDMX ratio and P53 expression (co-

relation coefficient = -0.437, $p < 0.001$). P53 expression in relation to the $\text{Log}_2(\text{MDM2}/\text{MDMX})$ scores is illustrated in Figure 4.5.

The subset of cases that did not over-express MDM2 or MDMX had apparently normal expression levels of P53 (n=9/11). This may indicate that the P53 - MDM pathways were intact in these cases and therefore the biomarkers remained at low levels. In turn, this might suggest a different mechanism of carcinogenesis in these cases.

Collectively, the observations made in this study invite careful characterisation of MDM2, MDMX and P53 proteins in tumours when considering *in-vivo* experimental evaluation of novel MDM2-specific or dual target MDM2/MDMX blocking compounds.

Table 4.1: Summary of the cytogenetic results for the liposarcoma cohort

Cytogenetic analysis		WDLS (n=43)	DDLS (n=9)	MXLS-RCLS (n=12)
Not attempted		1	1	2
Failed		3	1	1
MDM2 amplification by FISH	+ve	33	7	1(Probable)
	-ve	6	0	8
	No. of analysed cases	39	7	9
Chromosomal translocation by G band analysis and / or FISH	+ve	0	0	8
	-ve	4 ^o	2*	1 [†]
	No. of analysed cases	4	2	9
Findings confirming the histological diagnosis / total of successfully analysed cases		33/39	7/7	8/9

This is a tabular summary of the cytogenetic analysis tests that were conducted in the LS cohort. The data presented is a summary from analysing the cytogenetic results for each specimen as provided by the Yorkshire Regional Genetics Services. The methods used for cytogenetic analyses are detailed in Section 2.9.

The majority of the successfully-analysed cases (48/55) had concordant histological diagnosis and molecular features. Some inconsistencies were seen in WDLS.^o Two of these cases had *MDM2* amplification by FISH analysis. * These two cases showed *MDM2* amplification. † This case had a probable *MDM2* amplification. +ve = positive, -ve = negative.

Table 4.2: Contingency table of *MDM2* amplification and *MDM2* over-expression

<i>MDM2</i> amplification \ <i>MDM2</i> over-expression	Yes	No	Total
Yes	31	9	40
No	6	0	6
Total	37	9	46

A contingency table demonstrating the correlation between *MDM2* amplification and over-expression in WDLS and DDLS. Total number of WDLS and DDLS that were successfully analysed by FISH for *MDM2* amplification (n=46). *MDM2* protein over-expression (+/++) was determined by IHC and was based on the scoring protocol as detailed in Section 2.7.

Table 4.3: Stratified score summary of the analysed cohort

	MDMX -		MDMX +		MDMX ++		Total
	P53 -	P53 +	P53 -	P53 +	P53 -	P53 +	
MDM2 -	9	2	0	0	0	0	11
MDM2 +	4	1	4	0	0	2	11
MDM2 ++	4	0	12	1	3	22	42
Total	20		17		27		64

Immunohistochemistry scores for MDM2 and MDMX were stratified as follows: (-) normal expression: when <11% of cells had positive nuclear staining; (+) moderate over-expression: when 11 – 40% of cells had positive nuclear staining; (++) strong over-expression: when >40% of cells had positive nuclear staining. Scores for P53 were: (-) negative expression: when ≤10% of cells had positive nuclear staining; (+) positive expression: when 11% or more of cells had positive nuclear staining.

Colour codes: Yellow cell = negative staining for both MDM2 and MDMX; blue cell = co-expression of MDM2 and MDMX where higher MDM2 expression levels were seen compared to MDMX (Pattern –A) note mostly diminished levels of P53 were seen in this group; pink cell = co-expression of MDM2 and MDMX at proportionate levels (Pattern –B) note the associated positive expression of P53 in this group.

Table 4.4: FISH and IHC as diagnostic tools for WDLS and DDLS

	WDLS			DDLS			Lipoma			Ref.
	No. of cases	FISH(+)	IHC(+)	No. of cases	FISH(+)	IHC(+)	No. of cases	FISH(+)	IHC(+)	
	19	0/0 [†]	19/19	10	0/0 [†]	9/10	17	0/6 [†]	7/17	(90)
	48	47/48	10/48	5	5/5	5/5	25	ND	0/25	(88)
	27	4/5 [†]	26/27	14	4/8 [†]	9/14	24	0/0 [†]	0/24	(34)
	91	85/91	ND	64	60/64	ND	0	0	0	(194)
	44	41/41	44/44	61	53/55	58/61	49	0/0	3/49	(33)
	52	41/52 [§]	ND	0	0	0	324	7/324 [§]	ND	(205)
	5	5/5	ND	8	8/8	ND	23	0/0	ND	(206)
Total	286	223/242	99/138	162	130/140	81/90	462	7/330	10/115	
%		92%	71%		93%	90%		2%	7%	

This summary review of published literature indicates a marginal superiority for FISH as a diagnostic tool for WDLS and DDLS compared to IHC. It reveals the imperfections in both methods as diagnostic tools (no 100% results). † Test was done in selective or controversial cases; some studies subsequently changed the code of diagnosis based on FISH results as indicated by §. ND = not done.

Table 4.5: Characteristic features of liposarcomas with inconsistent FISH analysis

Age/ Gender	Site of tumour	Size cm	First diagnosis	MDM2 status by FISH	P53 mutation	IHC	IHC	IHC	Requested further tests	Second diagnosis after review
						MDM2	MDMX	P53		
85 / F	Lower limb	6*6*3	WDLS	Not amplified	D184N	84	70	62	13q deletion	Favours WDLS
73 / F	Lower limb	10*10*6	WDLS	Not amplified but 4X gain	Not done	32	18	1	None	Unchanged
67 / M	Lower limb	14*8*7	WDLS	Not amplified	None detected	25	5	46	13q deletion	?PML
62 / M	Lower limb	15*10*3	WDLS	Not amplified	Not done	80	32	6	13q deletion	?PML
53 / F	Upper limb	5*3*2	WDLS - Inflammatory	Not amplified	Lys292*FS	70	80	32	G band normal No 13q deletion	Unchanged
61 / M	Chest wall	4*2*2	WDLS	Not amplified	Not done	95	85	67	G band normal No 13q deletion	Unchanged
51 / F	Lower limb	20*8*8	MXLS	Possible amplification	Not done	99	46	32	None	Unchanged

A tabular summary of the key clinical and molecular features of the identified LS cases with inconsistent cytogenetic findings. Note that all cases presented in the lower limb and they were relatively small in size. The detected *P53* mutation and the presence of multiple copies of chromosome 12 may provide an alternative explanation to the driver of oncogenic changes. All cases had high expression of MDM2 on immunohistochemistry analysis indicating a possible complementary role in diagnosis in these controversial cases.

Table 4.6: Immunophenotype of liposarcomas in relation to their anatomical location

LS subtype	Number of cases	Retroperitoneal			Non-retroperitoneal		
		MDM2(+/**)	MDMX(+/**)	P53(+)	MDM2(+/**)	MDMX(+/**)	P53(+)
WDLS	43	7/7	4/7	2/7	27/36	20/36	10/36
DDLS	9	7/7	7/7	5/7	2/2	2/2	2/2
MXLS- RCLS	12	1/2	1/2	1/2	8/10	10/10	9/10

No variations were detected in the expression profiles of the analysed proteins in relation to the anatomical location of LS.

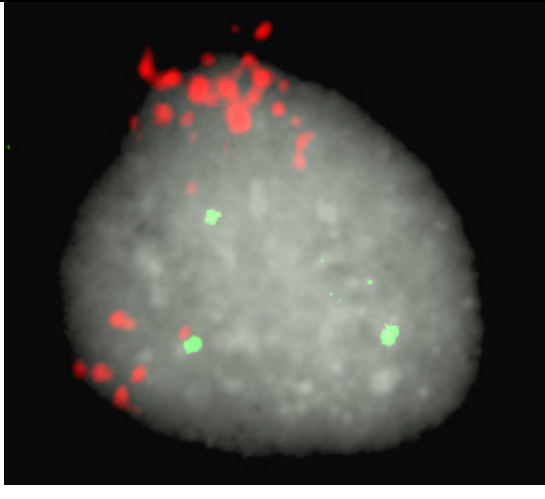
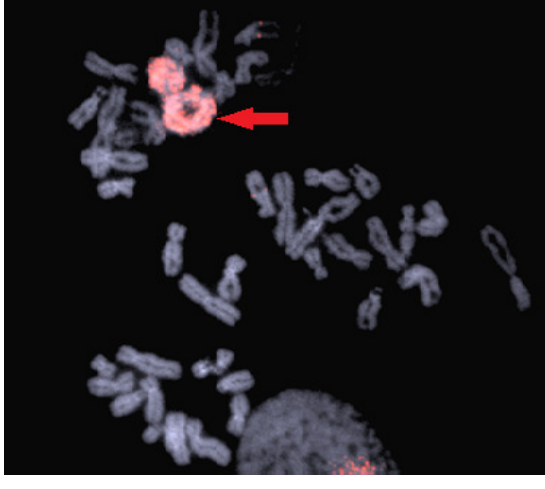
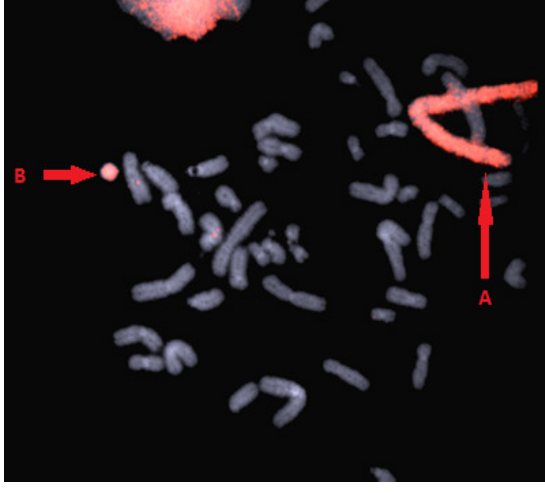
<p>A- FISH analysis of interphase cell demonstrating <i>MDM2</i> amplification, note high red signal in relation to green.</p>		
<p>B- Karyotype analysis showing ring chromosome 12 (indicated by arrow)</p>		
<p>C- Karyotype analysis showing giant chromosome 12 (A) and ring chromosome (B)</p>		

Figure 4.1: Examples of characteristic cytogenetic alterations in liposarcomas

Illustration of different cytogenetic alterations commonly seen in liposarcomas. A- FISH analysis of interphase cell. The red probe hybridises to *MDM2* and the green probe to chromosome 12 centromere as control. B and C- chromosomal spread showing ring chromosome 12 (B) and giant chromosome 12 (C) using *MDM2* red probe. Images were provided by Dr Paul Roberts, Yorkshire Regional Genetics Services.

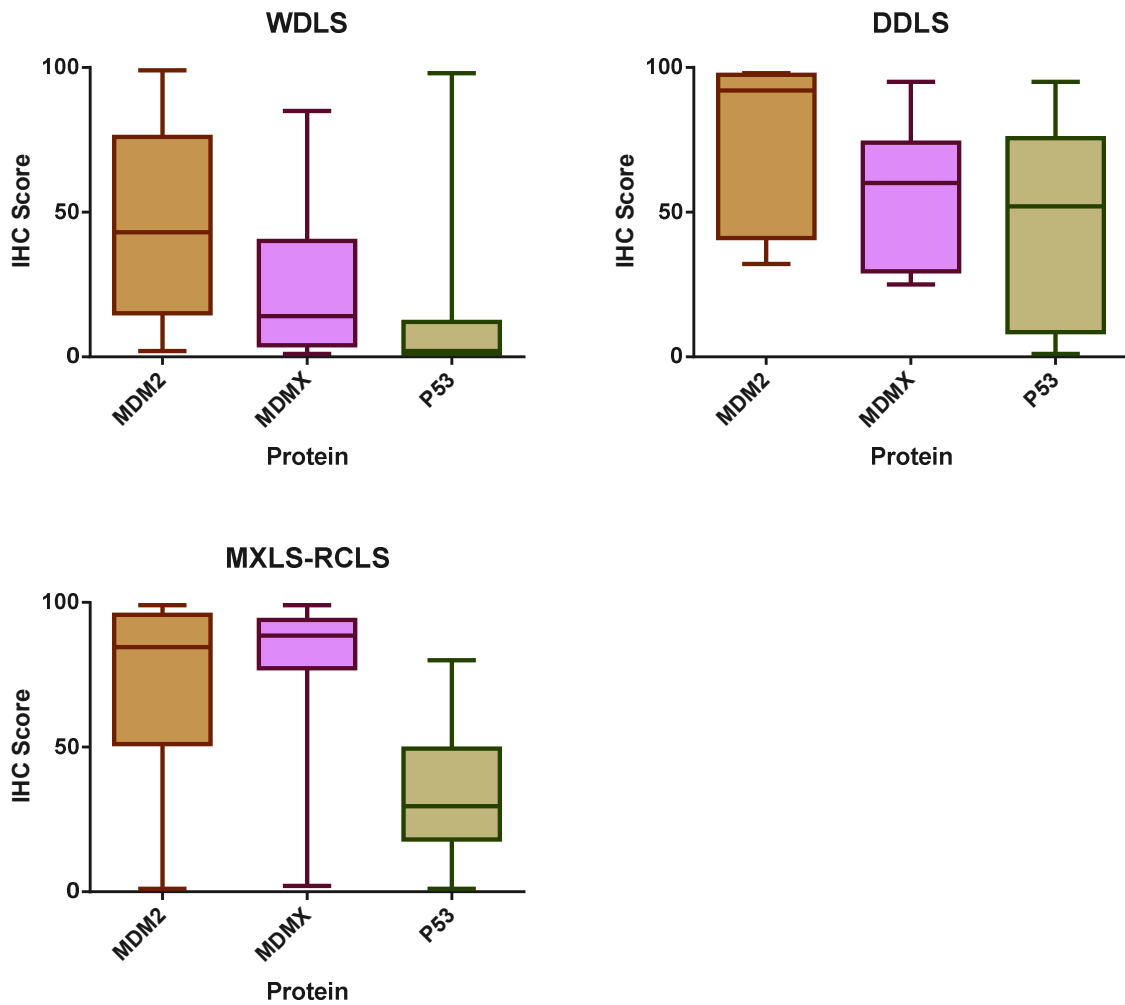


Figure 4.2: Subtype-specific expression levels of MDM2; MDMX; and P53

The box plots above illustrate the median score (lined); interquartile range (boxed); and the minimum to maximum score values (whiskers) for MDM2, MDMX and P53 in subtype-specific categorisation. All proteins were expressed at higher levels in DDLS and MXLS-RCLS compared to WDLs. MDM2 expression was higher in relation to MDMX in WDLs whereas both MDM2 and MDMX had comparable expressions in DDLS and MXLS-RCLS. P53 expression was increased with increasing MDMX. IHC = immunohistochemistry.

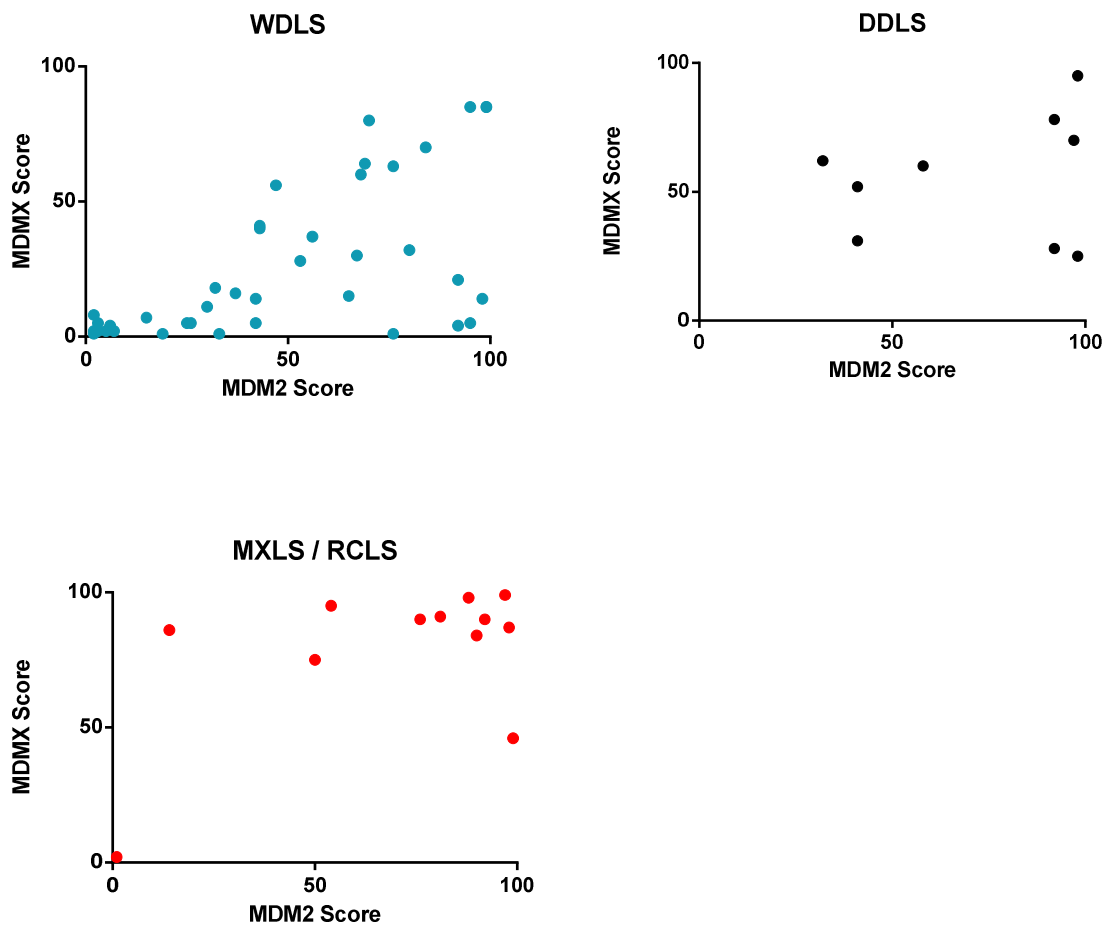


Figure 4.3: Co-expression patterns of MDM proteins in different subtypes of liposarcomas

The scatter plots above illustrate the co-expression values for MDM2 and MDMX in the various subtypes of LS. Different patterns of MDM2/MDMX expression levels were noted. A predilection to over-express MDM2 at higher levels in comparison to MDMX was a feature of WDLs, whereas all other LS subtypes had comparable MDM2 to MDMX expression levels on immunohistochemistry. The scatter plots demonstrate that the same individual cases often expressed both proteins. Data presented are the mean of the individual scores by two independent scorers.

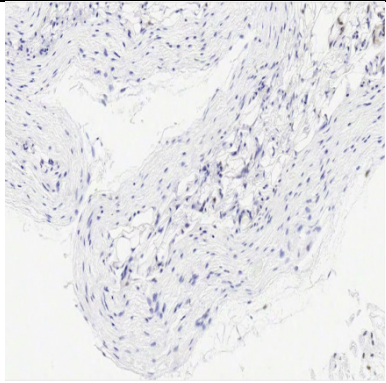
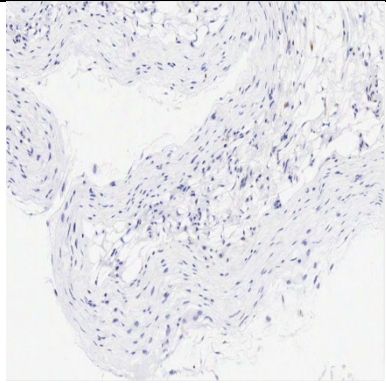
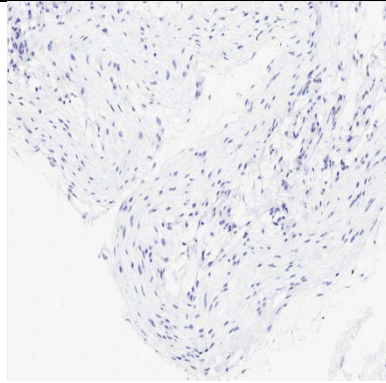
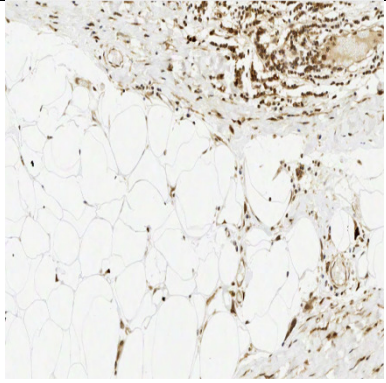
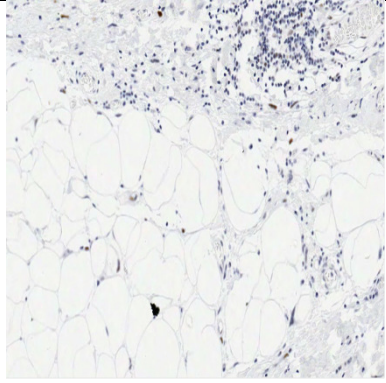
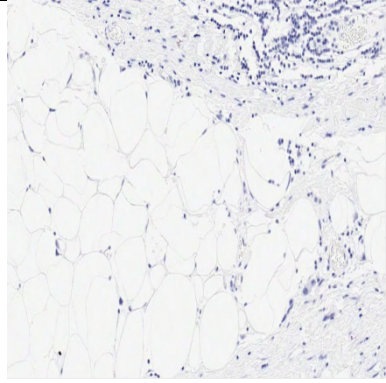
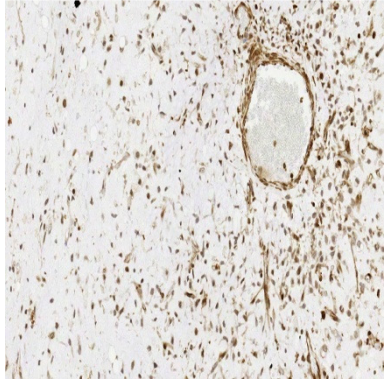
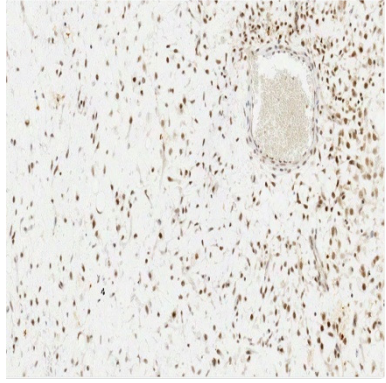
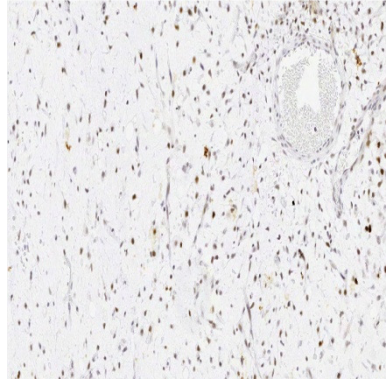
	MDM2	MDMX	P53
Normal expression Example: WDLS, case no. WD24			
Pattern -A Example: WDLS, case no. WD31			
Pattern-B Example: MXLS, case no. MR8			

Figure 4.4: Immunohistochemistry patterns for MDM2, MDMX and P53

Three distinct patterns of immunohistochemistry staining were identified: normal expression where none of the examined proteins was over-expressed; negative P53 expression with higher scores of MDM2 in comparison to MDMX (Pattern-A); positive P53 expression with comparable scores of MDM2 and MDMX (Pattern-B).

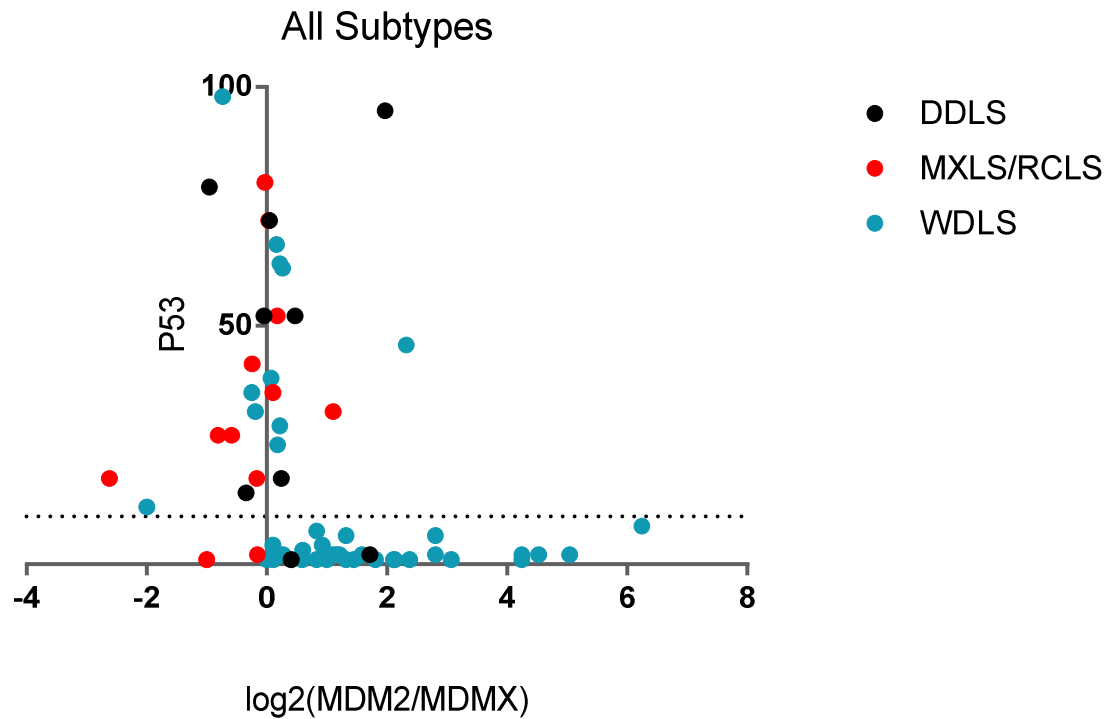


Figure 4.5: P53 expression in relation to the Log₂(MDM2/MDMX) scores in liposarcomas

The scatterplot above illustrates the P53 scores in relation to MDM2:MDMX ratio (expressed as log₂ [MDM2:MDMX] for range adjustment). The dotted line represents the 10% cut off value for positive P53. Across various subtypes of LS, higher P53 expression levels were detected when MDMX was co-expressed at comparable or higher levels in relation to MDM2 (Log₂[MDM2:MDMX]<1). Diminished P53 expression was noted when MDM2 was expressed at significantly higher levels than MDMX (Log₂[MDM2/MDMX]>1).

5 Genetic Analysis of P53

5.1 Aims

The aim of this Section is to assess if the detected P53 over-expression in the analysed cohort resulted from a somatic mutation rather than a genuine manifestation of P53 interaction with its cellular regulators. Sanger sequencing DNA analysis of *P53* was performed in 26 LSs of the total 28 cases that over expressed P53 in the described cohort, in addition to a subcutaneous lipoma that had normal P53, MDM2 and MDMX expression profile as a control sample.

5.2 DNA Extraction

Genomic DNA extraction from FFPE tissue and cell lines was performed according to the protocol in Section 2.10.1. Subsequently, the DNA concentration was quantified using the nanodrop technique and visualised with ethidium bromide following agarose gel electrophoresis (1% w/v agarose). Figure 5.1 shows a typical agarose gel visualisation of 10 genomic FFPE DNA samples. Samples that failed to yield suitable DNA matter were re-extracted until a satisfactory product was obtained.

5.3 Polymerase Chain Reaction

PCR amplification of *P53* exons 4 to 9 was performed in 26 samples. The presence of an amplicon of the correct size was verified by agarose gel electrophoresis. PCR amplification was successful in all cases but failed for exon 7 in three of these cases (case numbers: MR1, MR8 and WD31), despite frequent attempts. Examples of PCR amplicon visualisation by ethidium bromide following agarose gel electrophoresis are shown in Figure 5.2.

PCR amplicons were purified from unincorporated oligonucleotide primers using GenElute PCR clean up kit, according to the protocol in Section 2.10.2. Confirmation of retained amplicons post purification was performed by nanodrop and standard agarose gel

electrophoresis. Examples of post purification amplicon visualisation by ethidium bromide following agarose gel electrophoresis are shown in Figure 5.3.

5.4 Somatic Mutations of P53

Sanger sequencing DNA analysis was performed according to the protocol in Section 2.10.3. The presence of a sequence variant was identified by the visualisation of a variant peak and the corresponding decrease in the height of the wild type nucleotide peak when present. Table 5.1 summarises the detected P53 somatic mutations in the analysed cohort in terms of nucleotide and amino acid changes.

Five of the 26 cases (19%) were found to have previously-described pathological somatic heterozygous mutations: 1 missense mutation in exon 4, c.137C>T; p.Ser46Phe (Figure 5.4) in a MXLS that over-expressed MDM2 and MDMX (case no. MR1); 3 missense mutations in exon 5 namely c.392A>G; p.Asn131Ser (Figure 5.5) and c.511G>A; p.Glu171Lys (Figure 5.6) in a WDLS case that expressed normal levels of MDM2 and MDMX (case no. WD28); and c.550G>A; p.Asp184Asn (Figure 5.7) in two cases (MXLS and WDLS), which over-expressed both MDM2 and MDMX (case numbers MR8 and WD42).

A frame shift mutation was detected in exon 8, Lys292*FS (c.876DelAG) (Figure 5.8) in an inflammatory WDLS that also over-expressed MDM2 and MDMX (case no. WD39) . Table 5.2 summarises the clinical, histological and molecular features of these tumours.

Additionally, a nucleotide variant was found in exon 7, c.770T>A; p.Leu257Gln - rs28934577 (Figure 5.9), in sporadic cases including the control lipoma.

5.5 P53 Arg72Pro Polymorphism - rs1042522

A single nucleotide polymorphism (SNP) C>G at exon 4, codon 72, in the proline-rich domain of P53, which replaces arginine (Arg) with proline (Pro), has been reported to affect P53 functions. The Arg72 variant was found to induce apoptosis markedly better (121) and was linked to superior response to conventional chemotherapy, compared to the Pro72 variant (207). In light of these findings, this polymorphism was examined in the cohort of cases that over-expressed P53. The majority of cases were homozygous for the Arg72 variant (58%), 9

cases were found to be heterozygous and two cases were homozygous Pro72. The SNP's genotype is indicated in Table 5.1 while the electropherograms in Figure 5.10 illustrates examples of sequences for each of the variant genotypes.

5.6 Analysis of Results and Discussion

The sequence analysis of *TP53* encompassed all of the previously-described *P53* mutational hot spots found in all cancer types, as identified on the P53 International Agency for Research on Cancer IARC website (Figure 5.11). Mutational analysis was performed on 26 LSs that over-expressed *P53* and were identified at the start of the project. Subsequently 2 more cases were identified, but not sequenced as the data would not have changed the overall conclusion of this part of the thesis.

The clinical follow up of the 26 cases averaged between 22 and 64 months with a median of 47.5 months. All cases remained in regular follow up until January 2014 by LTHT. No evidence of recurrence or distant metastasis was detected in any of these cases. While the presence of the detected *P53* mutations did not seem to have influenced the prognosis of these cases, due to the limited numbers of cases and the relatively limited follow up period, a firm conclusion cannot be made.

5.6.1 Phenotypical Consequences of the Detected *P53* Somatic Mutations

The Ser46Phe missense mutation in the *N*-terminus domain of *P53* was previously reported in urinary bladder (208) and lymphoid tumours (209). *In vitro* cell line models have demonstrated an increased apoptotic activity of the 46Phe variant compared to the wild type protein. Consequently this variant was referred to as "super *P53*" by Nakamura *et al.* (210). The increased apoptotic activity may be a consequence of the variant *P53* protein having a higher affinity for the cytoplasmic protein clathrin. This interaction subsequently activates *P53*-dependent promoters of apoptosis and up-regulates the transactivation of genes downstream of *P53* (211).

The three other detected somatic missense mutations were all mapped to the DNA-binding domain, suggesting a disruption to *P53*'s ability to correctly bind DNA and therefore compromising its functions. Asn131Ser has been reported as a point mutation in

hepatocellular carcinoma (212) and breast cancers (213), either as a sole mutation or in conjunction with other P53 point mutations. Glu171Lys was reported in multiple malignancies including breast (214), pulmonary (215) and gastro-intestinal (216). Studies from haematological malignancies confirmed that Glu171Lys-mutant P53 was transcriptionally active (217) and gastric tumours with P53 mutations, including Glu171Lys, were found to over-express cyclo-oxygenase2 and had poorer prognosis (218). Asp184Asn was detected in two cases in the study cohort and has previously been reported in multiple malignancies including lymphomas (219); colorectal (220); and cervical tumours (221). The structure of the mutant P53 protein is not thought to be disrupted, but this mutation is believed to affect the sequence-specific binding of P53 to DNA (222).

The Leu257Gln variant was detected in 2 DDLs, 1 MXLS, 1 WDLS and 1 control lipoma. In the WDLS case, this variant was found in conjunction with other pathological P53 mutations (Glu171Lys, Asn131Ser). Leu257Gln is a relatively rare variant of uncertain clinical significance, which has been described sporadically. It was reported in early-stage colon cancer without lymph node or metastatic involvement (223), in carcinoma *in situ* of the urinary bladder (224), and it was found to have no dominant negative effect in oral cancers (225). While the Gln257 variant was reported to retain wild type P53 functions, it was also suggested that it may interfere with P53 overall activity (226). Additionally, Gln257 was reported to interact normally with MDM2 (227). As Leu257Gln was detected in the control subcutaneous lipoma that did not over-express P53, it was therefore reasonable to assume that this variant did not affect the P53 expression profile.

The described frame shift mutation in this study (Lys292*FS) has not previously been reported in STS or any other cancers according to IARC TP53 database. However, a sequence variant at position c.874A>T in the same codon was reported to result in nonsense mutation and a non-functional P53 (228). It is expected therefore that a frame shift at this position would have a substantial effect on the resultant protein's structure and function, since all subsequent amino acids are replaced by 10 novel amino acids (ASPRAAPREH*).

5.6.2 Significance of P53 Arg72Pro Polymorphism

Genotyping of the Arg72Pro polymorphism in this study detected the Pro72 variant in 42% of cases, whereas a previous study including 35 LSs from the Norwegian patients identified the Pro72 variant in 62% of tumours (82). It is possible that the difference in the variant's frequency is due to the small size of each tumour cohort. However, it may also reflect differences in the allele frequency between the English and Norwegian populations. The frequency of Pro72 allele in the general population germ line ranges from 70% in Africans to 23% among Western Europeans (229).

Arg72Pro polymorphism has been extensively reported in different cancers. It appears that patients with homozygous and heterozygous Pro72 variant had increased resistance to conventional chemotherapy and shorter progression free survival rates in non-small cell lung cancer (230) and advanced gastric cancers (231). On the other hand, the germ line Pro72 allele has not been associated with increased cancer susceptibility. On the contrary, germline homozygous and heterozygous Pro72 individuals were found to have increased longevity in human population studies (232, 233). Such discrepancy in prognosis between the polymorphism in normal compared to tumour tissue may be explained by the superior ability of the Arg72 variant to induce apoptosis, whereas Pro72 variant induces G1 arrest and is better at promoting P53-dependent DNA repair (233).

The two cases that displayed homozygous Pro polymorphism at codon 72 were found to have concomitant pathological mutations in the neighbouring exon 5: Glu171Lys and Asn131Ser in case no. WD28; and Asp184Asn in case no. WD42. In fact, 4 of the 5 detected mutations occurred in tumours carrying the proline-variant (adding cases MR8 and WD39). While the numbers in this study are too small to draw a valid conclusion about a correlation between P72 and a higher incidence of associated *P53* mutations, this finding may be important when taking into account the low prevalence of *P53* mutations in LSs, in general (approximately 20%). In agreement with this finding, Ohnstad *et al.* reported 48% of mutant *P53* (n=27), in a series of STSs, to have the Pro72 variant (82). Collectively, these findings emphasise the importance of examining the full length of *P53* for mutations when conducting studies that focus on Arg72Pro polymorphism.

5.6.3 *P53* Mutations in Relation to the Protein Expression Profiles

Screening *P53* for somatic and germline sequence variants in the cohort of *P53* over-expressing LSs revealed a *P53* somatic mutation incidence of 19% (n=5). If we assumed that the 3 cases which partially failed PCR amplification for exon 7 harboured a devastating mutation in exon 7, then the number of cases will rise to 6 as two of these cases were already found to have mutations in exon 4 and 5 (case numbers MR1 and MR8, respectively). Additionally, on the assumption that the two *P53* over-expressing cases that presented later in the study, and therefore were not subjected to genomic analysis of *P53*, were subsequently found to have a *P53* mutation, then the total incidence of *P53* mutation will rise to 28% (n=8 of 28 new total). These incidences remain within the expected range of *P53* mutations in LS in general, regardless of their *P53* protein expression profile, as previously reported in the literature (43, 44). In other words, the majority of LS cases (70 - 80%) that over-expressed *P53* were found to have retained a wild type *P53* status. In turn, this suggests that the detected high *P53* expression levels were a genuine manifestation of the interplay between *P53* and its cellular regulators, MDM2 and MDMX.

Table 5.1: Summary of *P53* somatic mutations in the analysed cohort

Case no.	SNP 72	Exon 4	Exon 5	Exon 6	Exon 7	Exon 8	Exon 9
DD1	CG						
DD2	GG						
DD3	GG				c.770T>A (Leu257Gln)		
DD4	GG						
DD6	GG				c.770T>A (Leu257Gln)		
DD7	CG						
DD8	GG						
MR1	GG	c.137C>T (Ser46Phe)					
MR2	GG						
MR4	GG						
MR5	GG						
MR6	GG				c.770T>A (Leu257Gln)		
MR7	GG						
MR8	CG		c.550G>A (Asp184Asn)				
MR10	CG						
MR11	CG						
MR12	GG						
WD2	CG						
WD14	CG						
WD28	CC		c.511G>A (Glu171Lys) c.392A>G (Asn131Ser)		c.770T>A (Leu257Gln)		
WD31	CG						
WD36	GG						
WD37	GG						
WD39	CG					c.876DelAG (Lys292*FS)	
WD40	GG						
WD42	CC		c.550G>A (Asp184Asn)				
B1 Lipoma control					c.770T>A (Leu257Gln)		

Colour key for Table 5.1

Failed to analyse	Partially failed to analyse	No mutations	Non-pathological variant	Pathological mutation
-------------------	-----------------------------	--------------	--------------------------	-----------------------

A tabular summary of the detected *P53* somatic mutations and SNP variants in the analysed cohort.

Table 5.2: Characteristics of P53 mutant cases in the analysed cohort

Case no.	Mutation	M/F	Age	Site	Size (cm)	Histology	Cytogenetic	IHC	IHC	IHC	Follow up [†] (months)	Significant events [§]
								MDM2	MDMX	P53		
MR1	Ser46Phe	M	70	Buttock	10*7*5	MXLS	t12:16	81	91	18	22	None
MR8	Asp184Asn	F	51	Thigh	20*8*8	MXLS	Not done	99	46	70	54	None
WD28	Asn131Ser Glu171Lys	M	72	Thigh	26*23*11	WDLS	<i>MDM2</i> amplification by FISH	2	8	12	64	None
WD39	Lys292*FS	F	53	Arm	5*3*2	WDLS inflammatory	Normal Karyotype by G-band	70	80	32	41	None
WD42	Asp184Asn	F	85	Leg	6*6*3	WDLS	<i>MDM2</i> not amplified by FISH	84	70	62	33	None

A tabular summary of the clinical, histological and molecular characteristics of LSs with detectable *P53* somatic mutation(s). [†]clinical follow up is based on clinician correspondence and data available from PPM; [§] Significant events included recurrence, distant metastasis or death.

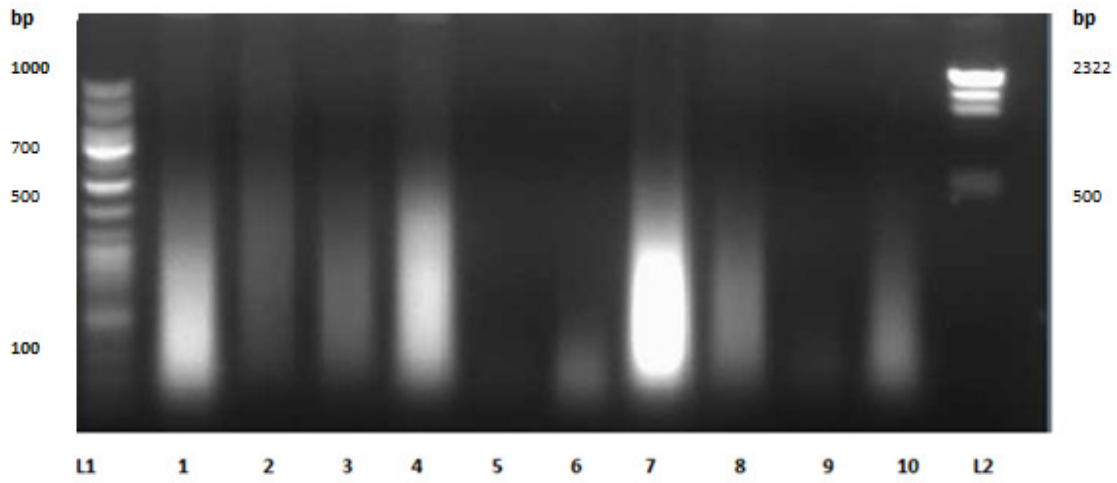


Figure 5.1: Agarose gel confirmation of genomic DNA extraction

Example of ethidium bromide-stained 1% agarose gel electrophoresis of DNA extraction for samples 1-10 (as numbered). Samples 5 and 9 were consequently repeated due to poor yield. L1 = ladder 1 (1kb ladder); L2 = ladder 2, Lambda DNA/Hind III Marker.

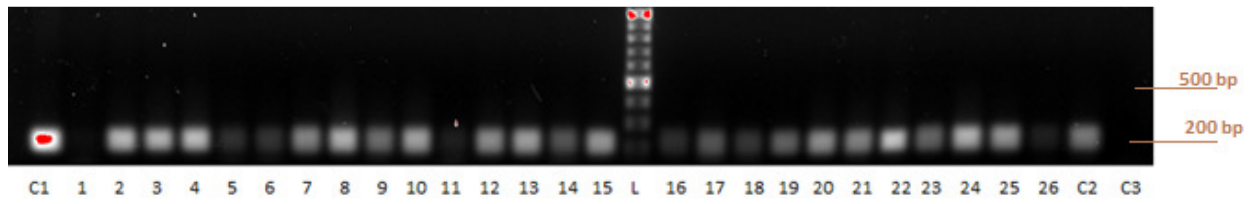


Figure 5.2: Agarose gel electrophoresis of PCR products for *P53* exon 5

Example of post-PCR agarose gel electrophoresis for *P53*-exon 5, samples 1-26 (as numbered). C1 = Control1, DNA control from human blood; C2 = Control 2, DNA extraction from a lipoma sample; C3 = Control 3, pure H₂O negative control; L = ladder, Gene ruler 100bp.

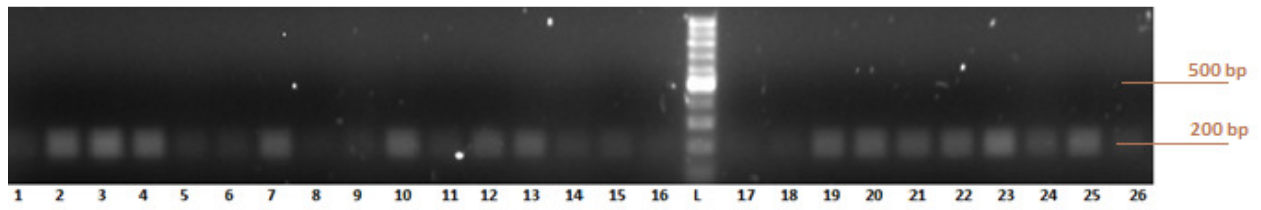


Figure 5.3: Agarose gel electrophoresis of post PCR purification products for *P53* exon 4

Example of post PCR purification agarose gel electrophoresis of P53-exon 4, samples 1-26 (as numbered). L = ladder, Gene ruler 100bp.

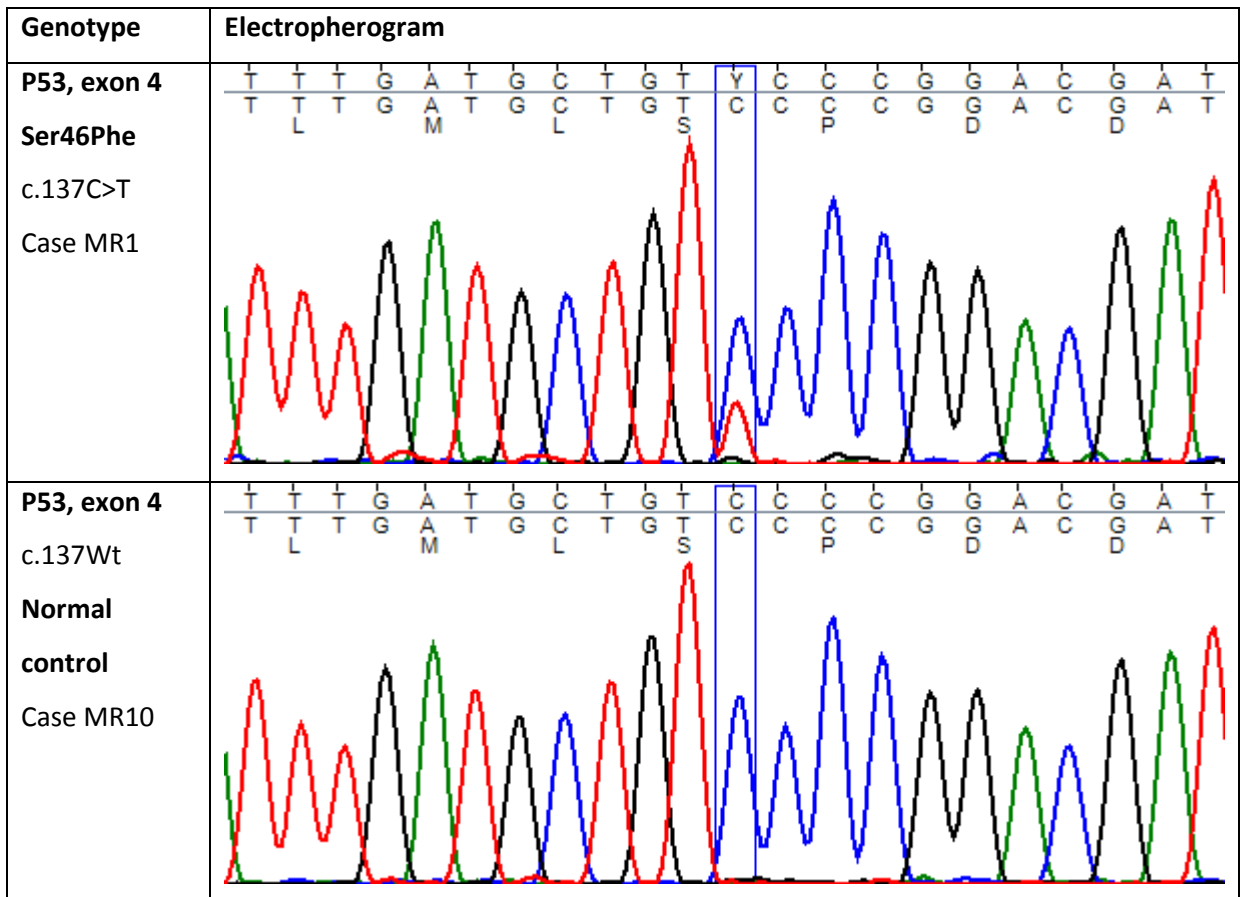


Figure 5.4: Electropherogram of sequence surrounding codon 46 demonstrating Ser46Phe

Electropherogram of *P53* exon 4 representing a heterozygous mutation C>T at residue 173 in case MR1 (top), in comparison to case MR10 as a control (bottom). The upper nucleotide sequence represents the sample's sequence while the lower two sequences identify the reference nucleotide and amino acid sequences respectively. Letter codes follow the International Union of Pure and Applied Chemistry (IUPAC) coding (Y = C+T). Wt=wild type.

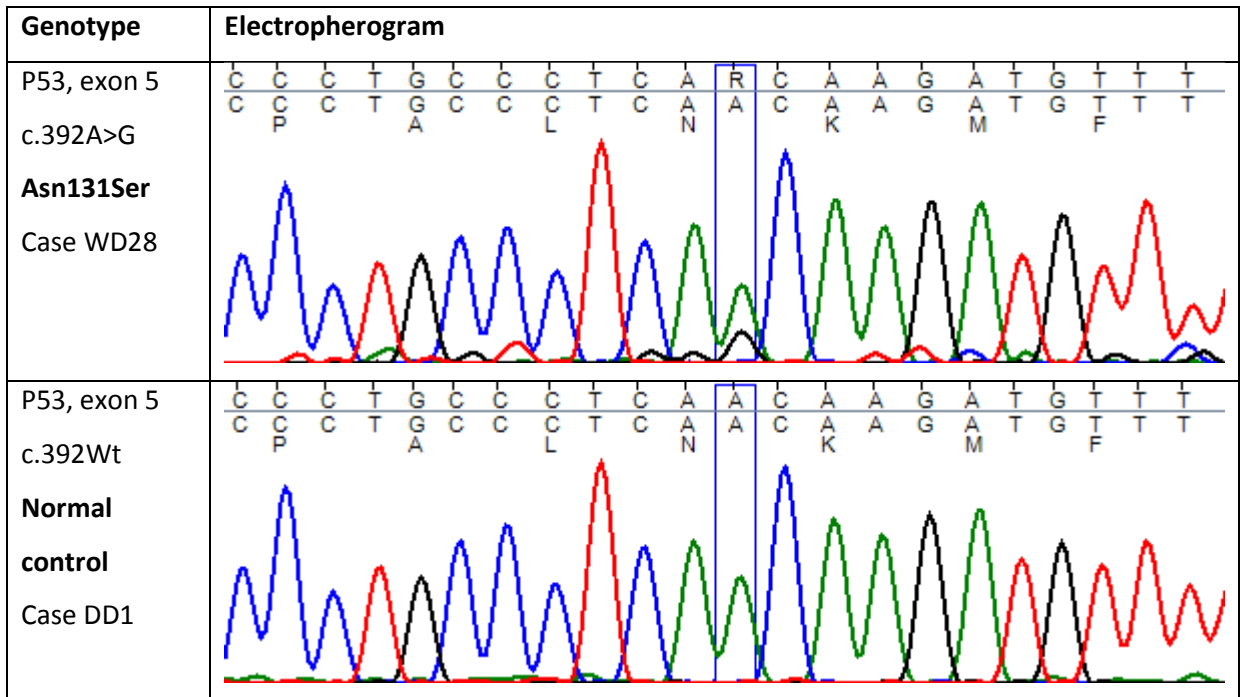


Figure 5.5; Electropherogram of sequence surrounding codon 131 demonstrating Asn131Ser

Electropherogram of *P53* exon 5 representing a heterozygous mutation A>G at residue 392 in case WD28 (top), in comparison to case DD1 as a control (bottom). The upper nucleotide sequence represents the sample's sequence while the lower two sequences identify the reference nucleotide and amino acid sequences respectively. Letter codes follow the International Union of Pure and Applied Chemistry (IUPAC) coding (R = A+G). Wt = wild type.

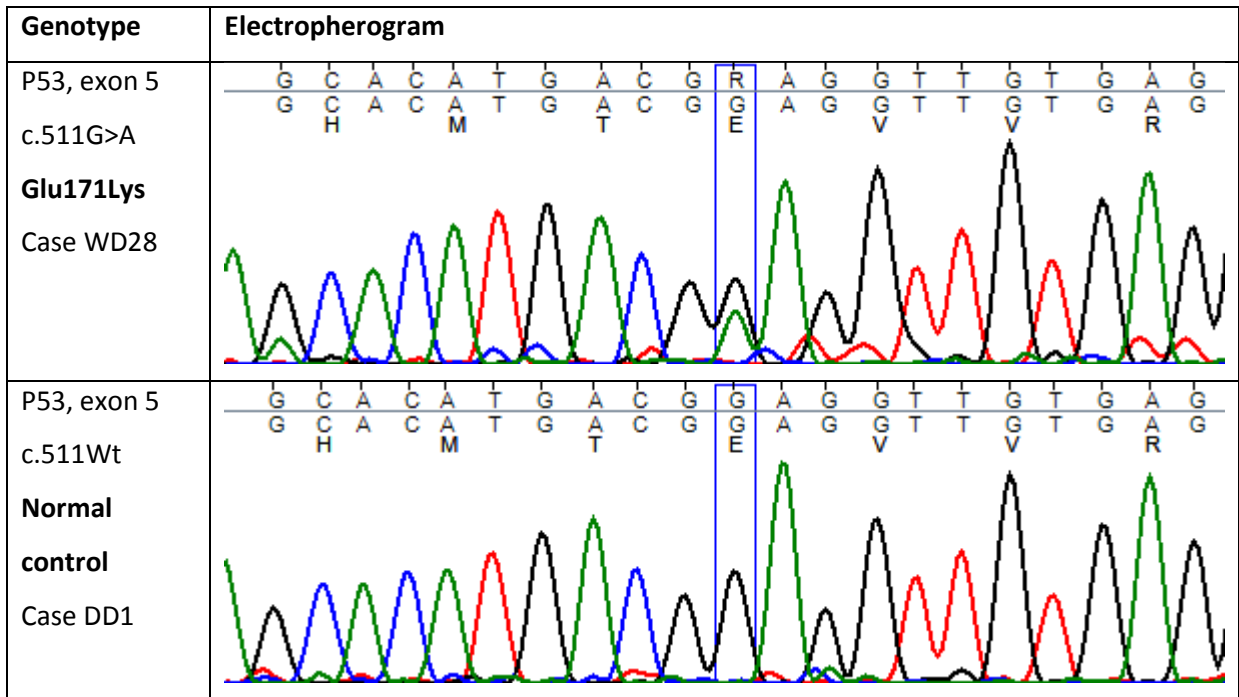


Figure 5.6: Electropherogram of sequence surrounding codon 171 demonstrating Glu171Lys

Electropherogram of *P53* exon 5 representing a heterozygous mutation G>A at residue 511 in case WD28 (top), in comparison to case DD1 as a control (bottom). The upper nucleotide sequence represents the sample's sequence while the lower two sequences identify the reference nucleotide and amino acid sequences respectively. Letter codes follow the International Union of Pure and Applied Chemistry (IUPAC) coding (R = A+G). Wt = wild type.

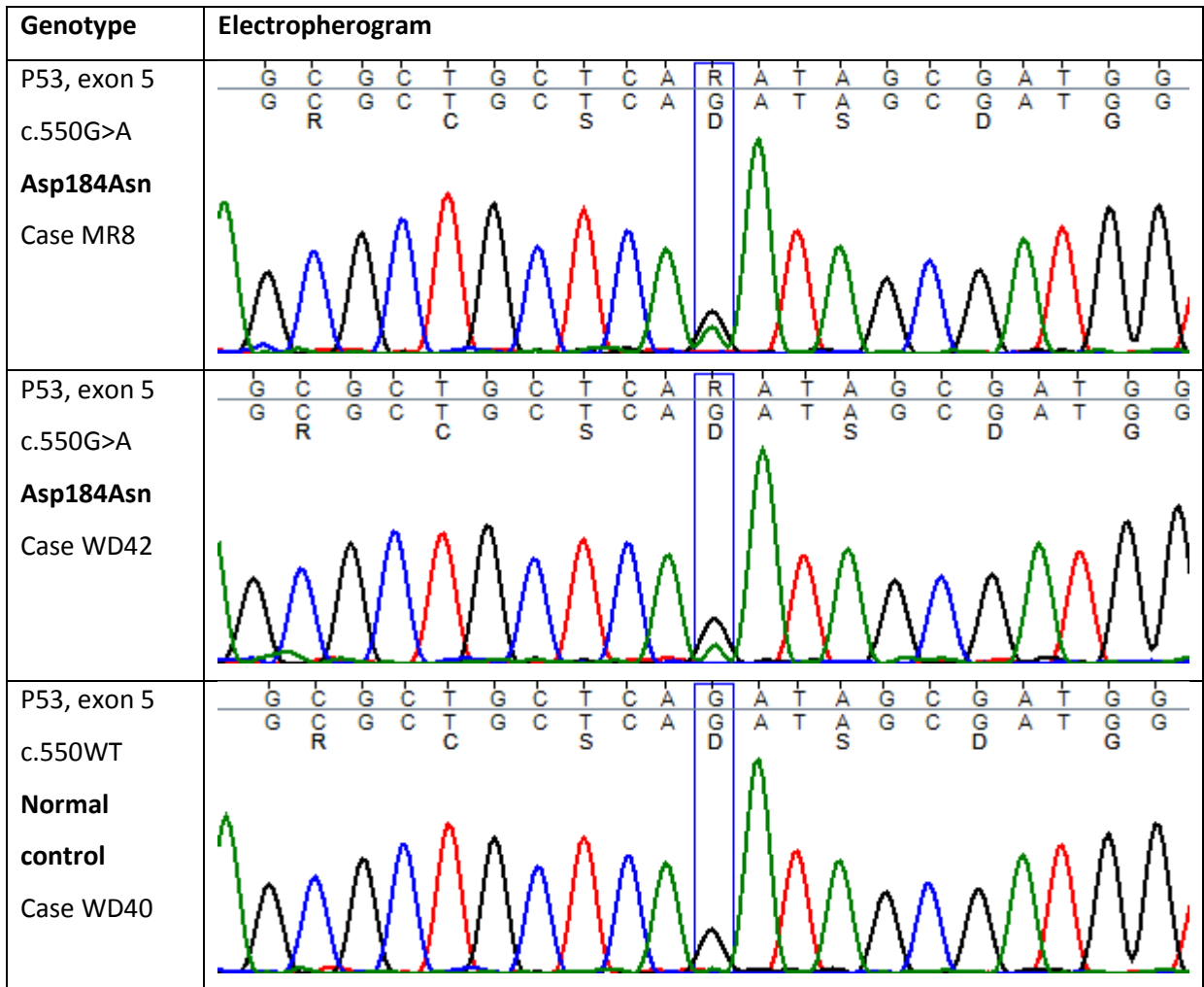


Figure 5.7: Electropherogram of sequence surrounding codon 184 demonstrating Asp184Asn

Electropherogram of *P53* exon 5 representing a heterozygous mutation G>A at residue 550 in cases MR8 and WD42 (top2), in comparison to case WD40 as a control (bottom). The upper nucleotide sequence represents the sample's sequence while the lower two sequences identify the reference nucleotide and amino acid sequences respectively. Letter codes follow the International Union of Pure and Applied Chemistry (IUPAC) coding (R = A+G). Wt = wild type.

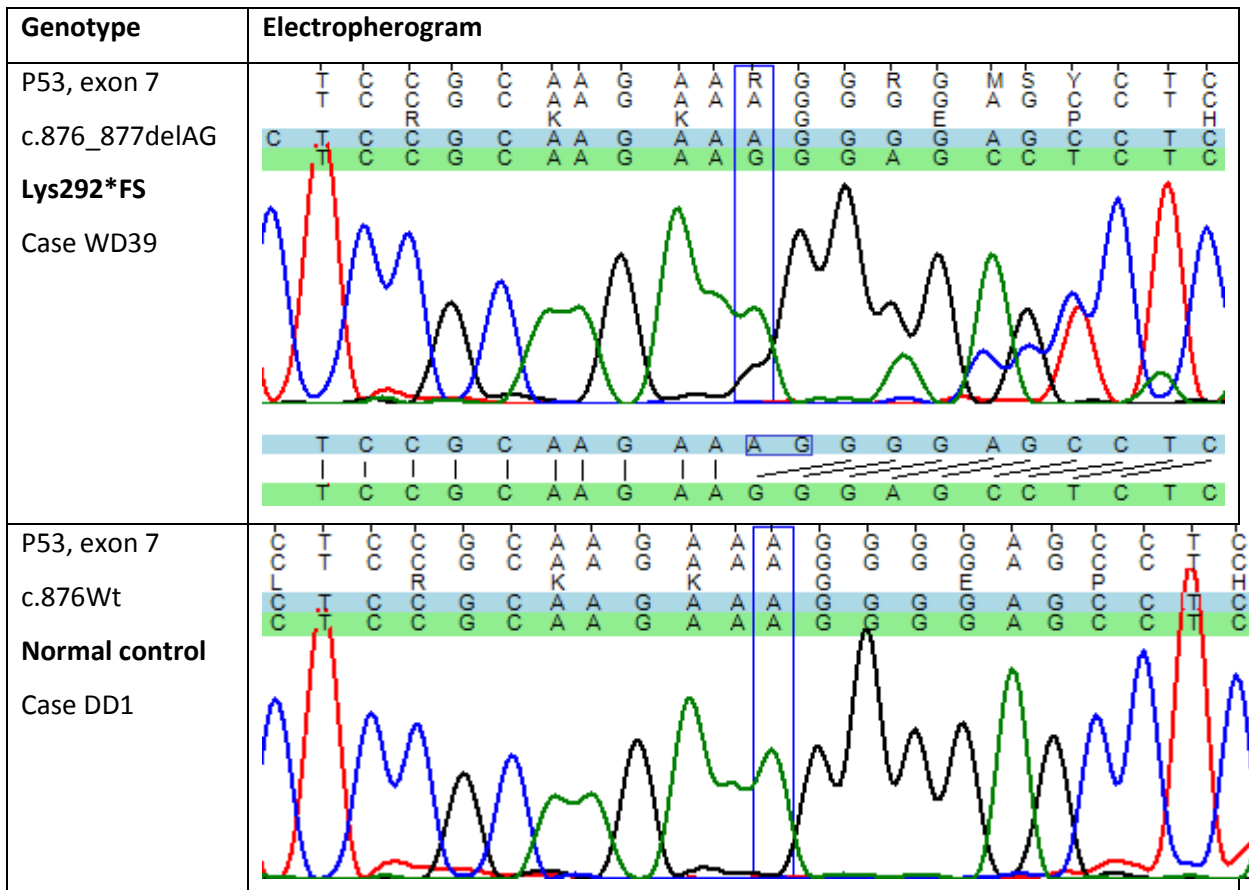


Figure 5.8: Electropherogram of sequence surrounding codon 292 demonstrating frame shift Lys292

Electropherogram of *P53* exon 8 representing a frame shift resulting from AG deletion at residue 876-877 in case WD39 (top) in comparison to case DD1 as a control (bottom). The upper nucleotide sequence represents the sample's sequence while the next two sequences identify the reference nucleotide and amino acid sequences respectively. The sequences in the blue bar again show the reference sequence while the sequence in the green bar shows the deduced sequence of the allele containing the deletion. It can be seen that the deduced sequence is transposed two positions 5' of the AG deletion. Due to the presence of the four consecutive G residues at and 3' to the deletion's location, it only manifests itself as changes in the peak heights these residues.

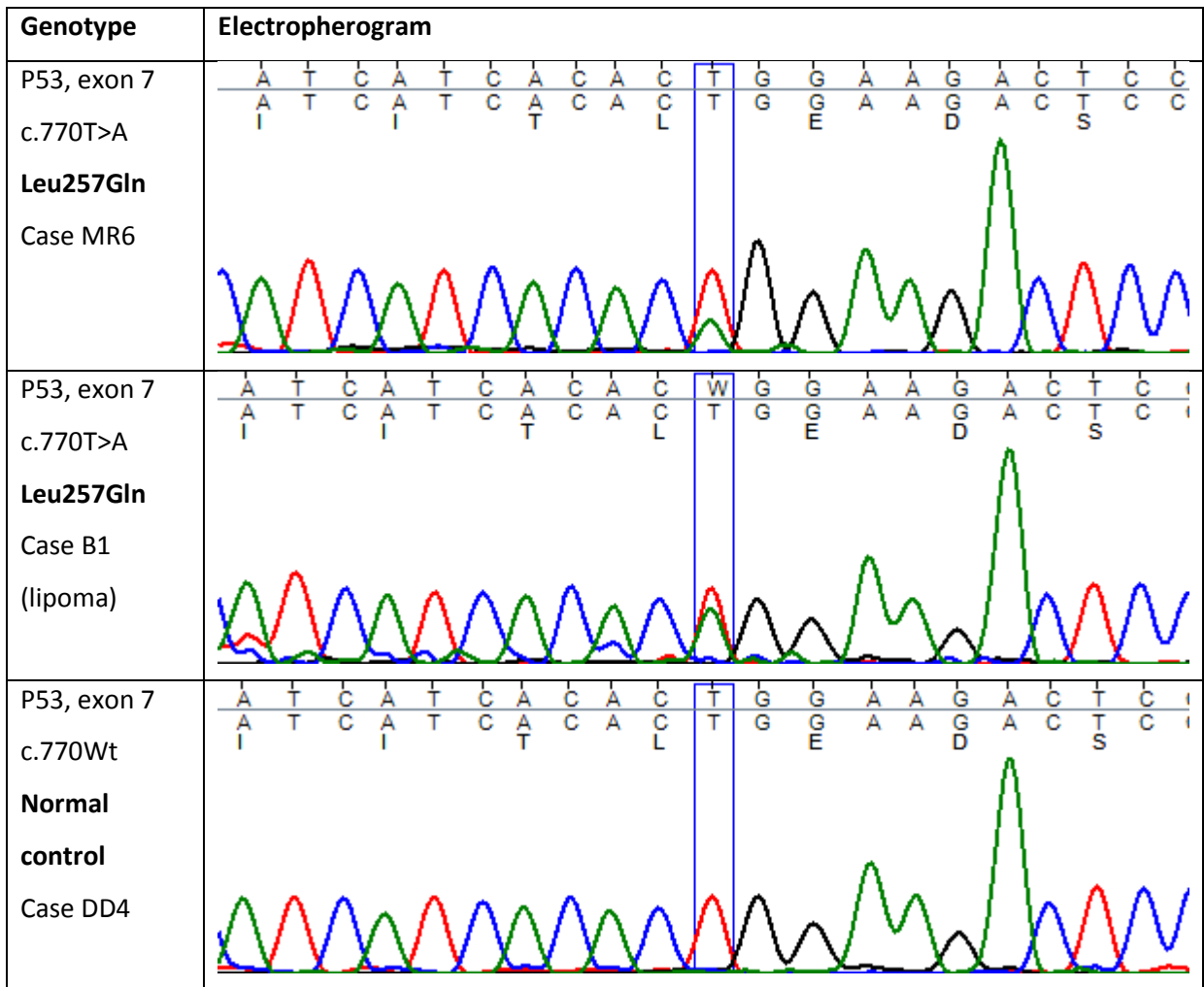


Figure 5.9: Electropherogram of sequence surrounding codon 257 demonstrating Leu257Gln

Electropherogram of *P53* exon 7 representing a heterozygous mutation T>A at residue 770 in cases MR6 and B1 (top2) as a demonstrative example, in comparison to case DD4 as a control (bottom). The upper nucleotide sequence represents the sample's sequence while the lower two sequences identify the reference nucleotide and amino acid sequences respectively. Letter codes follow the International Union of Pure and Applied Chemistry (IUPAC) coding (W = A+T). Wt = wild type.

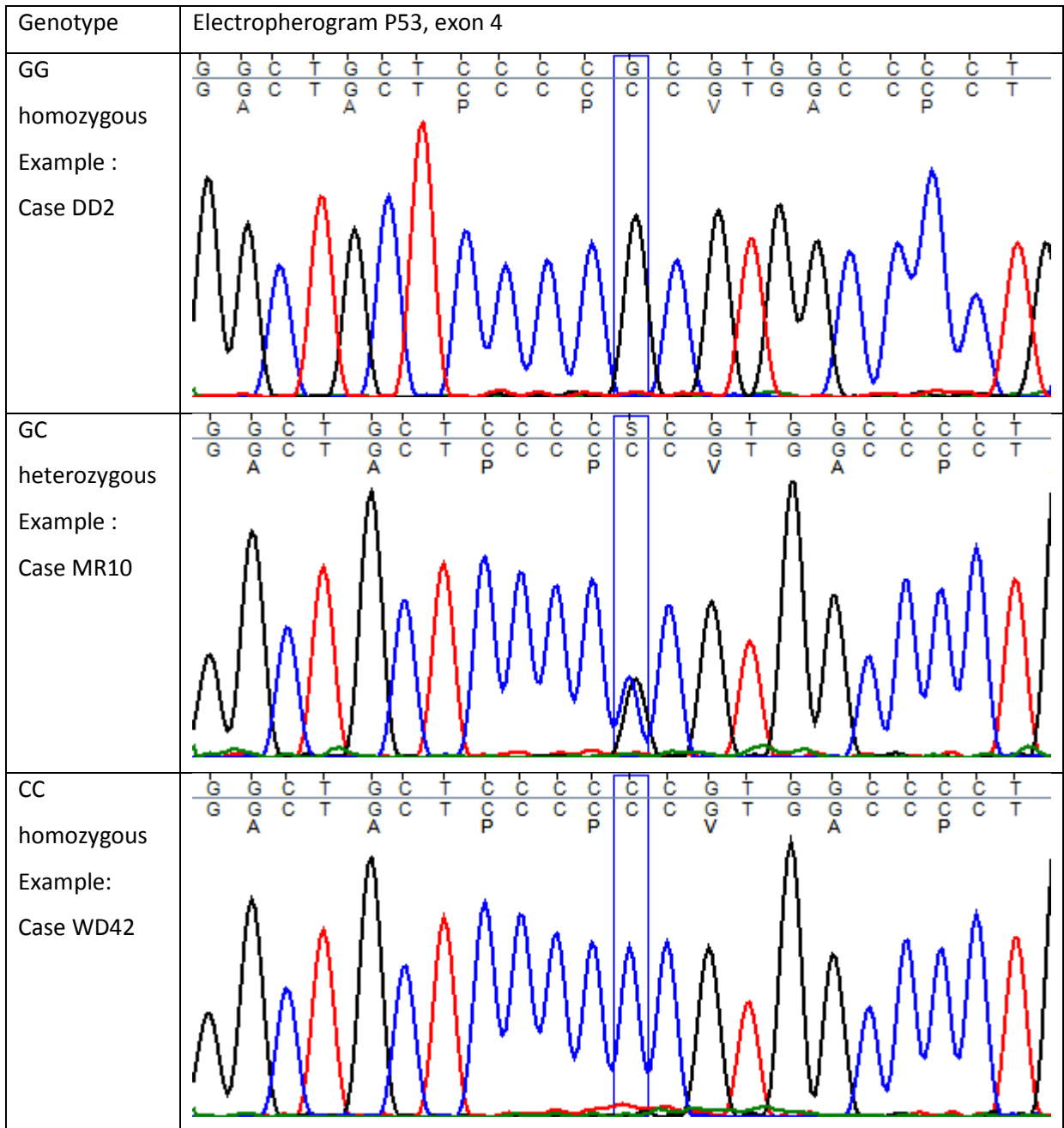


Figure 5.10: Electropherogram of sequence surrounding codon 72 demonstrating Arg72Pro polymorphism

Electropherogram of *P53* exon 4 representing SNP polymorphism at codon 72. GG homozygous resulting in Arginine variant, example case DD2 (top); GC heterozygous resulting in Arginine Proline variant, example case MR10 (middle); and CC homozygous resulting in Proline variant, example case WD42 (bottom). The upper nucleotide sequence represent the sample's sequence while the lower two sequences identify the reference nucleotide and amino acid sequences respectively.

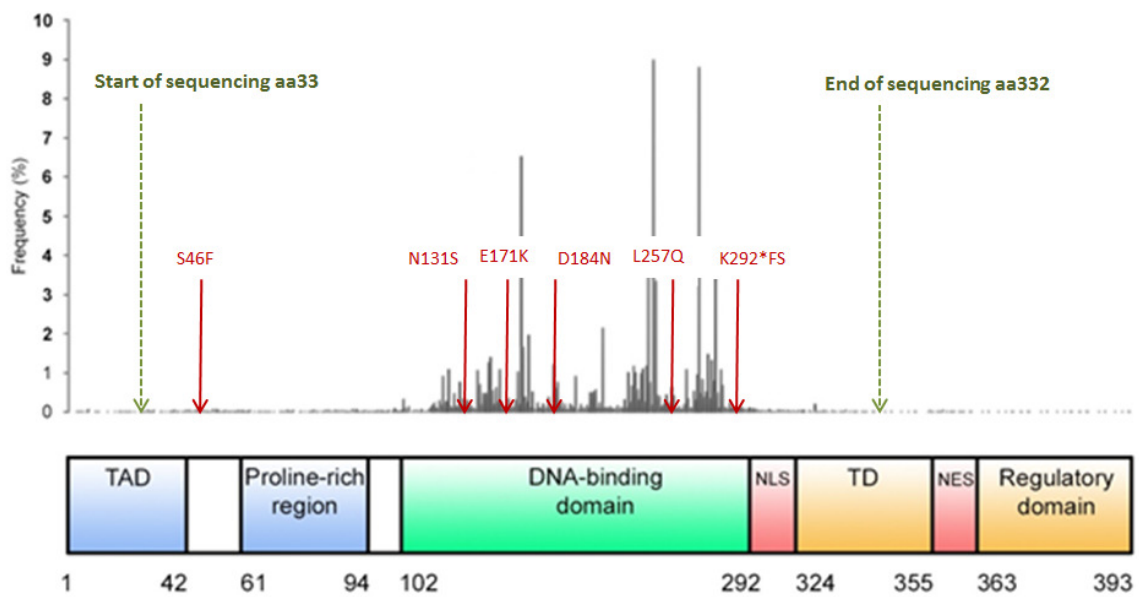


Figure 5.11 P53 structure and detected mutations

A schematic presentation of P53 and the frequency of detected mutations in cancers in general as per IARC TP53 database. The green arrows indicate the start and end of the sequenced area of P53. Detected mutations are indicated by the red arrows. TAD = Transactivation domain; TD = Tetramerisation domain; NES = nuclear export signal; NLS = nuclear localisation signal; aa = amino acid. Adopted from WA Freed-Pastor *et al.*, 2013 (54).

6 Other Soft Tissue Sarcomas and Benign Tumours

6.1 Aim

The aim of this Section is to examine a complementary small cohort of STSs (other than LSs) and benign lipomas to assess if they displayed cellular expression profiles of MDM and P53 proteins that were in line with the observed trends in the LS cohort.

This complementary cohort consisted of:

- A) Malignant tumours: 3 angiosarcomas and 1 inflammatory fibroblastic tumour
- B) Benign tumours: 3 lipomas, 1 leiomyoma and 1 intramuscular myxoma

The samples were processed and analysed using identical protocols to those employed in the analysis of the LS cohort.

6.2 Cytogenetics

Diagnostic cytogenetic analysis was performed in 4 of the 9 cases in the cohort, as a consequence of the tumours' appearances at the time of surgery. In the malignant cases, the 3 angiosarcomas were not analysed by FISH as LS was not initially suspected on clinical or radiological grounds. However, the inflammatory fibroblastic tumour was found to have *MDM2* amplification by FISH analysis. In the benign cases, all three benign lipomas were negative for *MDM2* amplification. The leiomyoma and myxoma cases were not subjected to cytogenetic analysis.

6.3 Immunohistochemistry

All cases were analysed by IHC and were scored using the same protocols as described earlier for the LS cohort. One angiosarcoma over-expressed MDM2 alone (case no. ST1) and another over-expressed MDMX alone (case no. ST3). Both cases had low P53 expression. However, the third angiosarcoma (case no. ST2) over-expressed all three proteins. In spite of a detectable *MDM2* amplification, the inflammatory fibroblastic tumour (case no. ST4) displayed low MDM2 and P53 protein expression profiles, with moderately over-expressed MDMX (+).

All three lipomas and the leiomyoma had low expression of MDM2, MDMX and P53. The intramuscular myxoma (case no. B5) demonstrated high expression levels (++) of MDM2 and MDMX with normal (low) P53 expression profile.

6.4 Discussion

6.4.1 Cytogenetic Results

The absence of MDM2 amplification by the cytogenetic FISH analysis of the three lipomas is in agreement with their benign histological evaluation. If the FISH analysis had revealed *MDM2* amplification in any of these cases, then the histological diagnosis would have been reviewed. It may be acceptable to have a histological diagnosis of LS that is not supported by *MDM2* amplification, but the contrary has not been reported.

The *MDM2* amplification displayed by the inflammatory fibroblastic tumour has been previously reported (234). These tumours are extremely rare and would require multicentre collaboration to obtain adequate numbers for analysis and characterisation.

6.4.2 Immunohistochemistry Results

The expression profile of MDM2 and P53 in the analysed angiosarcomas is consistent with a previous analysis that included 19 cases, which revealed that MDM2 and P53 were over-expressed in 68% and 53% of cases, respectively (235). However, we are not aware of any published studies that examined MDMX expression in angiosarcomas. Therefore, our observations of possible high frequency of MDMX over-expression in angiosarcomas invite further characterisation studies. Similarly, only limited data is available on the expression profile of MDM proteins in inflammatory fibroblastic tumours. One study, that included 15 cases, revealed that approximately 30% of these cancers over-expressed MDM2 (234).

While there are limited published data on the expression patterns of MDM2, MDMX and P53 in these tumour types, our observations of these proteins are in agreement with the expression pattern trends described earlier in LSs. The angiosarcoma case that displayed (++) profile for both MDM2 and MDMX, additionally over-expressed P53, as seen in the

“competitive” pattern; the other 2 angiosarcomas revealed low P53 levels in conjunction with a solitary over-expression of MDM2 or MDMX, as seen in the “collaborative” pattern (Figure 6.1). These observations are in agreement with the literature, which suggests that over-expression of one of the regulatory proteins may be sufficient for P53 inhibition / degradation.

Four of the 5 analysed benign cases displayed immunohistochemical profiles that are within the anticipated levels of normal (low) MDM / P53 interaction in non-malignant cells. The intramuscular myxoma, on the other hand, had shown high levels of MDM2 and MDMX with normal expression of P53. While this expression profile may represent an exception to the “competitive” pattern described earlier, such exceptions may be predicted in benign cases. A recent review of 11 myxomas did not detect *MDM2* amplification in any of these cases (236) and no published data regarding MDM2 expression in Intramuscular myxoma was found at the time of writing this report. However, it is known that some cells may over-express MDM2 without gene amplification, as seen within the LS results of this study.

The different tumours in this complementary cohort displayed a mosaic pattern of co-expression among the studied proteins, which may emphasise the significance of assessing these biomarkers jointly in order to obtain a meaningful picture of their complex interactions. It is remarkable how the expression patterns in this small cohort agreed with the described interplay between MDM2, MDMX and P53, observed in LSs in this study. Therefore, these patterns of protein interaction may represent a general feature of malignant cell molecular pathology that is not merely limited to LSs and may be anticipated in other cancers. Unfortunately, similar profiling studies in other cancers are lacking.

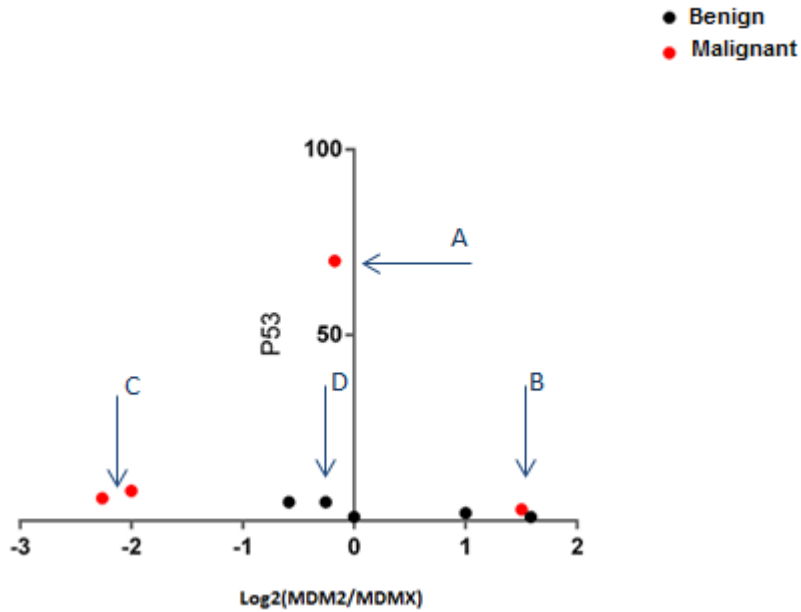


Figure 6.1: P53 expression in relation to Log2(MDM2/MDMX) scores in other STS and benign cases

A scatterplot representing the expression levels of P53 in relation to Log2(MDM2/MDMX) scores. A: angiosarcoma with (++) expression profile for (MDM2/MDMX/P53), consistent with “competitive” interplay pattern; B: angiosarcoma with solitary over-expression of MDM2; C: angiosarcoma and inflammatory fibroplastic tumour with solitary over-expression of MDMX, note the low level of P53 in B and C; D: intra-muscular myxoma with (++) expression profile. All benign cases retained low levels of activity for P53.

7 General Discussion

7.1 Significance of the Study

With the emergence of integrated cytogenetic and molecular genetic inputs into the STS diagnostics and classification system, a thorough evaluation of the molecular consequences of their pathognomonic events should similarly evolve to explore the prospects of future novel therapeutic approaches. This makes the MDM2 amplification in LS and its subsequent interplay with the tumour suppressor, P53 a very promising area for the development of therapeutic agents.

This study illustrates that the dynamic interactions between MDM proteins and P53 are a retained property in LS (and possibly other STS) tissues and does not merely represent a cell line observation. These interactions can be effectively assessed with simple, cost-effective techniques on FFPE human tissues. Previously, expression profiling of MDM2, MDMX and P53 was limited to cell line studies and therefore there were limitations in translating the outcomes into clinical use. This study also demonstrated that partial or selective analysis of MDM2 or MDMX alongside P53 may result in missing vital information about the characteristics of the examined tumours, and therefore may best be avoided.

The study has revealed that the MDM2 to MDMX ratio is an important factor in the expression levels of wild type P53. High P53 levels were seen when MDM2 and MDMX were equally over-expressed suggesting a possible competition between the two negative regulators to bind to P53 and therefore resulting in reduced P53 degradation. Conversely predominant MDM2 over-expression in relation to MDMX resulted in diminished levels of P53, suggesting a collaborative effort between MDM2 and MDMX to degrade P53. While the detected P53 may be functionally inactivated by the MDM2 and MDMX interactions, P53's activity may be rescued by the use of novel MDM2, MDMX and P53 binding antagonists. The conclusions of this study may give greater insight into the selection of antagonist drugs in future clinical trials exploring mechanisms to normalise the activity of wild type P53 in MDM2 and MDMX over-expressing tumours.

7.1.1 Role in Diagnostics

The results of this study, as well as other related previous analyses (as shown in Table 4.4) confirm clear superiority of molecular genetic testing as a diagnostic tool in LSs and STSs in general, compared to IHC testing. On the other hand, the IHC characterisation of LSs may provide an additional aid in the diagnostic toolkit, especially in cases where cytogenetic and molecular genetic assessments are not feasible or are inconclusive.

7.1.2 Role in Therapeutic Applications

Early STS cell line studies, which assessed the therapeutic response to a targeted MDM2 antagonist, utilising Nutlin-3a, have revealed a superior response in cell lines with *MDM2* gene amplification (162, 188). Since then, *MDM2* amplification has been considered the “benchmark” test to select cases for P53- MDM2 blocking trials. However, it is known that *MDM2* amplification and over-expression are not always correlated. As the novel blocking compounds interact with their targets at the protein-protein level, it may be inappropriate to solely adopt the gene amplification status as a predictor of response to this therapeutic approach. In addition, selecting cases based solely on their MDM2 status ignores the other, equally relevant, regulators of P53 and their role in the complex interplay of manipulating P53 cellular abundance and activity. An example of the complexity of the regulation of P53 activity was provided by Hu *et al.*, in their description of increased MDMX levels when treating MDM2 and MDMX positive cells with Nutlin-3a (164).

The earliest, proof of principle, clinical trial targeting *MDM2*-amplified WDLS and DDLS with the new generation of Nutlins (RG7112) has revealed disappointing results, with partial response in only one of the twenty recruited patients (163). Unfortunately, the study relied on the *MDM2* amplification status as a benchmark for selecting candidates and ignored the relevant MDMX role in the interaction. In light of the findings of this study, it would have been interesting to examine the MDM2, MDMX and P53 expression status in all these cases. Targeting P53-MDM2 interaction in cases that co-expressed MDMX may merely free P53 from one inhibitor (MDM2) to attach to another (MDMX), especially since Nutlins are known to have very poor affinity for MDMX.

It was not until very recently that the use of *MDM2* amplification as a benchmark test and a predictor of outcomes from Nutlin treatment was criticized, prompting the search for alternatives that recognised a holistic approach in the characterisation of candidate tumours for selective P53-MDM2 blocking trials (237). However, the majority of subsequent studies have failed to recognise the pivotal role of MDMX in P53 regulation. To date, the published results of this study represent the only call for simultaneous characterisation of MDM2, MDMX and P53, as a potential benchmark test for P53-MDM proteins antagonists (238).

In summary, cytogenetic and molecular genetic analysis is a key component in the diagnosis and classification of STSs, but it may not provide sufficient insights to be the selection criterion for targeted P53-MDM blocking therapies. This study proposes that IHC based characterisation of LSs may provide additional meaningful interpretation of cellular P53 availability and may guide the selection of single and /or dual affinity P53-MDM blocker compounds in future clinical trials.

7.2 Limitations of the Study

Similar to previous STSs studies, or any other rare cancers, concerns may be raised due to the sample size and the heterogeneity of the analysed tumour cohort, to reliably represent the disease as seen in the clinic. Typically, similar tumour profiling studies, examining other more common tumours, would probably involve more cases than used in this study. However, the study's final sample size was comparable to many other related analyses of similar rare tumour types and was sufficiently large to provide statistically-significant results.

As discussed in Chapter Four, and in contrast to the majority of cancers, STSs consist of a wide variety of tumour types resulting in a multifaceted classification system. Even the simple distinction between benign and malignant tumours in soft tissue neoplasms may occasionally prove to be extremely challenging and occasionally interpreter-dependent. This in turn, may provide a source of confusion and lack of consistency that may introduce classification errors in large, multi-centric trials or in literature reviews, where apparent homogenous tumour cohorts are in fact more heterogeneous than believed. However, one could hope that the introduction of the new WHO classification and the introduction of

molecular genetic based testing into STS tumour typing, may create a uniform mechanism towards a more objective, meaningful and synonymous categorisation for STSs, including the most challenging clinical cases.

7.3 Future Perspectives

To translate the findings of this study into the clinic, it will be necessary to conduct functional studies to evaluate the pharmacological effects of single and dual affinity blocking compounds in LSs, in light of their IHC profiles. Functional assessments have become increasingly important and clinically relevant with the advent of new MDM2 / MDMX blocking compounds of variable affinities. As some of these compounds are in phase I and phase II clinical trials, it is certainly vital to establish clear guidance for effective candidate selection with selective antagonist drug matching to these candidates. It is equally relevant to seek reliable predictors of outcome to further guide clinical trials.

Therefore, we propose functional studies utilising the Tissue Explant System introduced by Singh *et al.* (239) and later modified by Pishas *et al.* for the purpose of STS experiments (237). The system is designed to grow 1 mm³ pieces of freshly excised STS on a dental sponge immersed in a cocktail of RPMI media with 5% foetal bovine serum and other reagents. The tissue blocks can then be incubated with the drug of choice or a suitable control, at 37°C in a humidified atmosphere for a period of 48 hrs. Subsequently, tissue pieces may be harvested and evaluated for cellular activity, apoptosis, activity of P53 and its downstream pathways and any other parameters that may be relevant to objectively quantify the desired pharmacological response.

This proposed model of experiment may provide quantitative assessments as to the efficacy of different lead MDM blocking compounds. It may clarify the potential utility, and putative superiority, of dual MDM2 / MDMX blocking compounds, compared to single affinity MDM2 blockers, in cases that over-express both proteins by IHC. In addition, the alleged synergistic effect, obtained by adding conventional chemotherapy agents to MDM blockers can be scrutinised and detailed. Collectively, functional studies of this kind may provide a promising experimental platform for future clinical trials.

Finally, LSs are excellent candidates for targeted therapies of this pathway, as they mainly retain a wild type status of *P53* and demonstrate MDM2 amplification / over-expression in the majority of cases. Moreover, this promising approach of P53 reactivation is not limited to a certain subset of tumours and it may be applicable to a wide range of cancers after careful characterisation of their relevant MDM biomarkers.

I- References

1. Linch M, Miah AB, Thway K, Judson IR, Benson C. Systemic treatment of soft-tissue sarcoma [mdash] gold standard and novel therapies. *Nature Reviews Clinical Oncology*. 2014;11(4):187-202.
2. Dennis N, Francis M, Lawrence G. Soft Tissue Sarcoma Incidence and Survival. Birmingham: National Cancer Intelligence Network 2012 [updated 12/2012; cited 2013 07/2013]; Report]. Available from: http://www.ncin.org.uk/cancer_type_and_topic_specific_work/cancer_type_specific_work/sarcomas/.
3. WHO Classification of Soft Tissue Tumours. WHO; 2006 [cited 2013 10/2013]; STS classification]. Available from: <http://www.iarc.fr/en/publications/pdfs-online/pat-gen/bb5/bb5-classifsofttissue.pdf>.
4. Demicco EG. Sarcoma diagnosis in the age of molecular pathology. *Adv Anat Pathol*. 2013;20(4):264-74.
5. Jain S, Xu R, Prieto VG, Lee P. Molecular classification of soft tissue sarcomas and its clinical applications. *Int J Clin Exp Pathol*. 2010;3(4):416-28.
6. Fletcher CDM, Bridge, J.A., Hogendoorn, P., Mertens, F. WHO Classification of Tumours of Soft Tissue and Bone: World Health Organization; 2013.
7. Fletcher CD. The evolving classification of soft tissue tumours - an update based on the new 2013 WHO classification. *Histopathology*. 2013.
8. Singer S, Antonescu CR, Riedel E, Brennan MF. Histologic subtype and margin of resection predict pattern of recurrence and survival for retroperitoneal liposarcoma. *Annals of Surgery*. 2003;238(3):358.
9. Nijhuis PH, Sars PR, Plaat BE, Molenaar WM, Sluiter WJ, Hoekstra HJ. Clinico-pathological data and prognostic factors in completely resected AJCC stage I-III liposarcomas. *Annals of Surgical Oncology*. 2000;7(7):535-43.
10. Kinne DW, Chu FC, Huvos AG, Yagoda A, Fortner JG. Treatment of primary and recurrent retroperitoneal liposarcoma. *Cancer*. 1973;31(1):53-64.
11. Henricks WH, Chu YC, Goldblum JR, Weiss SW. Dedifferentiated liposarcoma: a clinicopathological analysis of 155 cases with a proposal for an expanded definition of dedifferentiation. *Am J Surg Pathol*. 1997;21(3):271-81.

12. Strauss DC, Hayes AJ, Thomas JM. Retroperitoneal tumours: review of management. *Ann R Coll Surg Engl.* 2011;93(4):275-80.
13. Pakos EE, Gogou PV, Apostolikas N, Batistatou A, Tsekeris PG. Factors associated with outcome in liposarcomas of the extremities and trunk. *J BUON.* 2010;15(3):518-23.
14. Conyers R, Young S, Thomas DM. Liposarcoma: molecular genetics and therapeutics. *Sarcoma.* 2011;2011.
15. Grimer R, Judson I, Peake D, Seddon B. Guidelines for the management of soft tissue sarcomas. *Sarcoma.* 2010;2010.
16. Brennan MF. Lessons learned from the study of soft tissue sarcoma. *Int J Surg.* 2013;11 Suppl 1:S8-10.
17. Mack TM. Sarcomas and other malignancies of soft tissue, retroperitoneum, peritoneum, pleura, heart, mediastinum, and spleen. *Cancer.* 1995;75(1 Suppl):211-44.
18. Weiss SW, Goldblum JR. *Enzinger and Weiss's Soft Tissue Tumors.* 5 ed. Philadelphia: Mosby Elsevier; 2008.
19. Gutierrez JC, Perez EA, Franceschi D, Moffat FL, Jr., Livingstone AS, Koniaris LG. Outcomes for soft-tissue sarcoma in 8249 cases from a large state cancer registry. *J Surg Res.* 2007;141(1):105-14.
20. Dei Tos AP, Doglioni C, Piccinin S, Sciot R, Furlanetto A, Boiocchi M, *et al.* Coordinated expression and amplification of the MDM2, CDK4, and HMGI-C genes in atypical lipomatous tumours. *J Pathol.* 2000;190(5):531-6.
21. Jones RL, Fisher C, Al-Muderis O, Judson IR. Differential sensitivity of liposarcoma subtypes to chemotherapy. *Eur J Cancer.* 2005;41(18):2853-60.
22. Hasegawa T, Seki K, Hasegawa F, Matsuno Y, Shimodo T, Hirose T, *et al.* Dedifferentiated liposarcoma of retroperitoneum and mesentery: varied growth patterns and histological grades-a clinicopathologic study of 32 cases. *Hum Pathol.* 2000;31(6):717-27.
23. Fletcher KCU, Krishnan K, Mertens F. *Pathology and Genetics of Tumours of Soft Tissue and Bone.* Lyon: IARC Press; 2002.
24. Schwab JH, Boland P, Guo T, Brennan MF, Singer S, Healey JH, *et al.* Skeletal metastases in myxoid liposarcoma: an unusual pattern of distant spread. *Ann Surg Oncol.* 2007;14(4):1507-14.

25. Chung PW, Dehesi BM, Ferguson PC, Wunder JS, Griffin AM, Catton CN, *et al.* Radiosensitivity translates into excellent local control in extremity myxoid liposarcoma: a comparison with other soft tissue sarcomas. *Cancer*. 2009;115(14):3254-61.
26. Hornick JL, Bosenberg MW, Mentzel T, McMenamin ME, Oliveira AM, Fletcher CD. Pleomorphic liposarcoma: clinicopathologic analysis of 57 cases. *Am J Surg Pathol*. 2004;28(10):1257-67.
27. Dodd LG. Update on liposarcoma: a review for cytopathologists. *Diagn Cytopathol*. 2012;40(12):1122-31.
28. Gebhard S, Coindre JM, Michels JJ, Terrier P, Bertrand G, Trassard M, *et al.* Pleomorphic liposarcoma: clinicopathologic, immunohistochemical, and follow-up analysis of 63 cases: a study from the French Federation of Cancer Centers Sarcoma Group. *Am J Surg Pathol*. 2002;26(5):601-16.
29. de Vreeze RS, de Jong D, Nederlof PM, Ariaens A, Tielen IH, Frenken L, *et al.* Added Value of Molecular Biological Analysis in Diagnosis and Clinical Management of Liposarcoma: A 30-Year Single-Institution Experience. *Ann Surg Oncol*. 2010;17(3):686-93.
30. Szymanska J, Virolainen M, Tarkkanen M, Wiklund T, Asko-Seljavaara S, Tukiainen E, *et al.* Overrepresentation of 1q21-23 and 12q13-21 in lipoma-like liposarcomas but not in benign lipomas: a comparative genomic hybridization study. *Cancer Genet Cytogenet*. 1997;99(1):14-8.
31. Pedeutour F, Forus A, Coindre JM, Berner JM, Nicolo G, Michiels JF, *et al.* Structure of the supernumerary ring and giant rod chromosomes in adipose tissue tumors. *Genes Chromosomes Cancer*. 1999;24(1):30-41.
32. Rieker RJ, Weitz J, Lehner B, Egerer G, Mueller A, Kasper B, *et al.* Genomic profiling reveals subsets of dedifferentiated liposarcoma to follow separate molecular pathways. *Virchows Arch*. 2010;456(3):277-85.
33. Binh MB, Sastre-Garau X, Guillou L, de Pinieux G, Terrier P, Lagace R, *et al.* MDM2 and CDK4 immunostainings are useful adjuncts in diagnosing well-differentiated and dedifferentiated liposarcoma subtypes: a comparative analysis of 559 soft tissue neoplasms with genetic data. *Am J Surg Pathol*. 2005;29(10):1340-7.
34. Pilotti GT, C Lavarino. Distinct mdm2/p53 expression patterns in liposarcoma subgroups: Implications for different pathogenetic mechanisms. *J Pathol* 1997;181(1):14-24.
35. Antonescu CR, Tschernyavsky SJ, Decuseara R, Leung DH, Woodruff JM, Brennan MF, *et al.* Prognostic impact of P53 status, TLS-CHOP fusion transcript structure, and histological grade in myxoid liposarcoma: a molecular and clinicopathologic study of 82 cases. *Clin Cancer Res*. 2001;7(12):3977-87.

36. Dal Cin P, Sciot R, Panagopoulos I, Aman P, Samson I, Mandahl N, *et al.* Additional evidence of a variant translocation t(12;22) with EWS/CHOP fusion in myxoid liposarcoma: clinicopathological features. *J Pathol.* 1997;182(4):437-41.
37. Guillou L, Aurias A. Soft tissue sarcomas with complex genomic profiles. *Virchows Arch.* 2010;456(2):201-17.
38. DeLeo AB, Jay G, Appella E, Dubois GC, Law LW, Old LJ. Detection of a transformation-related antigen in chemically induced sarcomas and other transformed cells of the mouse. *Proc Natl Acad Sci U S A.* 1979;76(5):2420-4.
39. Finlay CA, Hinds PW, Levine AJ. The p53 proto-oncogene can act as a suppressor of transformation. *Cell.* 1989;57(7):1083-93.
40. Donehower LA, Harvey M, Slagle BL, McArthur MJ, Montgomery CA, Jr., Butel JS, *et al.* Mice deficient for p53 are developmentally normal but susceptible to spontaneous tumours. *Nature.* 1992;356(6366):215-21.
41. Hollstein M, Sidransky D, Vogelstein B, Harris CC. p53 mutations in human cancers. *Science.* 1991;253(5015):49-53.
42. Petitjean A, Mathe E, Kato S, Ishioka C, Tavtigian SV, Hainaut P, *et al.* Impact of mutant p53 functional properties on TP53 mutation patterns and tumor phenotype: lessons from recent developments in the IARC TP53 database. *Hum Mutat.* 2007;28(6):622-9.
43. Taubert H, Meye A, Wurl P. Soft tissue sarcomas and p53 mutations. *Mol Med.* 1998;4(6):365-72.
44. Leach FS, Tokino T, Meltzer P, Burrell M, Oliner JD, Smith S, *et al.* p53 Mutation and MDM2 amplification in human soft tissue sarcomas. *Cancer Res.* 1993;53(10 Suppl):2231-4. Epub 1993/05/15.
45. Vousden KH, Lu X. Live or let die: the cell's response to p53. *Nat Rev Cancer.* 2002;2(8):594-604.
46. Li FP, Fraumeni JF, Jr. Soft-tissue sarcomas, breast cancer, and other neoplasms. A familial syndrome? *Ann Intern Med.* 1969;71(4):747-52.
47. Malkin D, Li FP, Strong LC, Fraumeni JF, Jr., Nelson CE, Kim DH, *et al.* Germ line p53 mutations in a familial syndrome of breast cancer, sarcomas, and other neoplasms. *Science.* 1990;250(4985):1233-8.
48. Ognjanovic S, Olivier M, Bergemann TL, Hainaut P. Sarcomas in TP53 germline mutation carriers: a review of the IARC TP53 database. *Cancer.* 2012;118(5):1387-96.

49. Oren M, Rotter V. Introduction: p53--the first twenty years. *Cell Mol Life Sci.* 1999;55(1):9-11.
50. Irwin MS, Kaelin WG. p53 family update: p73 and p63 develop their own identities. *Cell Growth Differ.* 2001;12(7):337-49.
51. Wang YV, Wade M, Wong E, Li YC, Rodewald LW, Wahl GM. Quantitative analyses reveal the importance of regulated Hdmx degradation for p53 activation. *Proc Natl Acad Sci U S A.* 2007;104(30):12365-70.
52. Lamb P, Crawford L. Characterization of the human p53 gene. *Mol Cell Biol.* 1986;6(5):1379-85.
53. Berger M, Vogt Sionov R, Levine AJ, Haupt Y. A role for the polyproline domain of p53 in its regulation by Mdm2. *J Biol Chem.* 2001;276(6):3785-90.
54. Freed-Pastor WA, Prives C. Mutant p53: one name, many proteins. *Genes Dev.* 2012;26(12):1268-86.
55. Bakalkin G, Selivanova G, Yakovleva T, Kiseleva E, Kashuba E, Magnusson KP, *et al.* p53 binds single-stranded DNA ends through the C-terminal domain and internal DNA segments via the middle domain. *Nucleic Acids Res.* 1995;23(3):362-9.
56. Khoury MP, Bourdon JC. The isoforms of the p53 protein. *Cold Spring Harb Perspect Biol.* 2010;2(3):a000927.
57. Hollstein M, Hainaut P. Massively regulated genes: the example of TP53. *J Pathol.* 2010;220(2):164-73.
58. Oren M. Decision making by p53: life, death and cancer. *Cell Death Differ.* 2003;10(4):431-42.
59. Vousden KH, Prives C. Blinded by the Light: The Growing Complexity of p53. *Cell.* 2009;137(3):413-31.
60. Reinhardt HC, Schumacher B. The p53 network: cellular and systemic DNA damage responses in aging and cancer. *Trends Genet.* 2012;28(3):128-36.
61. Zheltukhin AO, Chumakov PM. Constitutive and induced functions of the p53 gene. *Biochemistry (Mosc).* 2010;75(13):1692-721.
62. el-Deiry WS, Tokino T, Velculescu VE, Levy DB, Parsons R, Trent JM, *et al.* WAF1, a potential mediator of p53 tumor suppression. *Cell.* 1993;75(4):817-25.

63. Colman MS, Afshari CA, Barrett JC. Regulation of p53 stability and activity in response to genotoxic stress. *Mutat Res.* 2000;462(2-3):179-88.
64. Cory S, Adams JM. The Bcl2 family: regulators of the cellular life-or-death switch. *Nat Rev Cancer.* 2002;2(9):647-56.
65. Takimoto R, El-Deiry WS. Wild-type p53 transactivates the KILLER/DR5 gene through an intronic sequence-specific DNA-binding site. *Oncogene.* 2000;19(14):1735-43.
66. Symonds H, Krall L, Remington L, Saenz-Robles M, Lowe S, Jacks T, *et al.* p53-dependent apoptosis suppresses tumor growth and progression in vivo. *Cell.* 1994;78(4):703-11.
67. Maltzman W, Czyzyk L. UV irradiation stimulates levels of p53 cellular tumor antigen in nontransformed mouse cells. *Mol Cell Biol.* 1984;4(9):1689-94.
68. Huibregtse JM, Scheffner M, Howley PM. A cellular protein mediates association of p53 with the E6 oncoprotein of human papillomavirus types 16 or 18. *EMBO J.* 1991;10(13):4129.
69. Maheswaran S, Englert C, Bennett P, Heinrich G, Haber DA. The WT1 gene product stabilizes p53 and inhibits p53-mediated apoptosis. *Genes & Development.* 1995;9(17):2143-56.
70. Querido E, Marcellus RC, Lai A, Charbonneau R, Teodoro JG, Ketner G, *et al.* Regulation of p53 levels by the E1B 55-kilodalton protein and E4orf6 in adenovirus-infected cells. *Journal of Virology.* 1997;71(5):3788-98.
71. Fuchs SY, Adler V, Buschmann T, Yin Z, Wu X, Jones SN, *et al.* JNK targets p53 ubiquitination and degradation in nonstressed cells. *Genes & Development.* 1998;12(17):2658-63.
72. Duan W, Gao L, Druhan LJ, Zhu W-G, Morrison C, Otterson GA, *et al.* Expression of Pirh2, a newly identified ubiquitin protein ligase, in lung cancer. *Journal of the National Cancer Institute.* 2004;96(22):1718-21.
73. Węsierska-Gądek J, Wojciechowski J, Schmid G. Central and carboxy-terminal regions of human p53 protein are essential for interaction and complex formation with PARP-1. *Journal of Cellular Biochemistry.* 2003;89(2):220-32.
74. Honda R, Tanaka H, Yasuda H. Oncoprotein MDM2 is a ubiquitin ligase E3 for tumor suppressor p53. *FEBS Lett.* 1997;420(1):25-7.

75. Toledo F, Krummel KA, Lee CJ, Liu CW, Rodewald LW, Tang M, *et al.* A mouse p53 mutant lacking the proline-rich domain rescues Mdm4 deficiency and provides insight into the Mdm2-Mdm4-p53 regulatory network. *Cancer Cell*. 2006;9(4):273-85.
76. Kruse JP, Gu W. Modes of p53 regulation. *Cell*. 2009;137(4):609-22.
77. Shvarts A, Steegenga WT, Riteco N, van Laar T, Dekker P, Bazuine M, *et al.* MDMX: a novel p53-binding protein with some functional properties of MDM2. *EMBO J*. 1996;15(19):5349-57.
78. Shvarts A, Bazuine M, Dekker P, Ramos YF, Steegenga WT, Merckx G, *et al.* Isolation and identification of the human homolog of a new p53-binding protein, Mdmx. *Genomics*. 1997;43(1):34-42.
79. Rosai J, Akerman M, Dal Cin P, DeWever I, Fletcher CD, Mandahl N, *et al.* Combined morphologic and karyotypic study of 59 atypical lipomatous tumors. Evaluation of their relationship and differential diagnosis with other adipose tissue tumors (a report of the CHAMP Study Group). *Am J Surg Pathol*. 1996;20(10):1182-9.
80. Bartel F, Schulz J, Bohnke A, Blumke K, Kappler M, Bache M, *et al.* Significance of HDMX-S (or MDM4) mRNA splice variant overexpression and HDMX gene amplification on primary soft tissue sarcoma prognosis. *Int J Cancer*. 2005;117(3):469-75.
81. Ito M, Barys L, O'Reilly T, Young S, Gorbacheva B, Monahan J, *et al.* Comprehensive mapping of p53 pathway alterations reveals an apparent role for both SNP309 and MDM2 amplification in sarcomagenesis. *Clin Cancer Res*. 2011;17(3):416-26.
82. Ohnstad HO, Castro R, Sun J, Heintz KM, Vassilev LT, Bjerkehagen B, *et al.* Correlation of TP53 and MDM2 genotypes with response to therapy in sarcoma. *Cancer*. 2013;119(5):1013-22.
83. McLendon R, Friedman A, Bigner D, Van Meir EG, Brat DJ, Mastrogiannis GM, *et al.* Comprehensive genomic characterization defines human glioblastoma genes and core pathways. *Nature*. 2008;455(7216):1061-8.
84. Gembarska A, Luciani F, Fedele C, Russell EA, Dewaele M, Villar S, *et al.* MDM4 is a key therapeutic target in cutaneous melanoma. *Nat Med*. 2012;18(8):1239-47.
85. Tanière P, Martel-Planche G, Puttawibul P, Casson A, Montesano R, Chanvitan A, *et al.* TP53 mutations and MDM2 gene amplification in squamous-cell carcinomas of the esophagus in South Thailand. *Int J Cancer*. 2000;88(2):223-7.
86. Forslund A, Zeng Z, Qin L-X, Rosenberg S, Ndubuisi M, Pincas H, *et al.* MDM2 gene amplification is correlated to tumor progression but not to the presence of SNP309 or TP53 mutational status in primary colorectal cancers. *Mol Cancer Res*. 2008;6(2):205-11.

87. Lam S, Lodder K, Teunisse AF, Rabelink MJ, Schutte M, Jochemsen AG. Role of Mdm4 in drug sensitivity of breast cancer cells. *Oncogene*. 2010;29(16):2415-26.
88. Kimura H, Dobashi Y, Nojima T, Nakamura H, Yamamoto N, Tsuchiya H, *et al.* Utility of fluorescence in situ hybridization to detect MDM2 amplification in liposarcomas and their morphological mimics. *Int J Clin Exp Pathol*. 2013;6(7):1306-16.
89. Dei Tos AP, Doglioni C, Piccinin S, Maestro R, Mentzel T, Barbareschi M, *et al.* Molecular abnormalities of the p53 pathway in dedifferentiated liposarcoma. *J Pathol*. 1997;181(1):8-13.
90. Aleixo PB, Hartmann AA, Menezes IC, Meurer RT, Oliveira AM. Can MDM2 and CDK4 make the diagnosis of well differentiated/dedifferentiated liposarcoma? An immunohistochemical study on 129 soft tissue tumours. *J Clin Pathol*. 2009;62(12):1127-35.
91. Taubert H, Koehler T, Meye A, Bartel F, Lautenschlager C, Borchert S, *et al.* MDM2 mRNA level is a prognostic factor in soft tissue sarcoma. *Mol Med*. 2000;6(1):50-9.
92. Danovi D, Meulmeester E, Pasini D, Migliorini D, Capra M, Frenk R, *et al.* Amplification of Mdmx (or Mdm4) directly contributes to tumor formation by inhibiting p53 tumor suppressor activity. *Mol Cell Biol*. 2004;24(13):5835-43.
93. Ramos YF, Stad R, Attema J, Peltenburg LT, van der Eb AJ, Jochemsen AG. Aberrant expression of HDMX proteins in tumor cells correlates with wild-type p53. *Cancer Res*. 2001;61(5):1839-42.
94. Riemenschneider MJ, Knobbe CB, Reifenberger G. Refined mapping of 1q32 amplicons in malignant gliomas confirms MDM4 as the main amplification target. *Int J Cancer*. 2003;104(6):752-7.
95. Wade M, Li YC, Wahl GM. MDM2, MDMX and p53 in oncogenesis and cancer therapy. *Nat Rev Cancer*. 2013;13(2):83-96.
96. Tanimura S, Ohtsuka S, Mitsui K, Shirouzu K, Yoshimura A, Ohtsubo M. MDM2 interacts with MDMX through their RING finger domains. *FEBS Lett*. 1999;447(1):5-9.
97. Mayo LD, Turchi JJ, Berberich SJ. Mdm-2 phosphorylation by DNA-dependent protein kinase prevents interaction with p53. *Cancer Res*. 1997;57(22):5013-6.
98. Zuckerman V, Lenos K, Popowicz GM, Silberman I, Grossman T, Marine JC, *et al.* c-Abl phosphorylates Hdmx and regulates its interaction with p53. *J Biol Chem*. 2009;284(6):4031-9.

99. Kostic M, Matt T, Martinez-Yamout MA, Dyson HJ, Wright PE. Solution structure of the Hdm2 C2H2C4 RING, a domain critical for ubiquitination of p53. *J Mol Biol.* 2006;363(2):433-50.
100. Linares LK, Hengstermann A, Ciechanover A, Muller S, Scheffner M. HdmX stimulates Hdm2-mediated ubiquitination and degradation of p53. *Proc Natl Acad Sci U S A.* 2003;100(21):12009-14.
101. Ohtsubo C, Shiokawa D, Kodama M, Gaiddon C, Nakagama H, Jochemsen AG, *et al.* Cytoplasmic tethering is involved in synergistic inhibition of p53 by Mdmx and Mdm2. *Cancer Sci.* 2009;100(7):1291-9.
102. O'Keefe K, Li H, Zhang Y. Nucleocytoplasmic shuttling of p53 is essential for MDM2-mediated cytoplasmic degradation but not ubiquitination. *Mol Cell Biol.* 2003;23(18):6396-405.
103. Wade M, Wang YV, Wahl GM. The p53 orchestra: Mdm2 and Mdmx set the tone. *Trends Cell Biol.* 2010;20(5):299-309.
104. Li C, Chen L, Chen J. DNA damage induces MDMX nuclear translocation by p53-dependent and -independent mechanisms. *Mol Cell Biol.* 2002;22(21):7562-71.
105. Gu J, Kawai H, Nie L, Kitao H, Wiederschain D, Jochemsen AG, *et al.* Mutual dependence of MDM2 and MDMX in their functional inactivation of p53. *J Biol Chem.* 2002;277(22):19251-4.
106. Migliorini D, Danovi D, Colombo E, Carbone R, Pelicci PG, Marine JC. Hdmx recruitment into the nucleus by Hdm2 is essential for its ability to regulate p53 stability and transactivation. *J Biol Chem.* 2002;277(9):7318-23.
107. Sembritzki O, Hagel C, Lamszus K, Deppert W, Bohn W. Cytoplasmic localization of wild-type p53 in glioblastomas correlates with expression of vimentin and glial fibrillary acidic protein. *Neuro Oncol.* 2002;4(3):171-8.
108. Shaulsky G, Ben-Ze'ev A, Rotter V. Subcellular distribution of the p53 protein during the cell cycle of Balb/c 3T3 cells. *Oncogene.* 1990;5(11):1707-11.
109. Sigalas I, Calvert AH, Anderson JJ, Neal DE, Lunec J. Alternatively spliced mdm2 transcripts with loss of p53 binding domain sequences: transforming ability and frequent detection in human cancer. *Nat Med.* 1996;2(8):912-7.
110. Bartel F, Pinkert D, Fiedler W, Kappler M, Wurl P, Schmidt H, *et al.* Expression of alternatively and aberrantly spliced transcripts of the MDM2 mRNA is not tumor-specific. *Int J Oncol.* 2004;24(1):143-51.

111. Bartel F, Taylor AC, Taubert H, Harris LC. Novel mdm2 splice variants identified in pediatric rhabdomyosarcoma tumors and cell lines. *Oncol Res.* 2001;12(11-12):451-7.
112. Volk EL, Schuster K, Nemeth KM, Fan L, Harris LC. MDM2-A, a common Mdm2 splice variant, causes perinatal lethality, reduced longevity and enhanced senescence. *Dis Model Mech.* 2009;2(1-2):47-55.
113. Evans SC, Viswanathan M, Grier JD, Narayana M, El-Naggar AK, Lozano G. An alternatively spliced HDM2 product increases p53 activity by inhibiting HDM2. *Oncogene.* 2001;20(30):4041-9.
114. Iwakuma T, Lozano G. MDM2, an introduction. *Mol Cancer Res.* 2003;1(14):993-1000.
115. Fridman JS, Hernando E, Hemann MT, de Stanchina E, Cordon-Cardo C, Lowe SW. Tumor promotion by Mdm2 splice variants unable to bind p53. *Cancer Res.* 2003;63(18):5703-6.
116. Okoro DR, Arva N, Gao C, Polotskaia A, Puente C, Rosso M, *et al.* Endogenous Human MDM2-C Is Highly Expressed in Human Cancers and Functions as a p53-Independent Growth Activator. *PLoS One.* 2013;8(10):e77643.
117. Rallapalli R, Strachan G, Cho B, Mercer WE, Hall DJ. A novel MDMX transcript expressed in a variety of transformed cell lines encodes a truncated protein with potent p53 repressive activity. *J Biol Chem.* 1999;274(12):8299-308.
118. Lenos K, Grawenda AM, Lodder K, Kuijjer ML, Teunisse AF, Repapi E, *et al.* Alternate splicing of the p53 inhibitor HDMX offers a superior prognostic biomarker than p53 mutation in human cancer. *Cancer Res.* 2012;72(16):4074-84.
119. de Graaf P, Little NA, Ramos YF, Meulmeester E, Letteboer SJ, Jochemsen AG. Hdmx protein stability is regulated by the ubiquitin ligase activity of Mdm2. *J Biol Chem.* 2003;278(40):38315-24.
120. Phillips A, Teunisse A, Lam S, Lodder K, Darley M, Emaduddin M, *et al.* HDMX-L is expressed from a functional p53-responsive promoter in the first intron of the HDMX gene and participates in an autoregulatory feedback loop to control p53 activity. *J Biol Chem.* 2010;285(38):29111-27.
121. Dumont P, Leu JI, Della Pietra AC, 3rd, George DL, Murphy M. The codon 72 polymorphic variants of p53 have markedly different apoptotic potential. *Nat Genet.* 2003;33(3):357-65.
122. Assmann G, Voswinkel J, Mueller M, Bittenbring J, Koenig J, Menzel A, *et al.* Association of rheumatoid arthritis with Mdm2 SNP309 and genetic evidence for an allele-

specific interaction between MDM2 and p53 P72R variants: a case control study. *Clin Exp Rheumatol.* 2009;27(4):615-9.

123. Ohnstad HO, Castro R, Sun J, Heintz KM, Vassilev LT, Bjerkehagen B, *et al.* Correlation of TP53 and MDM2 genotypes with response to therapy in sarcoma. *Cancer.* 2012.

124. Liu J, Tang X, Li M, Lu C, Shi J, Zhou L, *et al.* Functional MDM4 rs4245739 genetic variant, alone and in combination with P53 Arg72Pro polymorphism, contributes to breast cancer susceptibility. *Breast cancer Research and Treatment.* 2013;140(1):151-7.

125. Wynendaele J, Bohnke A, Leucci E, Nielsen SJ, Lambertz I, Hammer S, *et al.* An illegitimate microRNA target site within the 3' UTR of MDM4 affects ovarian cancer progression and chemosensitivity. *Cancer Res.* 2010;70(23):9641-9.

126. Haupt Y, Maya R, Kazaz A, Oren M. Mdm2 promotes the rapid degradation of p53. *Nature.* 1997;387(6630):296-9.

127. Momand J, Zambetti GP, Olson DC, George D, Levine AJ. The mdm-2 oncogene product forms a complex with the p53 protein and inhibits p53-mediated transactivation. *Cell.* 1992;69(7):1237-45.

128. Shangary S, Wang S. Targeting the MDM2-p53 interaction for cancer therapy. *Clin Cancer Res.* 2008;14(17):5318-24.

129. Minsky N, Oren M. The RING domain of Mdm2 mediates histone ubiquitylation and transcriptional repression. *Mol Cell.* 2004;16(4):631-9.

130. Carter S, Bischof O, Dejean A, Vousden KH. C-terminal modifications regulate MDM2 dissociation and nuclear export of p53. *Nat Cell Biol.* 2007;9(4):428-35.

131. Li M, Brooks CL, Wu-Baer F, Chen D, Baer R, Gu W. Mono- versus polyubiquitination: differential control of p53 fate by Mdm2. *Science.* 2003;302(5652):1972-5.

132. Wade M, Wahl GM. Targeting Mdm2 and Mdmx in cancer therapy: better living through medicinal chemistry? *Mol Cancer Res.* 2009;7(1):1-11.

133. Plechanovova A, Jaffray EG, Tatham MH, Naismith JH, Hay RT. Structure of a RING E3 ligase and ubiquitin-loaded E2 primed for catalysis. *Nature.* 2012;489(7414):115-20.

134. Kawai H, Wiederschain D, Kitao H, Stuart J, Tsai KK, Yuan ZM. DNA damage-induced MDMX degradation is mediated by MDM2. *J Biol Chem.* 2003;278(46):45946-53.

135. Pan Y, Chen J. MDM2 promotes ubiquitination and degradation of MDMX. *Mol Cell Biol.* 2003;23(15):5113-21.

136. Sharp DA, Kratowicz SA, Sank MJ, George DL. Stabilization of the MDM2 oncoprotein by interaction with the structurally related MDMX protein. *J Biol Chem.* 1999;274(53):38189-96.
137. Jackson MW, Berberich SJ. MdmX protects p53 from Mdm2-mediated degradation. *Mol Cell Biol.* 2000;20(3):1001-7.
138. Pei D, Zhang Y, Zheng J. Regulation of p53: a collaboration between Mdm2 and Mdmx. *Oncotarget.* 2012;3(3):228-35.
139. Marine J-C, Francoz S, Maetens M, Wahl G, Toledo F, Lozano G. Keeping p53 in check: essential and synergistic functions of Mdm2 and Mdm4. *Cell Death Differ.* 2006;13(6):927-34.
140. Linares LK, Hengstermann A, Ciechanover A, Müller S, Scheffner M. HdmX stimulates Hdm2-mediated ubiquitination and degradation of p53. *Proc Natl Acad Sci U S A.* 2003;100(21):12009-14.
141. Mayo LD, Donner DB. A phosphatidylinositol 3-kinase/Akt pathway promotes translocation of Mdm2 from the cytoplasm to the nucleus. *Proc Natl Acad Sci U S A.* 2001;98(20):11598-603.
142. Lopez-Pajares V, Kim MM, Yuan ZM. Phosphorylation of MDMX mediated by Akt leads to stabilization and induces 14-3-3 binding. *J Biol Chem.* 2008;283(20):13707-13.
143. Sherr CJ, Weber JD. The ARF/p53 pathway. *Curr Opin Genet Dev.* 2000;10(1):94-9.
144. Tao W, Levine AJ. P19(ARF) stabilizes p53 by blocking nucleo-cytoplasmic shuttling of Mdm2. *Proc Natl Acad Sci U S A.* 1999;96(12):6937-41.
145. Ries S, Biederer C, Woods D, Shifman O, Shirasawa S, Sasazuki T, *et al.* Opposing effects of Ras on p53: transcriptional activation of mdm2 and induction of p19ARF. *Cell.* 2000;103(2):321-30.
146. Gilkes DM, Pan Y, Coppola D, Yeatman T, Reuther GW, Chen J. Regulation of MDMX expression by mitogenic signaling. *Mol Cell Biol.* 2008;28(6):1999-2010.
147. Zhang Z, Zhang R. p53-independent activities of MDM2 and their relevance to cancer therapy. *Current Cancer Drug Targets.* 2005;5(1):9-20.
148. Xiao ZX, Chen J, Levine AJ, Modjtahedi N, Xing J, Sellers WR, *et al.* Interaction between the retinoblastoma protein and the oncoprotein MDM2. *Nature.* 1995;375(6533):694-8.

149. Martin K, Trouche D, Hagemeyer C, Sorensen TS, La Thangue NB, Kouzarides T. Stimulation of E2F1/DP1 transcriptional activity by MDM2 oncoprotein. *Nature*. 1995;375(6533):691-4.
150. Jones SN, Roe AE, Donehower LA, Bradley A. Rescue of embryonic lethality in Mdm2-deficient mice by absence of p53. *Nature*. 1995;378(6553):206-8.
151. Montes de Oca Luna R, Wagner DS, Lozano G. Rescue of early embryonic lethality in mdm2-deficient mice by deletion of p53. *Nature*. 1995;378(6553):203-6.
152. Parant J, Chavez-Reyes A, Little NA, Yan W, Reinke V, Jochemsen AG, *et al*. Rescue of embryonic lethality in Mdm4-null mice by loss of Trp53 suggests a nonoverlapping pathway with MDM2 to regulate p53. *Nat Genet*. 2001;29(1):92-5.
153. Huang L, Yan Z, Liao X, Li Y, Yang J, Wang ZG, *et al*. The p53 inhibitors MDM2/MDMX complex is required for control of p53 activity in vivo. *Proc Natl Acad Sci U S A*. 2011;108(29):12001-6.
154. Itahana K, Mao H, Jin A, Itahana Y, Clegg HV, Lindstrom MS, *et al*. Targeted inactivation of Mdm2 RING finger E3 ubiquitin ligase activity in the mouse reveals mechanistic insights into p53 regulation. *Cancer Cell*. 2007;12(4):355-66.
155. Gannon HS, Woda BA, Jones SN. ATM phosphorylation of Mdm2 Ser394 regulates the amplitude and duration of the DNA damage response in mice. *Cancer Cell*. 2012;21(5):668-79.
156. Vassilev LT. Small-molecule antagonists of p53-MDM2 binding: research tools and potential therapeutics. *Cell Cycle*. 2004;3(4):419-21.
157. Grasberger BL, Lu T, Schubert C, Parks DJ, Carver TE, Koblisch HK, *et al*. Discovery and cocrystal structure of benzodiazepinedione HDM2 antagonists that activate p53 in cells. *J Med Chem*. 2005;48(4):909-12.
158. Ding K, Lu Y, Nikolovska-Coleska Z, Wang G, Qiu S, Shangary S, *et al*. Structure-based design of spiro-oxindoles as potent, specific small-molecule inhibitors of the MDM2-p53 interaction. *J Med Chem*. 2006;49(12):3432-5.
159. Vassilev LT, Vu BT, Graves B, Carvajal D, Podlaski F, Filipovic Z, *et al*. In vivo activation of the p53 pathway by small-molecule antagonists of MDM2. *Science*. 2004;303(5659):844-8.
160. Apontes P, Leontieva OV, Demidenko ZN, Li F, Blagosklonny MV. Exploring long-term protection of normal human fibroblasts and epithelial cells from chemotherapy in cell culture. *Oncotarget*. 2011;2(3):222-33.

161. Shangary S, Qin D, McEachern D, Liu M, Miller RS, Qiu S, *et al.* Temporal activation of p53 by a specific MDM2 inhibitor is selectively toxic to tumors and leads to complete tumor growth inhibition. *Proc Natl Acad Sci U S A.* 2008;105(10):3933-8.
162. Tovar C, Rosinski J, Filipovic Z, Higgins B, Kolinsky K, Hilton H, *et al.* Small-molecule MDM2 antagonists reveal aberrant p53 signaling in cancer: implications for therapy. *Proc Natl Acad Sci U S A.* 2006;103(6):1888-93.
163. Ray-Coquard I, Blay JY, Italiano A, Le Cesne A, Penel N, Zhi J, *et al.* Effect of the MDM2 antagonist RG7112 on the P53 pathway in patients with MDM2-amplified, well-differentiated or dedifferentiated liposarcoma: an exploratory proof-of-mechanism study. *Lancet Oncol.* 2012;13(11):1133-40.
164. Hu B, Gilkes DM, Farooqi B, Sebti SM, Chen J. MDMX overexpression prevents p53 activation by the MDM2 inhibitor Nutlin. *J Biol Chem.* 2006;281(44):33030-5.
165. Joseph TL, Madhumalar A, Brown CJ, Lane DP, Verma CS. Differential binding of p53 and nutlin to MDM2 and MDMX: Computational studies. *Cell Cycle.* 2010;9(6):1167-81.
166. Reed D, Shen Y, Shelat AA, Arnold LA, Ferreira AM, Zhu F, *et al.* Identification and characterization of the first small molecule inhibitor of MDMX. *J Biol Chem.* 2010;285(14):10786-96.
167. Bista M, Smithson D, Pecak A, Salinas G, Pustelny K, Min J, *et al.* On the mechanism of action of SJ-172550 in inhibiting the interaction of MDM4 and p53. *PLoS One.* 2012;7(6):e37518.
168. Bernal F, Wade M, Godes M, Davis TN, Whitehead DG, Kung AL, *et al.* A stapled p53 helix overcomes HDMX-mediated suppression of p53. *Cancer Cell.* 2010;18(5):411-22.
169. Verdine GL, Hilinski GJ. Stapled peptides for intracellular drug targets. *Methods Enzymol.* 2012;503(1):3-33.
170. Barakat K, Mane J, Friesen D, Tuszynski J. Ensemble-based virtual screening reveals dual-inhibitors for the p53-MDM2/MDMX interactions. *J Mol Graph Model.* 2010;28(6):555-68.
171. Macchiarulo A, Pellicciari R. MDM2/MDMX inhibitor peptide: WO2008106507. *Expert Opin Ther Pat.* 2009;19(5):721-6.
172. Phan J, Li Z, Kasprzak A, Li B, Sebti S, Guida W, *et al.* Structure-based design of high affinity peptides inhibiting the interaction of p53 with MDM2 and MDMX. *J Biol Chem.* 2010;285(3):2174-83.

173. Pazgier M, Liu M, Zou G, Yuan W, Li C, Li J, *et al.* Structural basis for high-affinity peptide inhibition of p53 interactions with MDM2 and MDMX. *Proc Natl Acad Sci U S A.* 2009;106(12):4665-70.
174. Czarna A, Popowicz GM, Pecak A, Wolf S, Dubin G, Holak TA. High affinity interaction of the p53 peptide-analogue with human Mdm2 and Mdmx. *Cell Cycle.* 2009;8(8):1176-84.
175. Li Q, Lozano G. Molecular pathways: targeting Mdm2 and Mdm4 in cancer therapy. *Clin Cancer Res.* 2013;19(1):34-41.
176. Zak K, Pecak A, Rys B, Wladyka B, Domling A, Weber L, *et al.* Mdm2 and MdmX inhibitors for the treatment of cancer: a patent review (2011-present). *Expert Opin Ther Pat.* 2013;23(4):425-48.
177. Yang Y, Ludwig RL, Jensen JP, Pierre SA, Medaglia MV, Davydov IV, *et al.* Small molecule inhibitors of HDM2 ubiquitin ligase activity stabilize and activate p53 in cells. *Cancer Cell.* 2005;7(6):547-59.
178. Herman AG, Hayano M, Poyurovsky MV, Shimada K, Skouta R, Prives C, *et al.* Discovery of Mdm2-MdmX E3 ligase inhibitors using a cell-based ubiquitination assay. *Cancer Discov.* 2011;1(4):312-25.
179. Roxburgh P, Hock AK, Dickens MP, Mezna M, Fischer PM, Vousden KH. Small molecules that bind the Mdm2 RING stabilize and activate p53. *Carcinogenesis.* 2012;33(4):791-8.
180. Issaeva N, Bozko P, Enge M, Protopopova M, Verhoef LG, Masucci M, *et al.* Small molecule RITA binds to p53, blocks p53-HDM-2 interaction and activates p53 function in tumors. *Nat Med.* 2004;10(12):1321-8.
181. Di Conza G, Buttarelli M, Monti O, Pellegrino M, Mancini F, Pontecorvi A, *et al.* IGF-1R/MDM2 relationship confers enhanced sensitivity to RITA in Ewing sarcoma cells. *Mol Cancer Ther.* 2012;11(6):1247-56.
182. Schuster K, Fan L, Harris LC. MDM2 splice variants predominantly localize to the nucleoplasm mediated by a COOH-terminal nuclear localization signal. *Mol Cancer Res.* 2007;5(4):403-12.
183. Kent WJ, Sugnet CW, Furey TS, Roskin KM, Pringle TH, Zahler AM, *et al.* The human genome browser at UCSC. *Genome Res.* 2002;12(6):996-1006.
184. Oda Y, Sakamoto A, Satio T, Kawauchi S, Iwamoto Y, Tsuneyoshi M. Molecular abnormalities of p53, MDM2, and H-ras in synovial sarcoma. *Mod Pathol.* 2000;13(9):994-1004.

185. Carr IM, Camm N, Taylor GR, Charlton R, Ellard S, Sheridan EG, *et al.* GeneScreen: a program for high-throughput mutation detection in DNA sequence electropherograms. *J Med Genet.* 2011;48(2):123-30.
186. Hu B, Gilkes DM, Chen J. Efficient p53 activation and apoptosis by simultaneous disruption of binding to MDM2 and MDMX. *Cancer Res.* 2007;67(18):8810-7.
187. Florenes VA, Maelandsmo GM, Forus A, Andreassen A, Myklebost O, Fodstad O. MDM2 gene amplification and transcript levels in human sarcomas: relationship to TP53 gene status. *J Natl Cancer Inst.* 1994;86(17):1297-302.
188. Muller CR, Paulsen EB, Noordhuis P, Pedeutour F, Saeter G, Myklebost O. Potential for treatment of liposarcomas with the MDM2 antagonist Nutlin-3A. *Int J Cancer.* 2007;121(1):199-205.
189. Li BH, Yang XZ, Li PD, Yuan Q, Liu XH, Yuan J, *et al.* IL-4/Stat6 activities correlate with apoptosis and metastasis in colon cancer cells. *Biochem Biophys Res Commun.* 2008;369(2):554-60.
190. Willenbring H, Sharma AD, Vogel A, Lee AY, Rothfuss A, Wang Z, *et al.* Loss of p21 permits carcinogenesis from chronically damaged liver and kidney epithelial cells despite unchecked apoptosis. *Cancer Cell.* 2008;14(1):59-67.
191. Pinheiro GS, Silva MR, Rodrigues CA, Kerbauy J, de Oliveira JS. Proliferating cell nuclear antigen (PCNA), p53 and MDM2 expression in Hodgkin's disease. *Sao Paulo Med J.* 2007;125(2):77-84.
192. Pishas KI, Al-Ejeh F, Zinonos I, Kumar R, Evdokiou A, Brown MP, *et al.* Nutlin-3a is a potential therapeutic for Ewing sarcoma. *Clin Cancer Res.* 2011;17(3):494-504.
193. Laboratory EMB. Transcription profiling of human multiple cancer cell lines. EMBL-EBI; 2013 [updated 2013; cited 2013 09/2013]; Available from: <http://www.ebi.ac.uk/gxa/experiment/E-MTAB-37/ENSG00000198625>.
194. Neuville A, Ranchere-Vince D, Dei Tos AP, Montesco MC, Hostein I, Toffolatti L, *et al.* Impact of molecular analysis on the final sarcoma diagnosis: a study on 763 cases collected during a European epidemiological study. *Am J Surg Pathol.* 2013;37(8):1259-68.
195. Nilsson M, Meza-Zepeda LA, Mertens F, Forus A, Myklebost O, Mandahl N. Amplification of chromosome 1 sequences in lipomatous tumors and other sarcomas. *Int J Cancer.* 2004;109(3):363-9.
196. Dahlén A, Debiec-Rychter M, Pedeutour F, Domanski HA, Höglund M, Bauer HC, *et al.* Clustering of deletions on chromosome 13 in benign and low-malignant lipomatous tumors. *Int J Cancer.* 2003;103(5):616-23.

197. Riemenschneider MJ, Büschges R, Wolter M, Reifenberger J, Boström J, Kraus JA, *et al.* Amplification and overexpression of the MDM4 (MDMX) gene from 1q32 in a subset of malignant gliomas without TP53 mutation or MDM2 amplification. *Cancer Res.* 1999;59(24):6091-6.
198. Laurie NA, Donovan SL, Shih CS, Zhang J, Mills N, Fuller C, *et al.* Inactivation of the p53 pathway in retinoblastoma. *Nature.* 2006;444(7115):61-6.
199. Arici A, Ozgur T, Ugras N, Yalcinkaya U. Immunohistochemical detection of p53 and MDM2 expressions in liposarcoma with World Health Organization classification. *Indian J Cancer.* 2013;50(3):164-9.
200. Kumar V, Misra S, Chaturvedi A. Retroperitoneal sarcomas- a challenging problem. *Indian J Surg Oncol.* 2012;3(3):215-21.
201. Thway K, Flora R, Shah C, Olmos D, Fisher C. Diagnostic utility of p16, CDK4, and MDM2 as an immunohistochemical panel in distinguishing well-differentiated and dedifferentiated liposarcomas from other adipocytic tumors. *Am J Surg Pathol.* 2012;36(3):462-9.
202. Sioletic S, Dal Cin P, Fletcher CD, Hornick JL. Well-differentiated and dedifferentiated liposarcomas with prominent myxoid stroma: analysis of 56 cases. *Histopathology.* 2013;62(2):287-93.
203. de Bruin EC, Taylor TB, Swanton C. Intra-tumor heterogeneity: lessons from microbial evolution and clinical implications. *Genome Med.* 2013;5(11):101.
204. Stad R, Little NA, Xirodimas DP, Frenk R, van der Eb AJ, Lane DP, *et al.* Mdmx stabilizes p53 and Mdm2 via two distinct mechanisms. *EMBO Rep.* 2001;2(11):1029-34.
205. Zhang H, Erickson-Johnson M, Wang X, Oliveira JL, Nascimento AG, Sim FH, *et al.* Molecular testing for lipomatous tumors: critical analysis and test recommendations based on the analysis of 405 extremity-based tumors. *Am J Surg Pathol.* 2010;34(9):1304-11.
206. Shimada S, Ishizawa T, Ishizawa K, Matsumura T, Hasegawa T, Hirose T. The value of MDM2 and CDK4 amplification levels using real-time polymerase chain reaction for the differential diagnosis of liposarcomas and their histologic mimickers. *Hum Pathol.* 2006;37(9):1123-9.
207. Sullivan A, Syed N, Gasco M, Bergamaschi D, Trigiante G, Attard M, *et al.* Polymorphism in wild-type p53 modulates response to chemotherapy in vitro and in vivo. *Oncogene.* 2004;23(19):3328-37.
208. Taylor JA, Li Y, He M, Mason T, Mettlin C, Vogler WJ, *et al.* p53 mutations in bladder tumors from arylamine-exposed workers. *Cancer Res.* 1996;56(2):294-8.

209. Hongyo T, Hoshida Y, Nakatsuka S, Syaifudin M, Kojya S, Yang WI, *et al.* p53, K-ras, c-kit and beta-catenin gene mutations in sinonasal NK/T-cell lymphoma in Korea and Japan. *Oncol Rep.* 2005;13(2):265-71.
210. Nakamura Y, Futamura M, Kamino H, Yoshida K, Nakamura Y, Arakawa H. Identification of p53-46F as a super p53 with an enhanced ability to induce p53-dependent apoptosis. *Cancer Science.* 2006;97(7):633-41.
211. Braithwaite AW, Royds JA, Jackson P. The p53 story: layers of complexity. *Carcinogenesis.* 2005;26(7):1161-9.
212. Pang A, Ng IO, Fan ST, Kwong YL. Clinicopathologic significance of genetic alterations in hepatocellular carcinoma. *Cancer Genet Cytogenet.* 2003;146(1):8-15.
213. Simao TA, Ribeiro FS, Amorim LM, Albano RM, Andrada-Serpa MJ, Cardoso LE, *et al.* TP53 mutations in breast cancer tumors of patients from Rio de Janeiro, Brazil: association with risk factors and tumor characteristics. *Int J Cancer.* 2002;101(1):69-73.
214. Crook T, Brooks LA, Crossland S, Osin P, Barker KT, Waller J, *et al.* p53 mutation with frequent novel condons but not a mutator phenotype in BRCA1- and BRCA2-associated breast tumours. *Oncogene.* 1998;17(13):1681-9.
215. King TC, Akerley W, Fan AC, Moore T, Mangray S, Hsiu Chen M, *et al.* p53 mutations do not predict response to paclitaxel in metastatic nonsmall cell lung carcinoma. *Cancer.* 2000;89(4):769-73.
216. Hasegawa M, Ohoka I, Yamazaki K, Hanami K, Sugano I, Nagao T, *et al.* Expression of p21/WAF-1, status of apoptosis and p53 mutation in esophageal squamous cell carcinoma with HPV infection. *Pathol Int.* 2002;52(7):442-50.
217. Bellon M, Baydoun HH, Yao Y, Nicot C. HTLV-I Tax-dependent and-independent events associated with immortalization of human primary T lymphocytes. *Blood.* 2010;115(12):2441-8.
218. Leung WK, To KF, Ng YP, Lee TL, Lau JY, Chan FK, *et al.* Association between cyclooxygenase-2 overexpression and missense p53 mutations in gastric cancer. *Br J Cancer.* 2001;84(3):335-9.
219. Kurniawan AN, Hongyo T, Hardjolukito ES, Ham MF, Takakuwa T, Kodariah R, *et al.* Gene mutation analysis of sinonasal lymphomas in Indonesia. *Oncol Rep.* 2006;15(5):1257-63.
220. Webley KM, Shorthouse AJ, Royds JA. Effect of mutation and conformation on the function of p53 in colorectal cancer. *J Pathol.* 2000;191(4):361-7.

221. Lee JS, Kim HS, Park JT, Lee MC, Park CS. Expression of vascular endothelial growth factor in the progression of cervical neoplasia and its relation to angiogenesis and p53 status. *Anal Quant Cytol Histol.* 2003;25(6):303-11.
222. Cho Y, Gorina S, Jeffrey PD, Pavletich NP. Crystal structure of a p53 tumor suppressor-DNA complex: understanding tumorigenic mutations. *Science.* 1994;265(5170):346-55.
223. Goh H-S, Yao J, Smith DR. p53 point mutation and survival in colorectal cancer patients. *Cancer Res.* 1995;55(22):5217-21.
224. Hartmann A, Schlake G, Zaak D, Hungerhuber E, Hofstetter A, Hofstaedter F, *et al.* Occurrence of chromosome 9 and p53 alterations in multifocal dysplasia and carcinoma in situ of human urinary bladder. *Cancer Res.* 2002;62(3):809-18.
225. Hassan NMM, Tada M, Hamada J-i, Kashiwazaki H, Kameyama T, Akhter R, *et al.* Presence of dominant negative mutation of TP53 is a risk of early recurrence in oral cancer. *Cancer Letters.* 2008;270(1):108-19.
226. Dearth LR, Qian H, Wang T, Baroni TE, Zeng J, Chen SW, *et al.* Inactive full-length p53 mutants lacking dominant wild-type p53 inhibition highlight loss of heterozygosity as an important aspect of p53 status in human cancers. *Carcinogenesis.* 2006;28(2):289-98.
227. Boutell JM, Hart DJ, Godber BL, Kozlowski RZ, Blackburn JM. Functional protein microarrays for parallel characterisation of p53 mutants. *Proteomics.* 2004;4(7):1950-8.
228. van Rensburg EJ, Engelbrecht S, van Heerden WF, Kotze MJ, Raubenheimer EJ. Detection of p53 gene mutations in oral squamous cell carcinomas of a black African population sample. *Hum Mutat.* 1998;11(1):39-44.
229. Reiling E, Lyssenko V, Boer JM, Imholz S, Verschuren WMM, Isomaa B, *et al.* Codon 72 polymorphism (rs1042522) of TP53 is associated with changes in diastolic blood pressure over time. *Eur J Hum Genet.* 2011;20(6):696-700.
230. Han JY, Lee GK, Jang DH, Lee SY, Lee JS. Association of p53 codon 72 polymorphism and MDM2 SNP309 with clinical outcome of advanced nonsmall cell lung cancer. *Cancer.* 2008;113(4):799-807.
231. Kim JG, Sohn SK, Chae YS, Song HS, Kwon K-Y, Do YR, *et al.* TP53 codon 72 polymorphism associated with prognosis in patients with advanced gastric cancer treated with paclitaxel and cisplatin. *Cancer Chemotherapy and Pharmacology.* 2009;64(2):355-60.
232. Orsted DD, Bojesen SE, Tybjaerg-Hansen A, Nordestgaard BG. Tumor suppressor p53 Arg72Pro polymorphism and longevity, cancer survival, and risk of cancer in the general population. *J Exp Med.* 2007;204(6):1295-301.

233. Bojesen SE, Nordestgaard BG. The common germline Arg72Pro polymorphism of p53 and increased longevity in humans. *Cell Cycle*. 2008;7(2):158-63.
234. Yamamoto H, Oda Y, Saito T, Sakamoto A, Miyajima K, Tamiya S, *et al.* p53 Mutation and MDM2 amplification in inflammatory myofibroblastic tumours. *Histopathology*. 2003;42(5):431-9.
235. Zietz C, Rossle M, Haas C, Sendelhofert A, Hirschmann A, Sturzl M, *et al.* MDM-2 oncoprotein overexpression, p53 gene mutation, and VEGF up-regulation in angiosarcomas. *Am J Pathol*. 1998;153(5):1425-33.
236. Tanas MR, Rubin BP, Tubbs RR, Billings SD, Downs-Kelly E, Goldblum JR. Utilization of fluorescence in situ hybridization in the diagnosis of 230 mesenchymal neoplasms: an institutional experience. *Arch Pathol Lab Med*. 2010;134(12):1797-803.
237. Pishas KI, Neuhaus SJ, Clayer MT, Schreiber AW, Lawrence DM, Perugini M, *et al.* Nutlin-3a efficacy in sarcoma predicted by transcriptomic and epigenetic profiling. *Cancer Res*. 2013;canres. 2424.013.
238. Touqan N, Diggle CP, Verghese ET, Perry S, Horgan K, Merchant W, *et al.* An observational study on the expression levels of MDM2 and MDMX proteins, and associated effects on P53 in a series of human liposarcomas. *BMC Clin Pathol*. 2013;13(1):32.
239. Singh B, Li R, Xu L, Poluri A, Patel S, Shaha AR, *et al.* Prediction of survival in patients with head and neck cancer using the histoculture drug response assay. *Head Neck*. 2002;24(5):437-42.

II- List of Abbreviations

aa	Amino Acid
Ab(s)	Antibodies
ARF	Alternative Reading Frame
Arg	Arginine
Asn	Asparagine
Asp	Aspartic acid
ATCC[®]	American Type Culture Collection
bp	Base Pair
BCA	Bicinchoninic Acid Assay
BSA	Bovine Serum Albumin
CGH	Comparative Genomic Hybridisation
DAPI	4',6-diamidino-2-phenylindole
dATP	Deoxyadenosine Triphosphate
dCTP	Deoxycytidine Triphosphate
DDLS	De-differentiated Liposarcoma
dGTP	Deoxyguanosine Triphosphate
DTT	Dithiothreitol
DMEM	Dulbecco's Modified Eagle's Medium
DMSO	Dimethyl sulfoxide
DNA	Deoxyribonucleic Acid
dNTP	Deoxynucleoside Triphosphates

DPBS	Dulbecco's Phosphate-Buffered Saline
dTTP	Deoxythymidine Triphosphate
EDTA	Ethylene di-amine tetra-acetic acid disodium salt
FCS	Foetal Calf Serum
FFPE	Formalin-Fixed Paraffin-Embedded
FISH	Fluorescence <i>in situ</i> Hybridization
Gln	Glutamine
Glu	Glutamic acid
HiDi	Highly Deionised
hr(s)	Hour(s)
HRP	Horseradish Peroxidase
IAPs	Inhibitor of Apoptosis Proteins
ICC	Immunocytochemistry
IHC	Immunohistochemistry
IARC	International Agency for Research on Cancer
IUPAC	International Union of Pure and Applied Chemistry
Kb	kilobase-pairs
KDa	Kilo Dalton
LDS	Lithium Dodecyl Sulphate
Leu	Leucine
LIMM	Leeds Institute of Molecular Medicine
LS(s)	Liposarcoma(s)

LTHT	Leeds Teaching Hospitals NHS Trust
Lys	Lysine
M	Molar
MDM	Murine Double Minute
MFH	Malignant Fibrous Histiocytoma
mg	milligram
ml	millilitre
mM	millimolar
nM	nanomolar
MXLS	Myxoid Liposarcoma
NCIN	National Cancer Intelligence Network
ND	Not Done
NES	Nuclear Export Signal
NLS	Nuclear Localisation Signal
ng	nanogram
nm	nanometre
NoLS	Nucleolar Localisation Signal
NP-40	Nonyl phenoxypolyethoxyethanol
PCR	Polymerase Chain Reaction
Phe	Phenylalanine
pM	picomolar
PMSF	Phenylmethanesulfonyl Fluoride

PPM	Patient Pathway Manager
Pro	Proline
RCLS	Round Cell Liposarcoma
RING	Really Interesting New Gene
RIPA	Radioimmunoprecipitation Assay
RPMI	Roswell Park Memorial Institute
SC	Spindle Cell
SDS	Sodium Dodecyl Sulphate
Ser	Serine
StR	Speciality Training Registrar
STS(s)	Soft Tissue Sarcoma(s)
TAD	Transactivation Domain
TBS	Tris-Buffered Saline
TD	Tetramerisation Domain
UK	United Kingdom
UCSC	University of California, Santa Cruz
v/v	volume/volume
v/w	volume/weight
WDLS	Well-Differentiated Liposarcoma
WHO	World Health Organisation
Wt	Wild Type
Zn	Zinc

μg	micrograms
μl	microlitres
μM	micromolar
μm	micrometre
°C	degrees Celsius
+ve	positive
-ve	negative

III- Appendices

List of Appendices:

- 1- Ethical Approval Letter and LTHT Research and Development Approval
- 2- Participants Information Sheet and Consent Form
- 3- Full Cohort of Study Participants

1- Ethical Approval Letter and Leeds Teaching Hospital Trust
Research and Development Approval

Leeds (Central) Research Ethics Committee

Yorkshire and Humber REC Office

Millside
Mill Pond Lane
Meanwood
Leeds
LS6 4EP

Telephone: 0113 3050108

Facsimile:

04 June 2010

Prof Sir Alexander F Markham
Professor of Medicine
University of Leeds
Leeds Institute of Molecular Medicine
St James's University Hospital
LS9 7TF

Dear Prof Sir Markham

Study Title: Interactions between P53 and its Main Cellular
Regulators in Tumour Tissues: Exploring the Potentials
for Future Therapies.

REC reference number: 10/H1313/34

Protocol number:

Thank you for your letter of 29 April 2010, responding to the Committee's request for further information on the above research and submitting revised documentation.

The further information was considered in correspondence by a sub-committee of the REC. A list of the sub-committee members is attached.

Confirmation of ethical opinion

On behalf of the Committee, I am pleased to confirm a favourable ethical opinion for the above research on the basis described in the application form, protocol and supporting documentation as revised, subject to the conditions specified below.

Ethical review of research sites

The favourable opinion applies to all NHS sites taking part in the study, subject to management permission being obtained from the NHS/HSCR&D office prior to the start of the study (see "Conditions of the favourable opinion" below).

Conditions of the favourable opinion

The favourable opinion is subject to the following conditions being met prior to the start of the study.

Management permission or approval must be obtained from each host organisation prior to the start of the study at the site concerned.

For NHS research sites only, management permission for research ("R&D approval") should be obtained from the relevant care organisation(s) in accordance with NHS research governance arrangements. Guidance on applying for NHS permission for research is available in the Integrated Research Application System or at <http://www.rdforum.nhs.uk>. *Where the only involvement of the NHS organisation is as a Participant Identification Centre, management permission for research is not required but the R&D office should be notified of the study. Guidance should be sought from the R&D office where necessary.*

Sponsors are not required to notify the Committee of approvals from host organisations.

It is the responsibility of the sponsor to ensure that all the conditions are complied with before the start of the study or its initiation at a particular site (as applicable).

Approved documents

The final list of documents reviewed and approved by the Committee is as follows:

Document	Version	Date
REC application		24 March 2010
Protocol		22 March 2010
Investigator CV	2	22 March 2010
Evidence of insurance or indemnity		08 October 2009
CV - Nader Touqan		24 March 2010
Participant Information Sheet	2	18 March 2010
Participant Consent Form	2	18 March 2010
Response to Request for Further Information		29 April 2010

Statement of compliance

The Committee is constituted in accordance with the Governance Arrangements for Research Ethics Committees (July 2001) and complies fully with the Standard Operating Procedures for Research Ethics Committees in the UK.

After ethical review

Now that you have completed the application process please visit the National Research Ethics Service website > After Review

You are invited to give your view of the service that you have received from the National Research Ethics Service and the application procedure. If you wish to make your views known please use the feedback form available on the website.

The attached document "*After ethical review – guidance for researchers*" gives detailed guidance on reporting requirements for studies with a favourable opinion, including:

- Notifying substantial amendments
- Adding new sites and investigators
- Progress and safety reports
- Notifying the end of the study

The NRES website also provides guidance on these topics, which is updated in the light of changes in reporting requirements or procedures.

We would also like to inform you that we consult regularly with stakeholders to improve our

service. If you would like to join our Reference Group please email referencegroup@nres.npsa.nhs.uk

10/H1313/34	Please quote this number on all correspondence
--------------------	---

Yours sincerely

Dr Margaret L Faulk
Chair

Email: Rachel.bell@leedspft.nhs.uk

 **Enclosures:** *List of names and professions of members who were present at the meeting and those who submitted written comments*

"After ethical review – guidance for researchers"

Copy to: *Mrs Rachel E de Souza*
R & D Office - Leeds Teaching Hospitals

□

Leeds (Central) Research Ethics Committee

Attendance at Sub-Committee of the REC meeting on 04 May 2010

Committee Members:



<i>Name</i>	<i>Profession</i>	<i>Present</i>	<i>Notes</i>
Dr Margaret L Faulk	Chair	Yes	
Ms Bren Torry	Lay Member	Yes	

Ref: Amanda Burt

11/11/2010

Prof Sir Alexander Markham
Leeds Teaching Hospitals NHS Trust
Level 7
Wellcome Trust Brenner Building
St James's University Hospital

Research & Development

Leeds Teaching Hospitals NHS Trust
34 Hyde Terrace
Leeds
LS2 9LN

Tel: 0113 392 2878
Fax: 0113 392 6397

r&d@leedsth.nhs.uk
www.leedsth.nhs.uk

Dear Prof Sir Alexander Markham

Re: LTHT R&D Approval of: Interactions between P53 and its Main Cellular Regulators in Tumour Tissues: Exploring the Potential for Future Therapies.
LTHT R&D Number: MM10/9511
REC: 10/H1313/34

I confirm that this study has R&D approval and the study may proceed at The Leeds Teaching Hospitals NHS Trust (LTHT). This organisational level approval is given based on the information provided in the documents listed below.

In undertaking this research you must comply with the requirements of the *Research Governance Framework for Health and Social Care* which is mandatory for all NHS employees. This document may be accessed on the R&D website http://www.leedsth.nhs.uk/sites/research_and_development/

R&D approval is given on the understanding that you comply with the requirements of the *Framework* as listed in the attached sheet "Conditions of Approval".

If you have any queries about this approval please do not hesitate to contact the R&D Department on telephone 0113 392 2878.

Indemnity Arrangements

The Leeds Teaching Hospitals NHS Trust participates in the NHS risk pooling scheme administered by the NHS Litigation Authority 'Clinical Negligence Scheme for NHS Trusts' for: (i) medical professional and/or medical malpractice liability; and (ii) general liability. NHS Indemnity for negligent harm is extended to researchers with an employment contract (substantive or honorary) with the Trust. The Trust only accepts liability for research activity that has been managerially approved by the R&D Department.

Chairman Mike Collier CBE Chief Executive Maggie Boyle

The Leeds Teaching Hospitals incorporating:

Chapel Allerton Hospital Leeds Dental Institute Seacroft Hospital
St James's University Hospital The General Infirmary at Leeds Wharfedale Hospital



WTA280

The Trust therefore accepts liability for the above research project and extends indemnity for negligent harm to cover you as principal investigator and the researchers listed on the Site Specific Information form. Should there be any changes to the research team please ensure that you inform the R&D Department and that s/he obtains an employment contract with the Trust if required.

Yours sincerely



Dr D R Norfolk
Associate Director of R&D

Approved documents

The documents reviewed and approved are listed as follows

<i>Document</i>	<i>Version</i>	<i>Date of document</i>
NHS R&D Form	3.0	26/02/2010
SSI Form	3.0	23/09/2010
Directorate Approval		05/10/2010
Radiology Approval	N/A	N/A
Labs Approval	Pathology	17/06/2010
Protocol		22/03/2010
REC Letter confirming favourable opinion		04/06/2010
Insurance	Zurich	29/09/2010
MHRA Clinical Trial Authorisation Letter	N/A	N/A
Patient information sheet (REC Approved)	2.0	18/03/2010
Consent form (REC Approved)	2.0	18/03/2010

2- Participant Information Sheet and Consent Form

**Interactions between P53 and its Main Cellular Regulators in Cancer
Tissues:
Exploring the Potential for Future Therapies**

Short Title: P53 Study

Information Sheet for Study Participants

Invitation

You are invited to take part in a research study. Before you decide, it is important for you to understand why the research is done and how it could affect you. Please take time to read this information sheet carefully. If anything is not clear, if you have any questions or if you would like more information then please do not hesitate to contact us (contact information below). Thank you for reading this.

1. What is the purpose of this study?

Each year, many thousands of people in the UK are diagnosed with cancer. Part of the treatment is having an operation to remove their cancers.

Cancer often forms as a result of changes in the DNA (which is what genes are made of) in cells. These changes are called mutations and are limited to the cancer cells; they are not present in the rest of the body.

P53 is a gene responsible for killing cancer cells in our bodies and its function is switched off in approximately 50 % of cancers by other genes or proteins that control it. Recent research has discovered molecules that could cancel the negative effects of these proteins and therefore restore the normal anti-cancer function of P53. This could be a promising future therapy in the fight against cancer.

We are interested in characterising various cancers from patients in our area, with regard to the status of P53 gene and its main regulating proteins. We will evaluate the potential beneficial effects of the novel molecules in treating cancers. To do this, we ask your permission to donate a small part of your cancer tissue for the purpose of this research.

2. Why have I been chosen?

You are invited to take part because you are going to have an operation for tumour.

3. Do I have to take part?

No, it is up to you to decide whether or not to take part. If after reading this information sheet carefully and asking as many questions as you wish, you decide to take part, we will then ask you to sign a consent form and to keep this information sheet for future reference. You are still free to withdraw at any time and without giving any reason. A decision to withdraw at any time or a decision not to take part, will not affect the standard care you receive.

REC Reference 10/H/1212/34

Date: 18/03/2010

Version 2

1

4. What will happen to me if I take part?

If you decide to take part, a series of extra tests will be carried out on your donated cancer tissues after the doctors have removed it in the operation. No blood tests or any other investigations are required from you. No additional follow up or clinic visits either. Taking part in the study will not affect, delay or alter any of the routine standard procedures that you receive during your treatment.

5. What is my donated cancer tissue tested for?

We will carry out some tests on a small part(s) of your cancer tissue after doctors have removed it from your body in the operation. These tests include: **Microscopic Appearance** - doctors will use a microscope to look at thin slices cut from your tissue. Sometimes, special colouring dyes are used to look at molecules in cells.

DNA abnormalities – This involves genetic analysis of the make up of your cancer cells looking for certain abnormalities in the DNA of P53 and its regulatory genes. *It is important to understand that the DNA changes we are studying are limited to the cancer cells and are not present in the rest of your body. Therefore, these mutations are not inheritable and would not have any bearings on your or other family members.*

Growing cells – When we receive your sample, we can grow some of the cells and investigate the effects a number of various new drugs on them.

6. Will the doctors take more samples than they would otherwise do, so that there is enough material for research?

No, your treatment is tailored to the exact needs of your disease and not to providing materials for research; this would be wrong and unethical. No extra samples will be removed for research purposes.

7. What other information will be collected in the study?

If you agree to take part, information routinely available from your medical notes will be used in the study. This includes the site and type of cancer you have, the pathology findings and the type of operation you had. This data will be anonymised.

8. Will Insurance companies have access to the results of the study?

No, your individual data are confidential and protected by the law.

9. What if the research discovers something unexpected about my condition?

This is extremely unlikely. In the rare event that this does happen, we will inform the doctor responsible for your care and they will get in touch with you. If you do not wish to know this, you can tell us by initializing the relevant box in the consent form.

10. What are the possible benefits of taking part?

There are no direct benefits to you, but the study may provide us with valuable information regarding potential therapies that could help others in the future. It will take years of extensive research to evaluate the efficiency and safety of these novel drugs before considering implementing them for human use.

11. What are the possible disadvantages of taking part?

There are no extra tests, procedures or burdens required from participants in the study.

12. Will the information obtained in the study be confidential?

All the information collected from you and your medical notes in the study will be kept strictly confidential at all times. The information will be held securely on paper and electronically at LGI, and at the Leeds Institute of Molecular Medicine, which is managing this research, under the provisions of the 1998 Data Protection Act.

Your donated sample will be given a serial number for the purpose of identification, but no personal details will be used during any stage of the study. Only appropriately-qualified members of the Research Team may confidentially review your medical records. In order to be able to check your notes, we will need to hold some information, such as your date of birth and hospital number, so that we can identify your notes accordingly. We will also hold a copy of your signed consent form.

The information collected about you may also be shown to authorised people from the UK Regulatory Authority and Independent Ethics Committee; this is to ensure that the study is carried out to the highest possible scientific standards. All will have a duty of confidentiality to you as a research participant.

13. What will happen to the results of the study?

The results of the study will be available after it finishes and will usually be published in a medical journal or be presented at a scientific conference. The data will be anonymous and none of the patients involved in the trial will be identified in any report or publication.

14. What will happen to my donated tissue after the study is over?

After the study is finished, samples left from your tissue could be disposed of lawfully or alternatively donated to an ethically approved research tissue bank that could utilize it for future research under the established strict ethical conduct. You will be asked to indicate your preference in the consent form.

15. What if I withdraw from the study?

If you withdraw from the study, we will continue to utilize your donated tissue but we will permanently destroy any identifying information related you in our database. If you preferred to withdraw consent for utilization of your tissue in the study then we will dispose of it lawfully.

16. Who is organising and funding the research?

The study is under the academic supervision of Prof Sir A. Markham (Professor of Medicine – University of Leeds) and clinical Supervision of Mr K. Horgan (Clinical Director of Breast / Sarcoma Services at Leeds Teaching Hospitals). Neither the hospital nor any of the study organisers receive any payment for your participation in the study.

Contact for further information

If you have any questions, or if you wish to participate or withdraw your consent then please do not hesitate to contact us. Please use the following contact details:

Mr Nader Touqan
Surgical Research Fellow

Breast Surgery Unit - LGI
LE1 3EX
Telephone: 07835104767
Email: n.touqan@leeds.ac.uk

Thank you for considering this study

PATIENT CONSENT FORM

Interactions between P53 and its main Cellular Regulators in Cancer Tissues: Exploring the Potential for Future Therapies

Patient ID: Initials: Date of Birth:

Patient initial each point

1. I confirm that I have read and understand the information sheet dated _____ (version _____) for the above study, have had the opportunity to ask questions. I understand that my participation is voluntary and that I am free to withdraw at any time without my medical care or legal rights being affected. I agree to take part in the study. _____
2. I understand that my medical records may be looked at by authorised individuals from the Sponsor for the study, the UK Regulatory Authority or the Independent Ethics Committee in order to check that the study is being carried out correctly. I give permission, provided that strict confidentiality is maintained, for these bodies to have access to my medical records for the above study and any further research that may be conducted in relation to it. _____
3. I understand that if I withdraw from the above study, the samples collected from me will remain to be used in analysing the results of the trial; I understand that my identity will remain anonymous. _____
4. I consent to the storage including electronic, of personal information for the purposes of this study. I understand that any information that could identify me will be kept strictly confidential and that no personal information will be included in the study report or other publication. _____
5. My tissue will not be used for research that involves reproductive cloning, however it may undergo genetic testing for the DNA makeup of my cancer cells. I understand the implications and give permission for that. _____
6. In the unlikely event that the research uncovers something unexpected about my condition, I do / do not wish to be informed. _____

Do wish to be informed Do NOT wish to be informed

7. After the study is finished, I do / do not wish to donate my tissue sample to an Ethically Approved Research Tissue bank for utilization in future research.

Do wish to donate Do NOT wish to donate

Name of the patient

Patient's signature and the date the patient signed the Consent form

Name of the Investigator taking written consent

Investigator's signature and date the Investigator signed the consent form

3-Full Cohort of Study Participants

Full Participants Cohort – WDLS

Case no.	Gender	Age	Site	Size (cm)	Histology	Grade	Cytogenetic results	Fresh sample	IHC score			P53 mutation
									MDM2	MDMX	P53	
WD1	F	85	Thigh (left)	14*13*3	WD LS	1	Failed	N	42	5	1	ND
WD2	M	65	Arm (right)	8*6*2	WD LS	1	Failed	N	99	85	63	None
WD3	F	74	Thigh (right)	19*16*10	WD LS	1	Failed	N	98	14	2	ND
WD4	F	72	Back	4*4*3	WD LS	1	MDM2 Amp	N	76	1	8	ND
WD5	F	45	Back	26*20*4	WD LS	1	MDM2 Amp	N	7	2	1	ND
WD6	F	65	Forearm (left)	14*6*4	WD LS	1	MDM2 Amp	N	2	1	1	ND
WD7	F	66	Retroperitoneal	40*35*10	WD LS	2	MDM2 Amp	Y	56	37	3	ND
WD8	F	60	Retroperitoneal	35*17*16	WD LS	1	MDM2 Amp	N	92	4	2	ND
WD9	F	40	Retroperitoneal	9*6*4	WD LS	1	MDM2 Amp	Y	65	15	1	ND
WD10	F	73	Shoulder (right)	16*7*4	WD LS	1	MDM2 Amp	N	2	2	1	ND
WD11	F	63	Thigh (left)	29*12*7	WD LS	1	MDM2 Amp	N	92	21	1	ND
WD12	F	74	Thigh (left)	8*10*5	WD LS	1	MDM2 Amp	N	42	14	2	ND
WD13	F	64	Thigh (right)	18*15*4	WD LS	1	MDM2 Amp	N	37	16	2	ND
WD14	F	78	Thigh (right)	14*10*10	WD LS	1	MDM2 Amp	N	68	60	25	None
WD15	F	56	Thigh (right)	17*12*4	WD LS	1	MDM2 Amp	N	43	40	4	ND
WD16	F	67	Thigh (right)	19*17*6	WD LS	1	MDM2 Amp	N	30	11	1	ND
WD17	F	47	Thigh (right)	21*14*5	WD LS	1	MDM2 Amp	N	69	64	1	ND
WD18	F	56	Thigh (right)	11*8*5	WD LS	1	MDM2 Amp	N	26	5	1	ND
WD19	F	60	Thigh (left)	20*15*4	WD LS	1	MDM2 Amp	N	32	18	7	ND

Full Participants Cohort – WDLS

Case no.	Gender	Age	Site	Size (cm)	Histology	Grade	Cytogenetic results	Fresh sample	IHC score			P53 mutation
									MDM2	MDMX	P53	
WD20	F	66	Retroperitoneal	27*11*9	WD LS	1	MDM2 Amp	Y	47	56	36	None
WD21	F	49	Retroperitoneal	12*7*2	WD LS	1	MDM2 Amp	Y	15	7	2	ND
WD22	M	71	Chest wall	9*9*5	WD LS	1	MDM2 Amp	N	2	2	1	ND
WD23	M	69	Chest wall	5*4*2	WD LS	1	MDM2 Amp	N	5	2	1	ND
WD24	M	50	Chest wall	9*7*1	WD LS	1	MDM2 Amp	N	6	4	1	ND
WD25	M	58	Gluteal (right)	25*17*5	WD LS	1	MDM2 Amp	N	67	30	2	ND
WD26	M	68	Retroperitoneal	21*15*4	WD LS	1	MDM2 Amp	N	19	1	1	ND
WD27	M	63	Thigh (left)	30*19*15	WD LS	1	MDM2 Amp	N	33	1	2	ND
WD28	M	72	Thigh (right)	26*23*11	WD LS	1	MDM2 Amp	N	2	8	12	Glu171Lys Asn131Ser
WD29	M	64	Thigh (right)	21*11*3	WD LS	1	MDM2 Amp	N	53	28	4	ND
WD30	M	44	Gluteal (left)	9*7*5	WD LS	1	MDM2 Amp	N	99	85	29	Failed Ex7
WD31	M	77	Thigh (left)	15*12*3	WD LS	1	MDM2 Amp	N	95	5	2	ND
WD32	M	83	Thigh (right)	28*26*12	WD LS	1	MDM2 Amp	N	98	14	6	ND
WD33	M	62	Pericardial	18*18*10	WD LS	1	MDM2 Amp	N	7	2	1	ND
WD34	M	71	Retroperitoneal	12*10*9	WD LS - Mixed	1	MDM2 Amp	Y	43	41	39	None
WD35	F	67	Thigh (right)	12*10*2	WD LS	1	MDM2 Amp - G band normal	N	76	63	2	ND

Full Participants Cohort – WDLS

Case no.	Gender	Age	Site	Size (cm)	Histology	Grade	Cytogenetic results	Fresh sample	IHC score			P53 mutation
									MDM2	MDMX	P53	
WD36	F	59	Thigh (left)	11*4*3	WD LS	1	MDM2 Amp G band normal	N	3	5	98	None
WD37	M	67	Thigh (left)	14*8*7	WD LS	1	MDM2 Normal 13q deletion	N	25	5	46	None
WD38	M	62	Thigh (right)	15*10*3	WD LS	1	MDM2 Normal 13q monosomy	N	80	32	6	ND
WD39	F	53	Arm (right)	5*3*2	WD LS – inflammatory	2	MDM2 Normal G band normal	N	70	80	32	Lys292*FS
WD40	M	61	Chest wall (right)	4*2*2	WD LS	1	MDM2 Normal G band normal	N	95	85	67	None
WD41	F	73	Leg (left)	10*10*6	WD LS	1	MDM2 Normal Gain Ch12	N	32	18	1	ND
WD42	F	85	Leg (right)	6*6*3	WD LS	1	MDM2 Normal 13q monosomy	N	84	70	62	Asp184Asn
WD43	M	73	Thigh (right)	9*6*4	WD LS	1	Not Done	N	3	2	1	ND

Full Participants Cohort – DDLS

Case no.	Gender	Age	Site	Size (cm)	Histology	Grade	Cytogenetic results	Fresh sample	IHC score			P53 mutation
									MDM2	MDMX	P53	
DD1	M	70	Back	19*10*4	DD LS	3	G band uncertain findings	N	32	62	79	None
DD2	M	62	Chest wall (right)	19*19*3	DD LS	3	MDM2 Amp G band normal	N	98	25	95	None
DD3	F	78	Retroperitoneal	20*18*8	DD LS	2	MDM2 Amp	Y	92	78	18	Leu257Gln
DD4	F	38	Retroperitoneal	20*18*18	DD LS	2	MDM2 Amp	N	41	52	15	None
DD5	M	63	Retroperitoneal	40*35*12	DD LS	2	MDM2 Amp	N	92	28	2	ND
DD6	M	65	Retroperitoneal	29*24*14	DD LS	3	MDM2 Amp	N	58	60	52	Leu257Gln
DD7	M	69	Retroperitoneal	25*20*14	DD LS	3	MDM2 Amp	Y	98	95	72	None
DD8	M	73	Retroperitoneal	23*20*8	DD LS	3	MDM2 Amp G band normal	N	97	70	52	None
DD9	F	64	Retroperitoneal	15*15*4	DD LS	3	Not attempted	N	41	31	1	ND

Full Participants Cohort – MXLS-RCLS

Case no.	Gender	Age	Site	Size (cm)	Histology	Grade	Cytogenetic results	Fresh sample	IHC score			P53 mutation
									MDM2	MDMX	P53	
MR1	M	70	Buttock (left)	10*7*5	MXLS	1	12:16 Translocation	N	81	91	18	Ser46Phe
MR2	M	47	Knee (right)	6*6*4	MXLS	3	12:16 Translocation	N	76	90	42	None
MR3	F	48	Thigh (left)	18*13*7	MXLS	1	CHOP rearrangement	N	88	98	2	ND
MR4	M	37	Thigh (left)	8*7*5	MXLS	3	CHOP rearrangement	N	50	75	27	None
MR5	M	44	Pelvic	17*11	MXLS	1	CHOP rearrangement	N	97	99	80	None
MR6	M	64	Chest wall (left)	9*7*	MXLS	2	Complex multiple translocations	N	98	87	52	Lue257Gln
MR7	F	53	Thigh (left)	6*6	MXLS	2	Not attempted	N	90	84	36	None
MR8	F	51	Thigh (left)	20*8*8	MXLS	2	Not attempted	N	99	46	32	Asp184Asn
MR9	M	44	Retroperitoneal	24*20	MXLS	2	Possible MDM2 Amp	N	1	2	1	ND
MR10	M	54	Thigh (left)	23*19*18	MXLS RCLS	3	12:16 Translocation	N	14	86	18	None
MR11	F	44	Thigh (left)	3*2*2	RCLS	3	12:16 Translocation	N	54	95	27	None
MR12	F	38	Thigh (right)	18*13*12	RCLS	3	Failed	N	92	90	72	None

Full Participants Cohort – Other STS and Benign Cases

Case no.	Gender	Age	Site	Size (cm)	Histology	Cytogenetic results	Fresh sample	IHC score			P53 mutation
								MDM2	MDMX	P53	
ST1	F	77	Chest wall	2.5	Angiosarcoma	ND	Y	17	6	3	ND
ST2	F	74	Breast	4	Angiosarcoma	ND	Y	39	44	70	ND
ST3	F	41	Breast	unknown	Angiosarcoma	ND	Y	5	24	6	ND
ST4	F	51	Retroperitoneal	17*12*14	Inflammatory fibroblastic tumour	MDM2 Amp	Y	3	12	8	ND
B1	F	31	Pelvic	9*8*3	Lipoma	MDM2 Normal	Y	6	3	2	None
B2	M	46	Axilla	5*4*2	Lipoma	MDM2 Normal	Y	2	3	5	ND
B3	M	35	Back	13*11*4	Lipoma	MDM2 Normal	Y	1	1	1	ND
B4	F	45	Retroperitoneal	20*14*10	Leiomyoma	ND	Y	3	1	1	ND
B5	F	73	Retroperitoneal	13*11*7	Intramuscular Myxoma	ND	Y	57	68	5	ND

Amp = Amplification; IHC = Immunohistochemistry; ND = Not Done; no. = number.